Department of AERONAUTICS and ASTRONAUTICS
STANFORD UNIVERSITY

RONALD E. FOERSTER
I. FLÜGGE-LOTZ

NEIGHBORING OPTIMAL FEEDBACK CONTROL OF MULTI-INPUT NONLINEAR DYNAMICAL SYSTEMS USING DISCONTINUOUS CONTROL

This research was sponsored by the National Aeronautics and Space Administration under Research Grant NASA NGL 05-020-007

MARCH
1970

SUDAAR
NO. 398

DEPARTMENT OF APPLIED MECHANICS

STANFORD UNIVERSITY
STANFORD, CALIFORNIA

NEIGHBORING OPTIMAL FEEDBACK CONTROL OF MULTI-INPUT NONLINEAR DYNAMICAL SYSTEMS USING DISCONTINUOUS CONTROL

by

Ronald E. Foerster

and

I. Flügge-Lotz

SUDAAR No. 398

March 1970

This research was sponsored by the National Aeronautics and Space Administration under Research Grant NASA NGL 05-020-007.

ABSTRACT

The calculation and implementation of the neighboring optimal feedback control law for multi-input nonlinear dynamical systems, using discontinuous control, is the subject of this study. The concept of neighboring optimal feedback control of systems with continuous, unbounded control functions has been investigated by others. A separate treatment of the problem is necessary, however, when the control function is discontinuous. This is often the case when optimal control of systems with bounded control inputs is desired. The differentiating features of this class of problems are the control discontinuities and the inherent system uncontrollability when the number of remaining switch times is less than the number of specified terminal constraints.

In this paper, a derivation of the neighboring optimal control law is presented, and a feedback mechanization of this control law is described. The neighboring control law is determined by minimizing the second-order terms in the expansion of the performance index about an optimal, nominal path. A distinction is made between real time along the neighboring path and nominal time along the nominal path. The concept of "time-to-go" is used to choose the nominal time. This concept is applied in two different ways, depending upon whether the terminal time is fixed or free. An open-loop algorithm which determines the number of neighboring switch times, the initial and final control functions, and the most appropriate nominal path , is presented. This algorithm initiates the feedback phase of the mechanization of the neighboring control law. The feedback mechanization allows for a possible reordering of the control-component switching sequence, and requires storage of only a small number of feedback gain matrices.

Three example problems, including the minimum-time satellite attitude-acquisition problem, are presented. These problems demonstrate the feasibility of neighboring optimal feedback control of systems with discontinuous control functions, and show the action of the neighboring control scheme when applied to states which do not lie in the immediate neighborhood of the nominal trajectory. For these particular examples, it was found that the neighboring control scheme works quite well even when the deviations in the neighboring state, away from the nominal, are large. When these deviations are large, however, the terminal constraints can no longer be satisfied exactly.

ACKNOWLEDGMENT

The authors would like to express their appreciation to Professor A. E. Bryson, Jr. for suggesting this topic and providing stimulating discussions during the course of this research. The authors also thank Professor G. F. Franklin for his helpful suggestions during the preparation of this manuscript.

This research was supported by the National Aeronautics and Space Administration under Research Grant NGL 05-020-007. This support is greatly appreciated.

TABLE OF CONTENTS

TABLE OF CONTENTS (Continued)

LIST OF TABLES

LIST OF ILLUSTRATIONS

LIST OF ILLUSTRATIONS (Continued)

LIST OF SYMBOLS

a	magnitude of orbit semi-major axis
B	rigid body
B^*	mass center of B
$\bar{b}_i$	unit vectors fixed in B and parallel to the principal axes of B, i = 1,2,3
c_i	cosine of θ_i, i = 1,2,3
$\bar{D}$	(N x n) matrix (see Eq. 3.50)
E	inertially fixed point mass (earth)
$\bar{E}(\cdot,\cdot)$	(1 x n) matrix (see Eq. 3.44 - Eq. 3.45)
$F'[\cdot],F[\cdot]$	(scalar) cost function of the final state
$f[\cdot,\cdot]$	(n x 1) vector function specifying the system dynamics
$\bar{G}_N$	(N x n) matrix (see Eq. 3.59)
$\bar{g}_N$	N^{th}-row of $\bar{G}_N$
$\bar{g}_0$	(1 x n) matrix (see Eq. 3.60)
$H[\cdot,\cdot,\cdot]$	(scalar) variational Hamiltonian (see Eq. 3.1)
$\bar{h}(\cdot)$	(scalar) function (see Eq. 3.43)
I_i	principal moments of inertia, i = 1,2,3
J	(scalar) performance index for neighboring path
$\bar{J}'',\bar{J}',\bar{J}$	(scalar) performance index for nominal path
J_ℓ	(N x N) matrix (see Eq. 3.52)
K	(scalar) positive gain (see Eq. 2.10)
k_i	inertia parameters, i = 1,2,3,(see Eq. C.2, Appendix C)
$L[\cdot,\cdot]$	(scalar) cost function along the trajectory
$\bar{M}$	(1 x n)matrix (see Eq. 3.32)
m	dimension of control vector

N	number of remaining switch times along the neighboring (and nominal) trajectory
$\bar{N}$	total number of switch times along the nominal trajectory
N'	integer less than or equal to $\bar{N}$
n	dimension of dynamical system
$\bar{P}$	(n x n) matrix (see Eq. 3.14)
q	number of terminal constraints
$\bar{R}(\cdot,\cdot)$	(n x ℓ) matrix (see Eq. 3.41)
r	orbital angular velocity
$S_{ij}(\cdot,\cdot)$	i^{th}-switching function for j^{th}-component of the control function
$S_f(\cdot,\cdot)$	final-time switching function
s	Laplace variable
s_i	sine of θ_i , i = 1,2,3
T_i	control torques, i = 1,2,3
$\bar{T}(\cdot,\cdot)$	(n x 1) matrix (see Eq. 3.40)
t	real time along the neighboring path
$\bar{t}$	nominal time along the nominal path
t_c	open-loop computation time (see Section 4.4)
t_{ij}	i^{th}-switch time associated with a step change in the j^{th}-component of the control function
t_s	(N x 1) switch-time vector (see Eq. 3.63)
$\bar{U}$	(n x n) matrix (see Eq. 3.39)
$u(\cdot)$	(m x 1) control vector
$\bar{V}$	(N x N)matrix (see Eq. 3.58)
W	(q x q) positive-definite weighting matrix (see Eq. 2.10)
$\bar{X}$	(N x N) matrix (see Eq. 3.49)
$x(\cdot)$	(n x 1) state vector
(x_E,y_E,z_E)	inertially fixed (earth fixed) reference frame

(x_B, y_B, z_B)	body fixed reference frame
(x_R, y_R, z_R)	orbitally fixed reference frame
$\bar{Y}$	(N x N) matrix (see Eq. 3.53)
$\bar{Z}$	(N x n) matrix (see Eq. 3.51)
β	(scalar) control angular acceleration bound (see Eq. 5.22)
β_i	(scalar) bound on control-component magnitude, i = 1,$\cdots$,m (see Eq. 2.2)
$\delta t_f, \delta t_{ij}$	(scalar) control parameters, i = 1,$\cdots$, N
δt_s	(N x 1) vector of switch-time perturbations (see Eq. 3.38)
$\delta x_I(\cdot)$	(n x 1) vector of first-order terms in the expansion of $\delta x(\cdot)$
$\delta x_{II}(\cdot)$	(n x 1) vector of second-order terms in the expansion of $\delta x(\cdot)$
ϵ	orbit eccentricity
θ	true anomaly
θ_i	three-axis Euler angles, i = 1,2,3 (see Appendix C)
$\lambda(\cdot)$	(n x 1) adjoint vector
ν	(q x 1) vector of Lagrange multipliers
$\bar{\rho}$	radius vector
τ	dummy variable of integration
$\Phi(\cdot,\cdot)$	(n x n) state transition matrix for Eq. 3.19
$\Psi[\cdot]$	(q x 1) vector of terminal constraints
$\bar{\omega}(\cdot,\cdot)$	(scalar) function (see Eq. 3.42)
ω_i	inertial angular velocity components, i = 1,2,3 (see Appendix C)

SPECIAL NOTATION

$\bar{(\ )}$	quantity associated with nominal path
$\dot{(\ )}$	differentiation with respect to time

$(\ )_0$	initial value
$(\ )_f$	final value
$(\ )_i$	i^{th}-component of a vector
$(\ )_{ij}$	the element in the i^{th}-row and j^{th}-column of a matrix
$(\ )^{-1}$	inverse of a matrix
$(\ )^T$	transpose of a matrix
$(\ )_{op}$	optimal value
$(\ )_{Min}$	minimum value
$\lvert\cdot\rvert$	absolute value function
$\lvert\lvert\cdot\rvert\rvert$	distance function (see Eq. 5.9)
$\Delta_i\alpha$	step change of a discontinuous vector $\alpha(\cdot)$ at time t_{ij} (see Eq. 3.9)
$\delta\alpha(\cdot)$	perturbation of a vector $\alpha(\cdot)$ (see Eq. 3.8)
$\delta x^i(\cdot)$	i^{th}-component of the vector $\delta x(\cdot)$
$\alpha(t_i^{\mp})$	value of vector $\alpha(t)$ at time $t \underset{\epsilon\to 0}{=} t_i \mp \epsilon, \epsilon > 0$

Let $\alpha(\cdot)$ be a (q x 1) vector, $x(\cdot)$ be a (n x 1) vector, and $y(\cdot)$ be a (m x 1) vector. Then the following notation is defined:

$$\alpha_x(\cdot) \equiv \begin{bmatrix} \dfrac{\partial\alpha_1(\cdot)}{\partial x_1} & \cdots & \dfrac{\partial\alpha_1(\cdot)}{\partial x_n} \\ \vdots & & \vdots \\ \dfrac{\partial\alpha_q(\cdot)}{\partial x_1} & \cdots & \dfrac{\partial\alpha_q(\cdot)}{\partial x_n} \end{bmatrix}$$

$$\alpha_x^j(\cdot) \equiv \begin{bmatrix} \dfrac{\partial\alpha_j(\cdot)}{\partial x_1} & \cdots & \dfrac{\partial\alpha_j(\cdot)}{\partial x_n} \end{bmatrix}$$

$$\alpha^{j}_{xy}(\cdot) \equiv \begin{bmatrix} \dfrac{\partial^2 \alpha_j(\cdot)}{\partial x_1 \partial y_1} & \cdots & \dfrac{\partial^2 \alpha_j(\cdot)}{\partial x_1 \partial y_m} \\ \vdots & & \vdots \\ \dfrac{\partial^2 \alpha_j(\cdot)}{\partial x_n \partial y_1} & \cdots & \dfrac{\partial^2 \alpha_j(\cdot)}{\partial x_n \partial y_m} \end{bmatrix}$$

CHAPTER I

INTRODUCTION

The calculation and implementation of optimal, discontinuous control laws for high-order systems is of current interest. A discontinuous control law is one that requires sudden changes of the control components from one discrete level to another. Optimal control laws which are discontinuous, often arise when the components of the control are bounded in magnitude. It is this class of optimization problems which is of interest in this study.

1.1 Problem Motivation

Minimum-time and minimum-fuel control laws are often discontinuous. Several techniques have been developed to find minimum-time and minimum-fuel open-loop control functions for a specified initial state. Only for some very special, low-order systems, have optimal feedback control laws been determined.

A problem involving a high-order, multi-input system, of current interest in the aerospace field, is the minimum-fuel or minimum-time attitude control of an orbiting satellite. This problem involves a 6th-order system with three bounded control inputs when three cold gas jets with bounded thrusts are used as the controlling mechanism. An optimal feedback control law, valid for all points in state-space, has proved all but impossible to obtain for a high-order system such as this. It is possible, however, to obtain a feedback control law, which is nearly optimal, and which is valid for a restricted region in state-space. Developing such a control scheme, applicable to multi-input, nonlinear, high-order systems, using discontinuous control, is the objective of this study.

The approach used here is similar to the approach used by others for systems with unbounded control and continuous control functions. A neighboring optimal feedback control law is derived which is valid for points in state-space that are in the neighborhood of an optimal, nominal trajectory. A neighboring optimal feedback control law is a control law which is based upon the state deviation from a nominal optimum path, and upon the open-loop control function used to generate the nominal path. The technique used to generate this control law is to expand the performance index, to second-order, about the nominal path, and then determine the control deviations, away from the nominal, by minimizing the second-order terms in the expansion.*

Three example problems, including the minimum-time attitude control problem mentioned above, are presented in this paper. The purpose of presenting these examples is twofold: 1) To demonstrate the feasibility of a neighboring optimal control scheme for systems possessing discontinuous control functions, and 2) to show the action of the neighboring control law when it is applied to states which do not lie in the immediate neighborhood of the nominal trajectory.

1.2 Previous Results

Several techniques have been discussed in the literature for solving optimization problems which result in optimal, discontinuous, open-loop control functions. Among the first-order algorithms developed to solve these optimization problems are those of Hales [1] and Wolske [2].**

---

* It will be shown, in Section 3.2, that the optimal nominal and neighboring control laws are identical to first-order.

** Numbers in brackets, [·], refer to references given at the end of this paper.

Hales' method is quite general, but convergence to the optimal solution is slow. The rate of convergence of Wolske's method is excellent, but his algorithm is restricted to handle only minimum-fuel problems.

Several second-order algorithms have also been developed to solve these problems. Among the most recent are those developed by Dyer and McReynolds [3,4], and Jacobson [5]. The theory upon which these algorithms are based is the same. The algorithm of Jacobson, however, appears to be superior since it is less sensitive to the initial choice of the control history. McNeal [6] also proposed a second-order algorithm which is based upon a somewhat different theoretical approach.

All of the above methods, however, are iterative techniques which converge to the open-loop solution of the optimization problem. The use of the second variation to obtain a neighboring optimal feedback control law was proposed, independently, by Breakwell et al. [7] and Kelley [8]. It was assumed by these authors, however, that the available control effort is unbounded, and that the control histories are continuous. Hence, this theory is not applicable to problems for which the optimal control law is discontinuous.

First McIntyre [9], and then McNeal [6], considered the problem of neighboring optimal feedback control with discontinuous control functions. Both authors expanded the performance index to second-order about an optimal, nominal path, and then determined the neighboring control law, in terms of deviations from the nominal control law, by minimizing the second-order terms in the expansion. Each author assumed that only one control variable of a multi-input dynamical system was discontinuous. In addition, McNeal considered the case where measurement noise and/or random disturbances act on the system. The

results of the present study, concerning systems with multi-dimensional discontinuous control functions, are basically in agreement with those results of McIntyre and McNeal which pertain to noise-free systems with a scalar discontinuous control function. The derivation here, however, is somewhat different from those of the other two authors.

Neither McNeal, nor McIntyre, made a distinction between real time, t, along the neighboring path, and nominal time, $\bar{t}$, along the nominal path. Hence, both authors implicitly assumed that $\bar{t} \equiv t$ in their mechanization of the neighboring control law. With this choice for the nominal time, the neighboring control law mechanization described by McNeal and McIntyre becomes open-loop after the nominal switch times and nominal final time, when the switch-time and final-time perturbations are positive.* This technique highly restricts the region in state-space for which the neighboring control law is applicable, and also could lead to excessive errors in multi-dimensional discontinuous control problems. The mere fact that the mechanization is not entirely a feedback mechanization is, of course, undesirable.

Speyer and Bryson [10], and Powers [11], did distinguish between real time and nominal time (index-time), for the case of neighboring optimal control of systems with continuous, unbounded control functions. Speyer and Bryson chose $\bar{t}$ such that estimated time-to-go until the final time is the same for both neighboring and nominal trajectories. Powers chose $\bar{t}$ such that a weighted distance between the neighboring current state and the nominal path is minimized. The technique of

---

* This fact is discussed in Section 4.4.

Powers appears to be difficult to implement when the system is high-order, whereas the method of Speyer and Bryson requires an accurate estimate of the final-time, which may be difficult to obtain when noise is present in the system. In each case, however, the mechanization of the neighboring control law is entirely a feedback mechanization. The "time-to-go" concept is used in the present study to choose $\bar{t}$ such that the neighboring, discontinuous control law is entirely a feedback control law.

Finally, both McIntyre and McNeal assume that the number of switch times and the initial control vector, for the neighboring path, are known. Davison and Monro [12] have developed a first-order, open-loop, iterative procedure for obtaining this information for minimum-time control problems. The neighboring feedback control law algorithm, described in the present paper, ascertains this information for any type of discontinuous control problem.

1.3 Contributions

The principal contributions of this study are the following:

1. A neighboring optimal control law, valid for states neighboring an optimal, nominal trajectory, is derived for systems which possess discontinuous optimal control functions. High-order, nonlinear systems, with multi-dimensional control functions, are considered. The problem whose solution determines the neighboring optimal control law, is reduced to the simplest form of a parameter optimization problem. The solution of this problem is obtained by solving a set of linear, coupled algebraic equations. This calculation is, therefore, easily performed on a digital computer.

2. A feedback mechanization of the neighboring control law is described. Switching functions for each component of the control vector are derived. These switching functions are constructed from

precalculated gains, which are, in turn, a function of the nominal time (a parameter associated with the nominal trajectory). Using the concept of "time-to-go" (see Section 4.2), two schemes, depending upon whether the terminal time is fixed or free, are proposed for choosing the nominal time. These schemes enlarge the region, in state-space, for which the feedback control scheme is applicable. When the mechanization of the feedback control law takes the form of a digital controller, a reordering of the sequence in which the control-components switch is possible.

3. An open-loop algorithm, which ascertains the number of switch times, the initial and final control vector, and the appropriate nominal trajectory, is described. This algorithm is used during the initial stages of the control scheme when the above information is not available. The algorithm is computationally simple, and thus the associated computation time has little effect, in general, upon the performance of the feedback phase of the control scheme.

4. The size of the region in state-space, about the nominal trajectory, for which the control scheme gives meaningful results, is investigated by considering three example problems. In order to give the neighboring control law a severe test, a third-order problem, with a highly nonlinear optimal switching surface, is considered. To demonstrate the feasibility of controlling high-order systems by the neighboring optimal feedback control technique, a 6^{th}-order system with three control inputs is discussed.

1.4 Organization of Work

The specific problem of interest in this study is formulated in Chapter II. The dynamical description of the system is given, and an

optimization problem is posed (Optimization Problem I). It has been shown by others that a neighboring optimal feedback control law cannot be derived from the solution of Optimization Problem I since exact satisfaction of terminal constraints is required. Therefore, a second optimization problem is posed (Optimization Problem II), which is free of terminal constraints, and from which a neighboring optimal feedback control law can be derived. The relationships between the solutions of these two optimization problems is discussed in detail.

The solution of Optimization Problem II is determined in Chapter III. The performance index is expanded, to second-order, about an optimal, nominal path, the nominal path being determined by solving Optimization Problem I. The control parameters (switch-time and final-time perturbations) are determined by minimizing the second-order terms in the expansion of the performance index. The equations which determine the control parameters are written in matrix form so that matrix algebra can easily be used to solve for these parameters. The resulting solution is then used to formulate a neighboring optimal feedback control law.

To implement the control law derived in Chapter III, it is necessary to determine the number of switch times, the initial and final control vectors, and the most appropriate nominal trajectory. An open-loop algorithm to accomplish this is presented in Chapter IV. The distinction between real and nominal time is discussed, and a technique for choosing the nominal time is described. The validity of this technique is supported by a heuristic argument and the results, obtained through its use, presented in Chapter V. The claim that this technique is always the best technique for choosing the

nominal time cannot be made. A feedback mechanization of the neighboring optimal control law is also described in Chapter IV. This mechanization requires that one monitor, simultaneously, the appropriate switching function for each component of the control vector. By so doing, one allows for the possibility of a reordering of the control-component switching sequence.

Three example problems are considered in Chapter V. The first two problems involve low-order, linear systems with scalar control inputs. The last problem involves a nonlinear, 6^{th}-order system with three control inputs. The first problem is the minimum-fuel settling-time problem for the $1/s^2$ plant. The intent of this problem is to demonstrate the use of the neighboring feedback control law mechanization for fixed terminal-time problems. The remaining two problems are the problem of minimum-time control of the $1/s(s^2 + 1)$ plant, and the minimum-time satellite attitude-acquisition problem. These problems demonstrate the use of the neighboring feedback control law mechanization for free terminal-time problems. It is felt that this choice of example problems gives a representative picture of the utility of neighboring optimal feedback control.

Finally, a summary of the basic results and conclusions of this study is presented in Chapter VI.

CHAPTER II

PROBLEM FORMULATION

In this chapter, the class of dynamical systems considered is defined and two optimization problems are posed, Optimization Problem I and Optimization Problem II. The nominal path, depicted schematically by Trajectory I in Fig. 2.1, and the nominal control law, for the initial nominal state $\bar{x}_o$, are determined by solving Optimization Problem I. The objective of this study is to solve Optimization Problem I for the optimal feedback control law for an initial state x_o, neighboring $\bar{x}_o$. The corresponding optimal trajectory is depicted schematically by Trajectory II in Fig. 2.1. In general, a neighboring optimal feedback control law for Optimization Problem I does not exist since terminal equality constraints are incorporated in the problem statement. The performance index of Optimization Problem I is therefore modified, and a free end-point optimization problem (Optimization Problem II) is posed. The solution of this problem gives a neighboring optimal feedback control law for initial state x_o, neighboring $\bar{x}_o$, which is a sub-optimal solution of Optimization Problem I with initial state x_o. The neighboring, sub-optimal trajectory is depicted schematically by Trajectory III in Fig. 2.1.

2.1 System Specification

The system dynamical equations are given by

$$\dot{x}(t) = f[x(t),u(t)] \ , \ x(t_o) = x_o \ , \tag{2.1}$$

where $x(t)$ is the $(n \times 1)$ state vector, $u(t)$ is the $(m \times 1)$

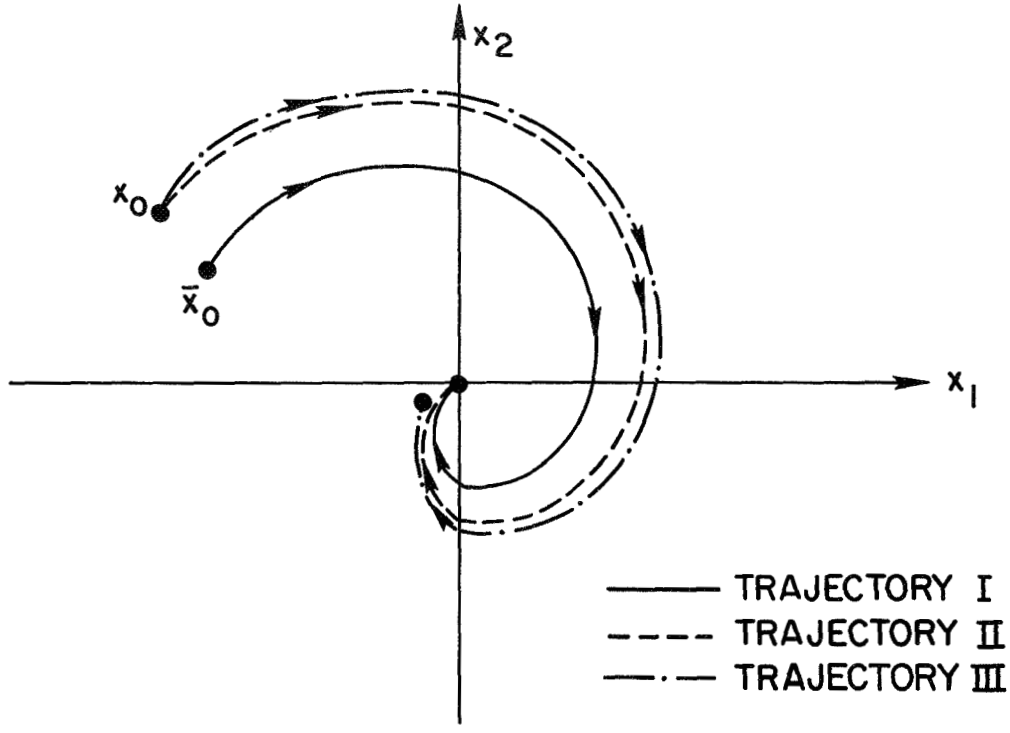

Figure 2.1. Two-Dimensional Example Trajectories Depicting the Nominal Path (I) , the Optimal Path Determined from Optimization Problem I(II) , and the Optimal Path Determined from Optimization Problem II (III).

control vector, $f[\cdot,\cdot]$ is an $(n \times 1)$ vector function, and x_o is the specified initial state vector. It is implicit in Eq. 2.1, and is assumed in the theory to follow, that time t never appears explicitly in the system dynamics or in the statement of the optimization problem.

This study is restricted to optimization problems which result in discontinuous control laws. It is therefore assumed that $f[x(t), u(t)]$ is a linear function of $u_i(t)$, $i = 1, \cdots, m$, and that

$$|u_i(t)| \leq \beta_i , \quad i = 1 , \cdots, m , \tag{2.2}$$

where β_i, $i = 1, \cdots, m$, are positive constants. It is assumed that $f[x(t), u(t)]$ is at least twice differentiable with respect to $x(t)$ in the time interval $[t_o, t_f]$, where t_f is the final time.

2.2 Optimization Problem

The solution of the optimization problem posed in this section, for the optimal control law for an initial state $\bar{x}_o$, defines the nominal path, $\bar{x}(\bar{t})$, $\bar{t} \in [\bar{t}_o, \bar{t}_f]$, and the nominal control history, $\bar{u}(\bar{t})$, $\bar{t} \in [\bar{t}_o, \bar{t}_f]$. All quantities associated with the nominal path will be indicated by a "bar" above their respective symbols. The need to distinguish between real time along a neighboring path, t, and nominal time, $\bar{t}$, will become evident in Section 3.4.

The scalar performance index of interest in this study is given by

$$\bar{J}'' = F'[\bar{x}(\bar{t}_f)] + \int_{\bar{t}_o}^{\bar{t}_f} L[\bar{x}(\bar{t}), \bar{u}(\bar{t})]d\bar{t} \tag{2.3}$$

where $F'[\bar{x}(\bar{t}_f)]$ is a scalar function of the final state and

$L[\bar{x}(\bar{t}) , \bar{u}(\bar{t})] , \bar{t} \in [\bar{t}_o, \bar{t}_f]$, is a scalar function of the control and state histories. The terminal equality constraints which are imposed upon the system are defined by

$$\Psi[\bar{x}(\bar{t}_f)] = 0 \tag{2.4}$$

where $\Psi[\bar{x}(\bar{t}_f)]$ is a $(q \times 1)$ vector function of the final state and $q \leq n$. The final time, $\bar{t}_f$, may or may not be specified. It is assumed that these terminal constraints are such that the initial state, for the system of Eq. 2.1, is controllable in the allowable time specified for the problem.

Again, to insure that the solution of the optimization problem will yield a discontinuous control law, it is necessary to assume that $L[\bar{x}(\bar{t}) , \bar{u}(\bar{t})]$ is at most a linear function of the components of $\bar{u}(\bar{t})$. To insure that the optimal control law is discontinuous, it is assumed that no singular arcs appear in the solution of the optimization problem posed below.* Finally, it is assumed that $F'[\cdot]$, $\Psi[\cdot]$, and $L[\cdot,\cdot]$ are at least twice differentiable with respect to $\bar{x}(\bar{t})$ in the time interval $[\bar{t}_o,\bar{t}_f]$.

Later theoretical considerations warrant a simplification in the performance index, $\bar{J}''$, at the expense of increasing the dimension of the state vector. When $L[\bar{x}(\bar{t}), \bar{u}(\bar{t})] , \bar{t} \in [\bar{t}_o, \bar{t}_f]$, is not identically zero, the state is augmented as follows:

$$\dot{\bar{x}}_{(n+1)} (\bar{t}) = L[\bar{x}(\bar{t}) , \bar{u}(\bar{t})] , \bar{x}_{(n+1)} (\bar{t}_o) = 0 . \tag{2.5}$$

---

* See [13], Chapter 8, for a definition and discussion of singular arcs.

The performance index, $\bar{J}''$, may thus be replaced by the performance index

$$\bar{J}' = F[\bar{x}(\bar{t}_f)] \tag{2.6}$$

where $F[\bar{x}(\bar{t}_f)] = F'[\bar{x}(\bar{t}_f)] + \bar{x}_{(n+1)}(\bar{t}_f)$.

To minimize the performance index $\bar{J}'$ subject to the terminal constraints, Eq. 2.4, the terminal constraints are adjoined to $\bar{J}'$ with a $(q \times 1)$ vector of Lagrange multipliers, ν , to form the augmented performance index:

$$\bar{J} = F[\bar{x}(\bar{t}_f)] + \nu^T \Psi[\bar{x}(\bar{t}_f)] . \tag{2.7}$$

The optimization problem for the nominal path is thus stated as follows:

Optimization Problem I

For the dynamical system defined by

$$\dot{\bar{x}}(\bar{t}) = f[\bar{x}(\bar{t}) , \bar{u}(\bar{t})] , \bar{x}(\bar{t}_o) = \bar{x}_o, \tag{2.8}$$

choose a control vector, $\bar{u}(\bar{t}), \bar{t} \in [\bar{t}_o, \bar{t}_f]$, subject to the control constraints (Eq.2.2), which minimizes $\bar{J}$ (Eq. 2.7), and choose ν such that the terminal constraints (Eq. 2.4) are satisfied.

2.3 Relaxation of Terminal Constraints

In [6], McNeal discusses and demonstrates the fact that, in general, a neighboring optimal feedback control law for Optimization Problem I does not exist for an initial state x_o, neighboring $\bar{x}_o$. Along the latter stages of the neighboring trajectory, the feedback gains of the neighboring control law become infinite. Specifically, for a fixed final time problem, when the number of remaining switch

times, N, along the neighboring path is less than the number of terminal constraints, q, the system is uncontrollable to the extent that N control decisions are insufficient in number to satisfy q terminal constraints. When t_f is free an additional control decision is available. For this class of problems, the system is uncontrollable once $(N + 1) < q$.

To alleviate the problem of uncontrollability, and hence insure the existence of a neighboring optimal feedback control law, a new optimization problem is posed in which insistence on exact satisfaction of the terminal constraints is relaxed. The solution of the new problem for the optimal control law for an initial state x_o, neighboring $\bar{x}_o$, will be an approximate solution of Optimization Problem I with initial state x_o.

Only approximate satisfaction of the terminal constraints will be required in the new optimization problem.* This may be accomplished by adding a penalty term to the performance index, $\bar{J}$ (Eq. 2.7), for non-satisfaction of the terminal constraints, and then formulating a free end-point optimization problem. The penalty term takes the form

$$\frac{K}{2} \Psi^T[x(t_f)]W\Psi[x(t_f)]$$

where K is a scalar positive constant and W is a $(q \times q)$ positive-definite weighting matrix. As K increases in magnitude from zero, the cost of non-satisfaction of Eq. 2.4 increases, and hence the components of $\Psi[x(t_f)]$ are reduced in magnitude by the control law.

---

* This approach was also followed by McNeal in [6].

The choice of W allows one to penalize certain components of $\Psi[x(t_f)]$, more than others, for being non-zero.

The new optimization problem, which will be solved in Chapter III to give a neighboring optimal feedback control law for points neighboring the nominal path, is thus stated as follows:

Optimization Problem II

For the dynamical system described by

$$\dot{x}(t) = f[x(t), u(t)], \quad x(t_o) = x_o, \tag{2.9}$$

choose a control vector, $u(t)$, $t \in [t_o, t_f]$, subject to the control constraints (Eq. 2.2), which minimizes the scalar performance index*

$$J = F[x(t_f)] + \nu^T \Psi[x(t_f)] + \frac{K}{2} \Psi^T[x(t_f)] W \Psi[x(t_f)], \tag{2.10}$$

where ν is the $(q \times 1)$ vector of Lagrange multipliers obtained in the solution of Optimization Problem I with the initial state $\bar{x}_o$, and x_o is an initial state neighboring $\bar{x}_o$.

---

* The $\nu^T \Psi[\cdot]$ term in the performance index (Eq. 2.10) is necessary to insure that, to first-order, Optimization Problem I is identical to Optimization Problem II. That is, the presence of this term insures that the nominal control law is identical to the neighboring control law, to first-order (see Section 3.2).

CHAPTER III

DERIVATION OF NEIGHBORING OPTIMAL FEEDBACK CONTROL LAW

The neighboring optimal feedback control law is determined by solving Optimization Problem II with an initial state x_o, neighboring the nominal path. The nominal path and control law are determined by solving Optimization Problem I with an initial state $\bar{x}_o$. Since it is assumed that x_o is a neighboring state of $\bar{x}_o$,* Optimization Problem II may be solved by expanding the performance index, Eq. 2.10, about the nominal path, and then determining the neighboring control law in terms of deviations in the nominal control law. It will be seen that, since the nominal path is optimal, the neighboring and nominal control laws are identical to first-order. In the analysis below, therefore, Eq. 2.10 is expanded to second-order, about the nominal path, and the second-order terms are then minimized with respect to the control parameters. This gives an approximate solution to Optimization Problem II which becomes exact as deviations in the neighboring path, away from the nominal path, approach zero.

The final time, $\bar{t}_f$, the final control vector,** $\bar{u}(\bar{t}_f^-)$, $\bar{N}$ switch times at which control discontinuities occur, and the associated control level changes, completely define the nominal control

---

* It is implicitly assumed that if x_o is in the neighborhood of $\bar{x}_o$, then each state $x(t)$, $t \in [t_o, t_f]$, is in the neighborhood of some state $\bar{x}(\bar{t}), \bar{t} \in [\bar{t}_o, \bar{t}_f]$.

** $\bar{u}(\bar{t}_i^{\mp})$ is, by definition, the value of the control vector at time $\bar{t} = \bar{t}_i \mp \epsilon$, where ϵ is a positive constant. This notation is used throughout the remainder of this work for quantities which are discontinuous at time $\bar{t}_i$.

history.* It is assumed that the number of switch times along the nominal path, denoted by $\bar{N}$, is identical to the number of switch times along the neighboring path. Thus, the final-time deviation away from $\bar{t}_f$, and the deviations in the $\bar{N}$ switch times away from their nominal values, are the control parameters which define the neighboring control law. Determining the optimal values of these deviations is the objective of this chapter.

3.1 Determination of Optimal Nominal Path

The nominal path and control law are determined by solving Optimization Problem I. It is assumed, for the present, that the terminal time is free. Problems with fixed terminal time are discussed at the end of this chapter.

The variational Hamiltonian for the system of Eq. 2.8 is defined to be

$$H[\bar{\lambda}(\bar{t}),\bar{x}(\bar{t}),\bar{u}(\bar{t})] \equiv \bar{\lambda}^T(\bar{t}) f[\bar{x}(\bar{t}),\bar{u}(\bar{t})] , \tag{3.1}$$

where $\bar{\lambda}(\bar{t})$ is the adjoint vector for the system. Pontryagin's "Minimum Principle" [14] gives a set of necessary conditions for $\bar{J}$ (Eq. 2.7) to have at least a local minimum. These necessary conditions for optimality of $\bar{u}(\bar{t})$ are stated as follows:

$$\dot{\bar{\lambda}}^T(\bar{t}) = -H_x[\bar{\lambda}(\bar{t}),\bar{x}(\bar{t}),\bar{u}(\bar{t})], \bar{t} \epsilon [\bar{t}_o, \bar{t}_f] \tag{3.2}$$

$$\bar{\lambda}^T(\bar{t}_f) = F_x[\bar{x}(\bar{t}_f)] + \nu^T \Psi_x[\bar{x}(\bar{t}_f)] \tag{3.3}$$

---

* The choice of specifying $\bar{u}(\bar{t}_f^-)$ instead of the seemingly more logical quantity, $\bar{u}(\bar{t}_o+)$, will be justified in Chapter IV.

$$\bar{\lambda}^T(\bar{t}_f) f[\bar{x}(\bar{t}_f), \bar{u}(\bar{t}_f)] = 0 \tag{3.4}$$

$$\bar{u}_{op}(\bar{t}) = \underset{\bar{u}(\bar{t})}{\text{Arg Min}} \; H[\bar{\lambda}(\bar{t}), \bar{x}(\bar{t}), \bar{u}(\bar{t})] \;, \; \bar{t} \epsilon [\bar{t}_o, \bar{t}_f] \tag{3.5}$$

Eq. (3.2)-(3.5), along with the dynamical equations (Eq. 2.8) and the terminal constraints (Eq. 2.4), are a mathematically consistent set of relationships that will yield an optimal control law, $\bar{u}_{op}(\bar{t})$, which will locally minimize $\bar{J}$. Eq. 3.4 is the transversality condition and need be satisfied only when the terminal time is free. Eq. 3.2 and Eq. 3.3 define $\bar{\lambda}(\bar{t})$, $\bar{t} \epsilon [\bar{t}_o, \bar{t}_f]$, and are the adjoint equations for the system of Eq. 2.8. The assumption that no singular arcs occur in the solution of this problem implies that the operation indicated in Eq. 3.5 can be performed to yield a well defined, discontinuous optimal control law.

Several techniques are described in the literature to solve this two-point boundary value problem. The solution takes the form of a state history, $\bar{x}(\bar{t}), \bar{t} \epsilon [\bar{t}_o, \bar{t}_f]$, and a control history. The control history is described by a set of $\bar{N}$ switch times, associated step changes in the magnitude of the components of the control function, the final control vector, and the final time. It is assumed that only one component of the control vector undergoes a step change at a given switch time.* The i^{th}-switch time, associated with a step change in $\bar{u}_j(\bar{t})$, is denoted by $\bar{t}_{ij}$. The associated step change in $\bar{u}_j(\bar{t})$

---

* It is highly unlikely that the numerical solution of the two-point boundary value problem will result in two control-vector components switching at exactly the same time.

is defined to be

$$\Delta_i \bar{u}_j \equiv \bar{u}_j(\bar{t}_{ij} -) - \bar{u}_j(\bar{t}_{ij} +), \quad i = 1,\cdots,\bar{N}; \quad j \in [1,\cdots,m] \ . \tag{3.6}$$

The $\bar{N}$ switch times are ordered as follows:

$$\bar{t}_o < \bar{t}_{\bar{N}j} < \bar{t}_{(\bar{N}-1)j} < \cdots < \bar{t}_{1j} < \bar{t}_f, \quad j \in [1,\cdots,m] \ . \tag{3.7}$$

Hence, the first subscript of $\bar{t}_{ij}$ indicates the number of remaining discontinuities in the control function in the time interval $[\bar{t}_{ij},\bar{t}_f)$. The second subscript indicates the component of the control function which is discontinuous at time $\bar{t}_{ij}$. An example control history is illustrated in Fig. 3.1 in order to further clarify the notation introduced in Eq. 3.6 and Eq. 3.7.

When specifying the sequence of nominal switch times by $\bar{t}_{ij}$, $i = 1, \cdots, \bar{N}$; $j \in [1,\cdots,m]$, it is implied that j assumes a sequence of values which defines the order in which the components of the nominal control function undergo step changes. This same sequence, determined by the chosen nominal path, also defines the sequence of values which j assumes when specifying the neighboring switch times and the switch-time perturbations (see Section 3.2).

It is assumed, in the remainder of this chapter, that Optimization Problem I has been solved. The following quantities are therefore considered to be prescribed: $\bar{t}_{ij}$, $i = 1,\cdots,\bar{N}$; $j \in [1,\cdots,m]$; $\Delta_i \bar{u}_j$, $i = 1,\cdots,\bar{N}$; $j \in [1,\cdots,m]$; $\bar{t}_f$; $\bar{u}(\bar{t}_f-)$; $\bar{x}(\bar{t}), \bar{t} \in [\bar{t}_o,\bar{t}_f]$; ν .

3.2 Expansion of Performance Index About the Nominal Path

Define the perturbation, $\delta\alpha(t)$, of a vector $\alpha(t)$ to be

$$\delta\alpha(t) \equiv \alpha(t) - \bar{\alpha}(\bar{t}) \ , \tag{3.8}$$

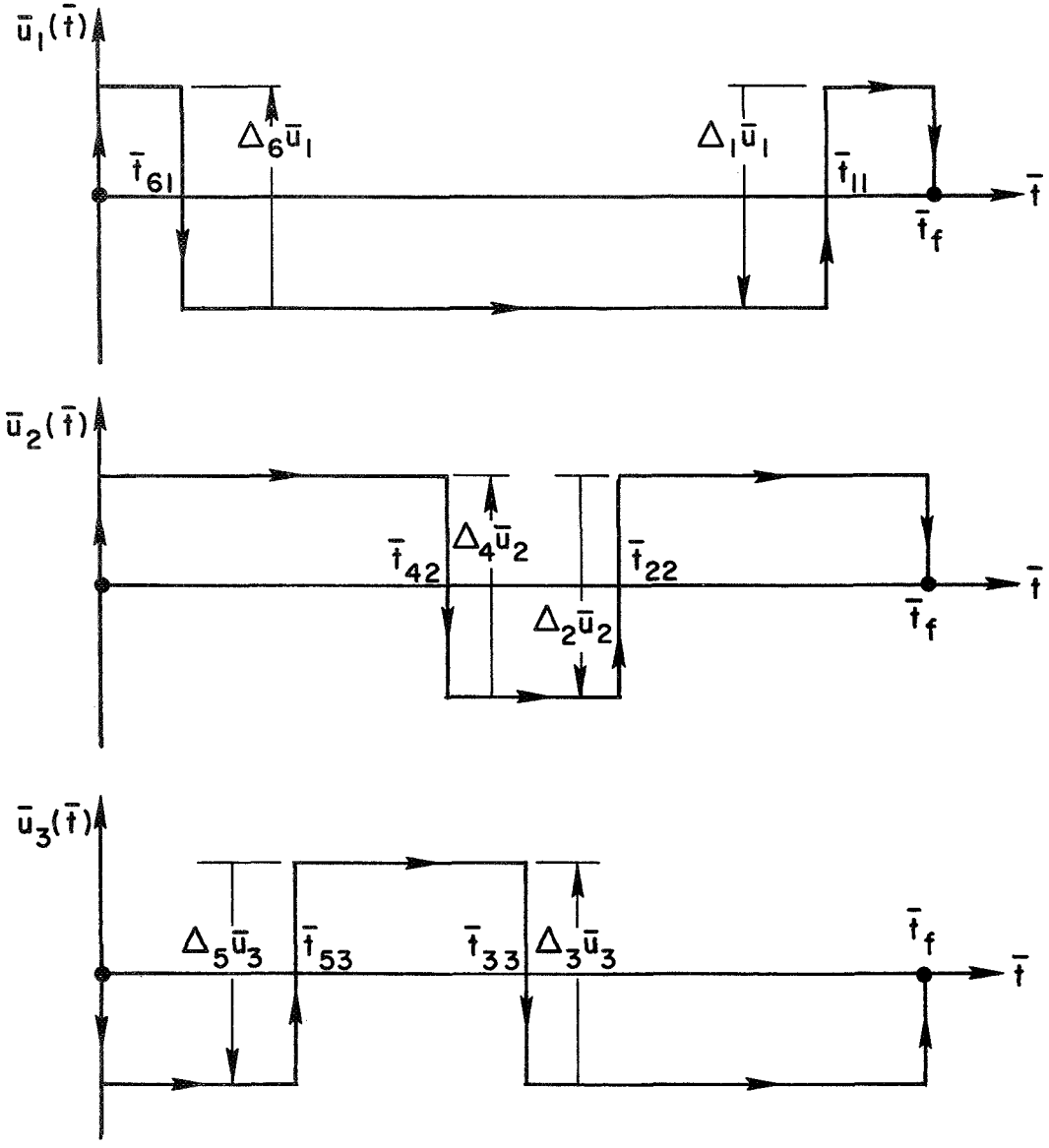

Figure 3.1. An Example Control History Which Demonstrates the Use of the Notation Introduced in Eq. 3.6 and Eq. 3.7.

and define the step change, $\Delta_i\alpha$,* of a discontinuous vector α (t) at time t_{ij} , to be

$$\Delta_i\alpha \equiv \alpha(t_{ij} -) - \alpha(t_{ij} +) \ . \tag{3.9}$$

This notation will be used extensively in the following theory.

The control parameters to be determined are the final-time perturbation,

$$\delta t_f \equiv t_f - \bar{t}_f \ , \tag{3.10}$$

and the switch-time perturbations,

$$\delta t_{ij} \equiv t_{ij} - \bar{t}_{ij} \ , \ i = 1,\cdots,\bar{N}; \ j\epsilon[1,\cdots,m] \ . \tag{3.11}$$

These perturbations are assumed to be positive in the following analysis. The results obtained below, however, are invariant to the sign of the control perturbations. This is true since all state and control perturbations are assumed to be infinitesimal. Furthermore, this assumption and Eq. 3.7 imply that the neighboring switch times satisfy the following inequalities:

$$t_o < t_{\bar{N}j} < t_{(\bar{N}-1)j} < \cdots < t_{2j} < t_{1j} < t_f \ , \ j\epsilon[1,\cdots,m] \ . \tag{3.12}$$

Eq. 3.12 is utilized, below, in the derivation of the neighboring optimal control law.**

---

* This notation has already been used in Eq. 3.6 for a scalar.

** It should be kept in mind that the mathematical developments in this chapter are, strictly speaking, valid only when the perturbations are infinitesimal. When the results of this chapter are applied to problems with finite perturbations, some of the relationships used to calculate the optimal control law, valid for infinitesimal perturbations, are no longer satisfied. In particular, allowance is made, in Chapter IV, for a possible reordering of the neighboring switch times (i.e. allowance is made for possible non-satisfaction of Eq. 3.12).

In this section, the performance index will be expanded to second-order in the initial-state, the final-time, and the switch-time perturbations. Writing J (Eq. 2.10) in terms of t_f and δt_f, and then expanding to second-order in $\delta x(\bar{t}_f + \delta t_f)$, the performance index may be written

$$J = F[\bar{x}(\bar{t}_f)] + \left[F_x[\bar{x}(\bar{t}_f)] + \nu^T \Psi_x[\bar{x}(\bar{t}_f)]\right] \delta x(\bar{t}_f + \delta t_f)$$
$$+ \tfrac{1}{2} \delta x^T(\bar{t}_f + \delta t_f)\Big[F_{xx}[\bar{x}(\bar{t}_f)] + K\Psi_x^T[\bar{x}(\bar{t}_f)]\, W\Psi_x[\bar{x}(\bar{t}_f)] \qquad (3.13)$$
$$+ (\nu^T \Psi[\bar{x}(\bar{t}_f)])_{xx}\Big] \delta x(\bar{t}_f + \delta t_f)$$

where the fact that $\Psi[\bar{x}(\bar{t}_f)] = 0$ has been utilized. Define the (n x n) symmetric matrix $\bar{P}$ as follows:*

$$\bar{P} \equiv F_{xx}[\bar{x}(\bar{t}_f)] + K\Psi_x^T[\bar{x}(\bar{t}_f)]\, W\Psi_x[\bar{x}(\bar{t}_f)] + (\nu^T \Psi[\bar{x}(\bar{t}_f)])_{xx} . \qquad (3.14)$$

Substituting Eq. 3.14 and Eq. 3.3 into Eq. 3.13 then gives

$$J = F[\bar{x}(\bar{t}_f)] + \bar{\lambda}^T(\bar{t}_f)\delta x(\bar{t}_f + \delta t_f) + \tfrac{1}{2}\delta x^T(\bar{t}_f + \delta t_f)\bar{P}\delta x(\bar{t}_f + \delta t_f). \qquad (3.15)$$

Since $F[\bar{x}(\bar{t}_f)]$ is independent of the control parameters, it is omitted in the expression for J in the remainder of this discussion.

The expansion of $\delta x(\bar{t}_f + \delta t_f)$ to second-order in δt_f and $\delta x(\bar{t}_f)$ is written**

$$\delta x(\bar{t}_f + \delta t_f) = \bar{f}(\bar{t}_f)\delta t_f + [I_n + \bar{f}_x(\bar{t}_f)\delta t_f]\delta x(\bar{t}_f) + \tfrac{1}{2}\dot{\bar{f}}(\bar{t}_f)\delta t_f^2 , \qquad (3.16)$$

---

* The last term in Eq. 3.14 was not obtained by McNeal (see [6], Eq. 3.5).

** In the remainder of this paper, a function, $\alpha[\cdot,\cdot]$, of the nominal state and control vectors, is written $\bar{\alpha}(\bar{t})$, i.e. $f[\bar{x}(\bar{t}), \bar{u}(\bar{t})] \equiv \bar{f}(\bar{t})$.

where I_n is the n^{th}-order identity matrix. The fact that $\delta u(t_f) = 0$ was used in writing Eq. 3.16.* This fact again follows from Eq. 3.7 and the assumption that the switch-time perturbations are infinitesimal. Now, $\delta x(\bar{t}_f)$ may be written

$$\delta x(\bar{t}_f) \equiv \delta x_I(\bar{t}_f) + \delta x_{II}(\bar{t}_f) + \cdots \tag{3.17}$$

where $\delta x_I(\bar{t}_f)$ gives the first-order terms in the expansion of $\delta x(\bar{t}_f)$, and $\delta x_{II}(\bar{t}_f)$ gives the second-order terms. The dynamical equations which specify $\delta x_I(\bar{t})$ and $\delta x_{II}(\bar{t})$, $\bar{t}_o \leq \bar{t} \leq \bar{t}_f$, are given by Eq. A.1 and Eq. A.6 in Appendix A, respectively. Substituting $\delta x(\bar{t}_f)$, from Eq. 3.17, into Eq. 3.16, and then substituting this result into Eq. 3.15, J may be written, after rearranging terms,

$$\begin{aligned} J = {} & [\bar{\lambda}^T(\bar{t}_f) + \bar{\lambda}^T(\bar{t}_f)\bar{f}_x(\bar{t}_f)\delta t_f + \bar{f}^T(\bar{t}_f)\bar{P}\delta t_f]\delta x_I(\bar{t}_f) \\ & + \tfrac{1}{2}\delta x_I^T(\bar{t}_f)\bar{P}\delta x_I(\bar{t}_f) + \tfrac{1}{2}[\bar{f}^T(\bar{t}_f)\bar{P}\bar{f}(\bar{t}_f) + \bar{\lambda}^T(\bar{t}_f)\dot{\bar{f}}(\bar{t}_f)]\delta t_f^2 \\ & + \bar{\lambda}^T(\bar{t}_f)\delta x_{II}(\bar{t}_f) \ , \end{aligned} \tag{3.18}$$

where terms higher than second-order have been omitted, and Eq. 3.4 was utilized to eliminate the $\bar{\lambda}^T(\bar{t}_f)\bar{f}(\bar{t}_f)$ term.

The perturbation, $\delta x_I(\bar{t})$, is the first-order solution of the first-order perturbed dynamical equations. These equations, between nominal switch times, are written

$$\dot{\delta x}(\bar{t}) = \bar{f}_x(\bar{t})\delta x(\bar{t}) + \bar{f}_u(\bar{t})\delta u(\bar{t}); \ \delta x(\bar{t}_o) = \delta x_o \ . \tag{3.19}$$

---

* From Eq. 3.8, $\delta u(t_f) = 0$ implies that $\bar{u}(\bar{t}_f) = u(t_f)$. Hence, it is necessary to choose a nominal path such that $\bar{u}(\bar{t}_f) = u(t_f)$ in order to mechanize the results of this chapter (see Section 4.3).

To solve Eq. 3.19 for $\delta x(\bar{t})$, the fact that $\bar{t}_{ij} + \delta t_{ij} < \bar{t}_{(i-1)j}$, $i = 2,\cdots,\bar{N}$; $j \in [1,\cdots,m]$, and $\bar{t}_{1j} + \delta t_{1j} < \bar{t}_f$, $j \in [1,\cdots,m]$, is utilized. These inequalities are again a consequence of Eq. 3.7 and the assumption that the switch-time perturbations are infinitesimal. From Appendix A, Eq. A.5, the first-order solution of Eq. 3.19 for $\delta x(\bar{t}_f)$ is*

$$\delta x_I(\bar{t}_f) = \Phi(\bar{t}_f,\bar{t}_o)\,\delta x_o + \sum_{i=1}^{\bar{N}} \Phi(\bar{t}_f,\bar{t}_{ij})\,\Delta_i \bar{f}\,\delta t_{ij} \tag{3.20}$$

where $\Phi(\cdot,\cdot)$ is the state transition matrix for Eq. 3.19.

Note that $\Phi(\bar{t}_f,\bar{t})$ satisfies the adjoint equations for the system of Eq. 3.19:

$$\dot{\Phi}(\bar{t}_f,\bar{t}) = -\Phi(\bar{t}_f,\bar{t})\,\bar{f}_x(\bar{t}). \tag{3.21}$$

Also, recall from Eq. 3.2, that $\bar{\lambda}(\bar{t})$ satisfies

$$\dot{\bar{\lambda}}^T(\bar{t}) = -\bar{\lambda}^T(\bar{t})\bar{f}_x(\bar{t}). \tag{3.22}$$

Thus, $\bar{\lambda}^T(\bar{t})$ may be written

$$\bar{\lambda}^T(\bar{t}) = \bar{\lambda}^T(\bar{t}_f)\Phi(\bar{t}_f,\bar{t}). \tag{3.23}$$

Using Eq. 3.23, Eq. 3.20, and the definition of the Hamiltonian (Eq. 3.1), one obtains the following results:

$$\bar{\lambda}^T(\bar{t}_f)\delta x_I(\bar{t}_f) = \bar{\lambda}^T(\bar{t}_o)\delta x_o + \sum_{i=1}^{\bar{N}} \Delta_i \bar{H}\delta t_{ij} = \bar{\lambda}^T(\bar{t}_o)\delta x_o\ . \tag{3.24}$$

---

* It is hereafter understood that j, in the sequence $\bar{t}_{ij}$, $i = 1,\cdots,\bar{N}$, assumes a sequence of values defined by the nominal path, and hence the notation $j \in [1,\cdots,m]$ will be omitted.

The last equality is valid since the nominal path is optimal and hence $\Delta_i \bar{H} = 0$, $i = 1,\cdots,\bar{N}$. Thus $\bar{\lambda}^T(\bar{t}_f)\delta x_I(\bar{t}_f)$ may be omitted in Eq. 3.18 since this term is independent of the control parameters.

Now, using Eq. 3.1 in Eq. 3.18, and using the fact that

$$\dot{\bar{f}}(\bar{t}_f) = \bar{f}_x(\bar{t}_f)\ \bar{f}(\bar{t}_f)\ , \tag{3.25}$$

J is rewritten as

$$J = [\bar{H}_x(\bar{t}_f) + \bar{f}^T(\bar{t}_f)\bar{P}]\ \delta x_I(\bar{t}_f)\delta t_f + \tfrac{1}{2}\delta x_I^T(\bar{t}_f)\bar{P}\delta x_I(\bar{t}_f) \tag{3.26}$$

$$+ \tfrac{1}{2}[\bar{f}^T(\bar{t}_f)\bar{P}\bar{f}(\bar{t}_f) + \bar{H}_x(\bar{t}_f)\bar{f}(\bar{t}_f)]\delta t_f^2 + \bar{\lambda}^T(\bar{t}_f)\delta x_{II}(\bar{t}_f)\ .$$

From Appendix A, Eq. A.18, the i^{th}-component of $\delta x_{II}(\bar{t}_f)$ is given by

$$\delta x_{II}^i(\bar{t}_f) = \tfrac{1}{2}\int_{\bar{t}_o}^{\bar{t}_f}\sum_{j=1}^{n}\Phi_{ij}(\bar{t}_f,\tau)\delta x_I^T(\tau)\bar{f}_{xx}^j(\tau)\delta x_I(\tau)d\tau \tag{3.27}$$

$$+\left[\sum_{k=1}^{\bar{N}}\left\{\Phi(\bar{t}_f,\bar{t}_{kj})[\Delta_k\bar{f}_x\delta x_I(\bar{t}_{kj})\delta t_{kj} + \tfrac{1}{2}\left(-\bar{f}_x(\bar{t}_{kj}^+)\Delta_k\bar{f} + \Delta_k\bar{f}_x\bar{f}(\bar{t}_{kj}^-)\right)\delta t_{kj}^2]\right\}\right]_i ,$$

where, from Eq. A.4 in Appendix A, $\delta x_I(\bar{t}_{kj})$ is given by

$$\delta x_I(\bar{t}_{kj}) = \Phi\ (\bar{t}_{kj},\bar{t}_o)\delta x_o + \sum_{i=k+1}^{\bar{N}}\Phi(\bar{t}_{kj},\bar{t}_{ij})\Delta_i\bar{f}\delta t_{ij},\ k=1,\cdots,\bar{N}\ . \tag{3.28}$$

It follows from Eq. 3.28 that

$$\delta x_I(\bar{t}) = \Phi(\bar{t},\bar{t}_o)\delta x_o + \sum_{i=k}^{\bar{N}} \Phi(\bar{t},\bar{t}_{ij})\Delta_i \bar{f}\delta t_{ij},$$

$$\bar{t}_{kj} < \bar{t} \leq \bar{t}_{(k-1)j},\ k = 2,\cdots,\bar{N},$$

$$\bar{t}_{kj} < \bar{t} \leq \bar{t}_f \quad ,\quad k = 1 \ , \tag{3.29}$$

$$\delta x_I(\bar{t}) = \Phi(\bar{t},\bar{t}_o)\delta x_o \ ,\ \bar{t}_o \leq \bar{t} \leq \bar{t}_{\bar{N}j} \ .$$

Finally, substituting Eq. 3.27 into Eq. 3.26, and making use of Eq. 3.23 and Eq. 3.1, the performance index is written

$$\begin{aligned} J = {} & [\bar{H}_x(\bar{t}_f) + \bar{f}^T(\bar{t}_f)\bar{P}]\delta x_I(\bar{t}_f)\delta t_f + \tfrac{1}{2}\,\delta x_I^T(\bar{t}_f)\bar{P}\delta x_I(\bar{t}_f) \\ & + \tfrac{1}{2}\,[\bar{f}^T(\bar{t}_f)\bar{P}\bar{f}(\bar{t}_f) + \bar{H}_x(\bar{t}_f)\bar{f}(\bar{t}_f)]\delta t_f^2 \\ & + \tfrac{1}{2}\int_{\bar{t}_o}^{\bar{t}_f} \delta x_I^T(\tau)\bar{H}_{xx}(\tau)\delta x_I(\tau)d\tau + \sum_{k=1}^{\bar{N}} [\Delta_k \bar{H}_x \delta x_I(\bar{t}_{kj})\delta t_{kj} \\ & + \tfrac{1}{2}\,(-\bar{H}_x(\bar{t}_{kj}^+)\Delta_k \bar{f} + \Delta_k \bar{H}_x \bar{f}(\bar{t}_{kj}^-))\,\delta t_{kj}^2\ ] \ . \end{aligned} \tag{3.30}$$

The integral term in Eq. 3.30 is derived in Appendix B, Eq. B.1.

In the following sections, J, as it appears in Eq. 3.30, will be minimized by choosing optimal values of δt_f and δt_{ij}, $i = 1,\cdots,\bar{N}$. It should be noted that each term in Eq. 3.30 is of second-order in the state, the switch-time, and the final-time perturbations. This means that, to first-order, the neighboring optimal feedback control law is identical to the nominal control law. This follows from the fact that the nominal path is optimal, and the fact

that the first-order necessary conditions of optimality for Optimization Problem I are identical to those for Optimization Problem II.

3.3 Calculation of Final-Time and Switch-Time Perturbations

The performance index, J, as it is expressed in Eq. 3.30, is a function of δt_f, δt_{kj}, $k = 1,\cdots,\bar{N}$, and prescribed quantities defined by the nominal path. When $\delta x_I(\bar{t}_f)$ (Eq. 3.20), $\delta x_I(\bar{t}_{kj})$, $k = 1,\cdots,\bar{N}$ (Eq. 3.28), and $\delta x_I(\bar{t}), \bar{t} \epsilon [\bar{t}_o, \bar{t}_f]$ (Eq. 3.29), are substituted into Eq. 3.30, the functional dependence of J upon the control parameters is explicit. The control parameters are constraint-free. Thus, Optimization Problem II is reduced to the simplest form of a parameter optimization problem.

The control parameters are, therefore, determined by solving a set of $(\bar{N} + 1)$ algebraic equations obtained by differentiating J with respect to δt_f, δt_{kj}, $k = 1,\cdots,\bar{N}$, and equating to zero. The resulting control law necessarily gives J a stationary value. To insure that this stationary value is a minimum, the matrix of second partial derivatives with respect to $\delta t_f, \delta t_{kj}$, $k = 1,\cdots,\bar{N}$, must be positive-definite. Since the nominal control law is minimizing, this sufficiency calculation will in general not be necessary. It is conceivable, however, that a neighboring control law could give J a local maximum value. This problem is not considered in this study, and thus the sufficiency calculation is omitted.

From Eq. 3.20, Eq. 3.28, and Eq. 3.29, it is seen that $\delta x_I(\bar{t}_f)$, $\delta x_I(\bar{t}_{kj})$, $k = 1,\cdots,\bar{N}$, and $\delta x_I(\bar{t}), \bar{t} \epsilon [\bar{t}_o, \bar{t}_f]$, are independent of δt_f. Differentiating J with respect to δt_f and equating to

zero thus gives

$$\frac{\partial J}{\partial \delta t_f} = [\bar{H}_x(\bar{t}_f) + \bar{f}^T(\bar{t}_f)\bar{P}]\delta x_I(\bar{t}_f) + [\bar{f}^T(\bar{t}_f)\bar{P}\bar{f}(\bar{t}_f) + \bar{H}_x(\bar{t}_f)\bar{f}(\bar{t}_f)]\delta t_f = 0 \ . \tag{3.31}$$

Define the (1 x n) vector $\bar{M}$ to be

$$\bar{M} \equiv [\bar{f}^T(\bar{t}_f)\bar{P}\bar{f}(\bar{t}_f) + \bar{H}_x(\bar{t}_f)\bar{f}(\bar{t}_f)]^{-1} [\bar{H}_x(\bar{t}_f) + \bar{f}^T(\bar{t}_f)\bar{P}] \ . \tag{3.32}$$

Then, solving Eq. 3.31 for δt_f gives

$$\delta t_f = -\bar{M}\delta x_I(\bar{t}_f) \ . \tag{3.33}$$

Now form $\bar{N}$ equations, to determine δt_{kj}, $k = 1,\cdots,\bar{N}$, by equating to zero the derivatives of J with respect to δt_{kj}, $k = 1,\cdots,\bar{N}$:

$$\frac{\partial J}{\partial \delta t_{kj}} = [\bar{H}_x(\bar{t}_f)\delta t_f + \bar{f}^T(\bar{t}_f)\bar{P}\delta t_f + \delta x_I^T(\bar{t}_f)\bar{P}]\left[\frac{\partial \delta x_I(\bar{t}_f)}{\partial \delta t_{kj}}\right] + \frac{\partial}{\partial \delta t_{kj}}\left[\frac{1}{2}\int_{\bar{t}_o}^{\bar{t}_f} \delta x_I^T(\tau)\bar{H}_{xx}(\tau)\delta x_I(\tau)d\tau\right]$$
$$+ \Delta_k \bar{H}_x \delta x_I(\bar{t}_{kj}) + (-\bar{H}_x(\bar{t}_{kj}^+)\Delta_k \bar{f} + \Delta_k \bar{H}_x \bar{f}(\bar{t}_{kj}^-))\delta t_{kj}$$
$$+ \sum_{\ell=1}^{\bar{N}} \Delta_\ell \bar{H}_x \left[\frac{\partial \delta x_I(\bar{t}_{\ell j})}{\partial \delta t_{kj}}\right] \delta t_{\ell j} = 0, \ k = 1,\cdots,\bar{N}. \tag{3.34}$$

Differentiation of Eq. 3.20 with respect to δt_{kj}, $k = 1,\cdots,\bar{N}$, gives

$$\frac{\partial \delta x_I(\bar{t}_f)}{\partial \delta t_{kj}} = \Phi(\bar{t}_f, \bar{t}_{kj})\Delta_k \bar{f}, \ k = 1,\cdots,\bar{N}, \tag{3.35}$$

and differentiation of Eq. 3.28 with respect to δt_{kj}, $k=1,\cdots,\bar{N}$, gives

$$\left.\begin{aligned} \frac{\partial \delta x_I(\bar{t}_{ij})}{\partial \delta t_{kj}} &= \Phi(\bar{t}_{ij},\bar{t}_{kj})\Delta_k\bar{f}, \quad k > i \\ \frac{\partial \delta x_I(\bar{t}_{ij})}{\partial \delta t_{kj}} &= 0 \qquad\qquad , \quad k \le i \end{aligned}\right\} k=1,\cdots,\bar{N};\ i=1,\cdots,\bar{N}. \tag{3.36}$$

The second term in Eq. 3.34 is evaluated in Appendix B and given by Eq. B.6. Now substitute Eq. 3.33, Eq. 3.35, Eq. 3.36, and Eq. B.6 into Eq. 3.34, and rearrange terms:

$$\begin{aligned} &[\Phi(\bar{t}_f,\bar{t}_{kj})\Delta_k\bar{f}]^T[\bar{P}-\bar{H}_x^T(\bar{t}_f)\bar{M}-\bar{P}\bar{f}(\bar{t}_f)\bar{M}]\delta x_I(\bar{t}_f) \\ &+\sum_{\ell=2}^{k}\left\{\int_{\bar{t}_{\ell j}}^{\bar{t}_{(\ell-1)j}}[\Phi(\tau,\bar{t}_{kj})\Delta_k\bar{f}]^T\bar{H}_{xx}(\tau)[\Phi(\tau,\bar{t}_o)\delta x_o\right. \\ &\left.+\sum_{i=\ell}^{\bar{N}}\Phi(\tau,\bar{t}_{ij})\Delta_i\bar{f}\delta t_{ij}]d\tau\right\}+\int_{\bar{t}_{1j}}^{\bar{t}_f}[\Phi(\tau,\bar{t}_{kj})\Delta_k\bar{f}]^T\bar{H}_{xx}(\tau)[\Phi(\tau,\bar{t}_o)\delta x_o \\ &+\sum_{i=1}^{\bar{N}}\Phi(\tau,\bar{t}_{ij})\Delta_i\bar{f}\delta t_{ij}]d\tau \\ &+\Delta_k\bar{H}_x\delta x_I(\bar{t}_{kj})+(-\bar{H}_x(\bar{t}_{kj}^+)\Delta_k\bar{f}+\Delta_k\bar{H}_x\bar{f}(\bar{t}_{kj}^-))\delta t_{kj} \\ &+\sum_{\ell=1}^{k-1}\Delta_\ell\bar{H}_x\Phi(\bar{t}_{\ell j},\bar{t}_{kj})\Delta_k\bar{f}\delta t_{\ell j}=0,\quad k=1,\cdots,\bar{N}. \end{aligned} \tag{3.37}$$

Since δt_f has been eliminated, Eq. 3.37 represents $\bar{N}$ linear, coupled equations for the $\bar{N}$ control parameters δt_{kj}, $k=1,\cdots,\bar{N}$. To solve these $\bar{N}$ equations for the control parameters, they will first be written in matrix form. To accomplish this, the following notation is introduced:

$$\delta t_s \equiv \begin{bmatrix} \delta t_{1j} \\ \cdot \\ \cdot \\ \cdot \\ \delta t_{Nj} \end{bmatrix} \tag{3.38}$$

$$\bar{U} \equiv \bar{P} - \bar{H}_x^T(\bar{t}_f)\bar{M} - \bar{P}\bar{f}(\bar{t}_f)\bar{M} \tag{3.39}$$

$$\bar{T}(\bar{t}_{ij},\bar{t}_{\ell j}) \equiv \Phi(\bar{t}_{ij},\bar{t}_{\ell j})\Delta_\ell \bar{f} \tag{3.40}$$

$$\bar{R}(\bar{t}_{ij},\bar{t}_{\ell j}) \equiv [\bar{T}(\bar{t}_{ij},\bar{t}_{1j}) \cdots \bar{T}(\bar{t}_{ij},\bar{t}_{\ell j})] \tag{3.41}$$

$$\bar{\omega}(\bar{t}_{ij},\bar{t}_{\ell j}) \equiv \Delta_i \bar{H}_x \bar{T}(\bar{t}_{ij},\bar{t}_{\ell j}) \tag{3.42}$$

$$\bar{h}(\bar{t}_{ij}) \equiv -\bar{H}_x(\bar{t}_{ij}^+)\Delta_i \bar{f} + \Delta_i \bar{H}_x \bar{f}(\bar{t}_{ij}^-) \tag{3.43}$$

$$\bar{E}(\bar{t}_{ij},\bar{t}_{\ell j}) \equiv \int_{\bar{t}_{ij}}^{\bar{t}_{(i-1)j}} \bar{T}^T(\tau,\bar{t}_{\ell j})\bar{H}_{xx}(\tau)\Phi(\tau,\bar{t}_f)d\tau, \quad i=2,\cdots,\bar{N} \tag{3.44}$$

$$\bar{E}(\bar{t}_{1j},\bar{t}_{\ell j}) \equiv \int_{\bar{t}_{1j}}^{\bar{t}_f} \bar{T}^T(\tau,\bar{t}_{\ell j})\bar{H}_{xx}(\tau)\Phi(\tau,\bar{t}_f)d\tau \tag{3.45}$$

Using this notation, $\delta x_I(\bar{t}_f)$ is written (see Eq. 3.20)

$$\delta x_I(\bar{t}_f) = \Phi(\bar{t}_f,\bar{t}_o)\delta x_o + \bar{R}(\bar{t}_f,\bar{t}_{Nj})\delta t_s \tag{3.46}$$

and $\Delta_k \bar{H}_x \delta x_I(\bar{t}_{kj})$ is written

$$\Delta_k \bar{H}_x \delta x_I(\bar{t}_{kj}) = \Delta_k \bar{H}_x \Phi(\bar{t}_{kj},\bar{t}_o)\delta x_o + \sum_{i=k+1}^{\bar{N}} \bar{\omega}(\bar{t}_{kj},\bar{t}_{ij})\delta t_{ij}. \tag{3.47}$$

Substituting Eq. 3.46 and Eq. 3.47 into Eq. 3.37, using the above notation, using the properties of the state transition matrix, and rearranging terms, then gives

$$[\bar{T}^T(\bar{t}_f,\bar{t}_{kj})\bar{U} + \Delta_k\bar{H}_x\Phi(\bar{t}_{kj},\bar{t}_f) + \sum_{i=1}^{k}\bar{E}(\bar{t}_{ij},\bar{t}_{kj})]\Phi(\bar{t}_f,\bar{t}_o)\delta x_o$$

$$+ \sum_{\ell=1}^{k}\left\{\bar{E}(\bar{t}_{\ell j},\bar{t}_{kj})\sum_{i=\ell}^{\bar{N}}\bar{T}(\bar{t}_f,\bar{t}_{ij})\delta t_{ij}\right\} + \bar{T}^T(\bar{t}_f,\bar{t}_{kj})\bar{U}\bar{R}(\bar{t}_f,\bar{t}_{\bar{N}j})\delta t_s$$

$$+ \bar{h}(\bar{t}_{kj})\delta t_{kj} + \sum_{i=k+1}^{\bar{N}}\bar{\omega}(\bar{t}_{kj},\bar{t}_{ij})\delta t_{ij} + \sum_{i=1}^{k-1}\bar{\omega}(\bar{t}_{ij},\bar{t}_{kj})\delta t_{ij} = 0,$$

$$k=1,\cdots,\bar{N}. \qquad (3.48)$$

Finally, the following notation is introduced in order to write Eq. 3.48 in matrix form:

$$\bar{X} \equiv \begin{bmatrix} \bar{h}(\bar{t}_{ij}) & \bar{\omega}(\bar{t}_{1j},\bar{t}_{2j}) & \cdots & \bar{\omega}(\bar{t}_{1j},\bar{t}_{\bar{N}j}) \\ \bar{\omega}(\bar{t}_{1j},\bar{t}_{2j}) & \bar{h}(\bar{t}_{2j}) & \cdots & \bar{\omega}(\bar{t}_{2j},\bar{t}_{\bar{N}j}) \\ \vdots & \vdots & & \vdots \\ \bar{\omega}(\bar{t}_{1j},\bar{t}_{\bar{N}j}) & \bar{\omega}(\bar{t}_{2j},\bar{t}_{\bar{N}j}) & \cdots & \bar{h}(\bar{t}_{\bar{N}j}) \end{bmatrix} \qquad (3.49)$$

$$\bar{D} \equiv \begin{bmatrix} \Delta_1\bar{H}_x\Phi(\bar{t}_{1j},\bar{t}_f) \\ \vdots \\ \Delta_{\bar{N}}\bar{H}_x\Phi(\bar{t}_{\bar{N}j},\bar{t}_f) \end{bmatrix} \qquad (3.50)$$

$$\bar{Z} \equiv \begin{bmatrix} \bar{E}(\bar{t}_{1j}, \bar{t}_{1j}) \\ \sum_{\ell=1}^{2} \bar{E}(\bar{t}_{\ell j}, \bar{t}_{2j}) \\ \vdots \\ \sum_{\ell=1}^{\bar{N}} \bar{E}(\bar{t}_{\ell j}, \bar{t}_{\bar{N}j}) \end{bmatrix} \tag{3.51}$$

$$J_{\ell} \equiv \begin{bmatrix} 0 & | & 0 \\ - - & | & - - \\ 0 & | & I_{(\bar{N}-\ell+1)} \end{bmatrix} \begin{matrix} \uparrow \\ \bar{N} \\ \downarrow \end{matrix} \qquad \begin{matrix} \\ \\ \bar{N} \end{matrix} \tag{3.52}$$

$$\bar{Y} \equiv \begin{bmatrix} \bar{E}(\bar{t}_{1j}, \bar{t}_{1j})\bar{R}(\bar{t}_f, \bar{t}_{\bar{N}j})I_{\bar{N}} \\ \sum_{\ell=1}^{2} \bar{E}(\bar{t}_{\ell j}, \bar{t}_{2j})\bar{R}(\bar{t}_f, \bar{t}_{\bar{N}j})J_{\ell} \\ \vdots \\ \sum_{\ell=1}^{\bar{N}} \bar{E}(\bar{t}_{\ell j}, \bar{t}_{\bar{N}j})\bar{R}(\bar{t}_f, \bar{t}_{\bar{N}j})J_{\ell} \end{bmatrix} \tag{3.53}$$

Using the above notation, the $\bar{N}$ equations in Eq. 3.48 may now be written in the following compact form:

$$[\bar{R}^T(\bar{t}_f, \bar{t}_{\bar{N}j})\bar{U}+\bar{D}+\bar{Z}]\Phi(\bar{t}_f, \bar{t}_o)\delta x_o + [\bar{Y}+\bar{R}^T(\bar{t}_f, \bar{t}_{\bar{N}j})\dot{\bar{U}}\bar{R}(\bar{t}_f, \bar{t}_{\bar{N}j}) + \bar{X}]\delta t_s = 0 \ . \tag{3.54}$$

Solving Eq. 3.54 for δt_s gives

$$\delta t_s = -[\bar{Y}+\bar{R}^T(\bar{t}_f, \bar{t}_{\bar{N}j})\dot{\bar{U}}\bar{R}(\bar{t}_f, \bar{t}_{\bar{N}j}) + \bar{X}]^{-1}[\bar{R}^T(\bar{t}_f, \bar{t}_{\bar{N}j})\bar{U}+\bar{D}+\bar{Z}]\Phi(\bar{t}_f, \bar{t}_o)\delta x_o . \tag{3.55}$$

Substituting Eq. 3.46 into Eq. 3.33, δt_f becomes

$$\delta t_f = -\bar{M}\Phi(\bar{t}_f,\bar{t}_o)\delta x_o - \bar{M}\bar{R}(\bar{t}_f,\bar{t}_{\bar{N}j})\delta t_s. \tag{3.56}$$

The above theory applies to free terminal-time problems. When t_f is specified, $\delta t_f \equiv 0$, and hence $\bar{M} \equiv 0$. If $\bar{U}$ is replaced by $\bar{P}$ (see Eq. 3.39), then Eq. 3.55 also gives the switch-time perturbations for fixed terminal-time problems.

When the system dynamics are linear in the state, as well as in the control, then $\bar{E}(\cdot,\cdot) \equiv 0$ since $\bar{H}_{xx}(\bar{t}) \equiv 0$, $\bar{t}\epsilon[\bar{t}_o,\bar{t}_f]$. Thus $\bar{Z} \equiv 0$ and $\bar{Y} \equiv 0$. Also, $\Delta_i\bar{H}_x \equiv 0$, $i=1,\cdots,\bar{N}$, and hence $\bar{D} \equiv 0$ and $\bar{\omega}(\cdot,\cdot) \equiv 0$. For this system, the final-time perturbation is given by Eq. 3.56 and the switch-time perturbations are modified to become:

$$\delta t_s = -[\bar{R}^T(\bar{t}_f,\bar{t}_{\bar{N}j})\bar{U}\bar{R}(\bar{t}_f,\bar{t}_{\bar{N}j})+\bar{V}]^{-1}\,\bar{R}^T(\bar{t}_f,\bar{t}_{\bar{N}j})\bar{U}\Phi(\bar{t}_f,\bar{t}_o)\delta x_o \tag{3.57}$$

where $\bar{V}$ is defined to be

$$\bar{V} \equiv -\begin{bmatrix} \bar{H}_x(\bar{t}_{1j}^+)\Delta_1\bar{f} & & 0 \\ & \ddots & \\ 0 & & \bar{H}_x(\bar{t}_{\bar{N}j}^+)\Delta_{\bar{N}}\bar{f} \end{bmatrix}. \tag{3.58}$$

Note that the coefficients of $\Phi(\bar{t}_f,\bar{t}_o)\delta x_o$ in Eq. 3.55 and Eq. 3.57 are completely defined by the nominal path. They can, therefore, be precalculated, and then applied to any initial state x_o, neighboring $\bar{x}_o$. The neighboring optimal feedback control law for the dynamical system of Eq. 2.1 is derived from the results of this section in the next section. Implementation of this control law is discussed in Chapter IV.

3.4 Neighboring Optimal Feedback Control Law

Denote the number of switch times along the neighboring path by N.* Define the $(N \times n)$ matrix, $\bar{G}_N$, to be

$$\bar{G}_N \equiv [\bar{Y}+\bar{R}^T(\bar{t}_f,\bar{t}_{Nj})\bar{U}\bar{R}(\bar{t}_f,\bar{t}_{Nj})+\bar{X}]^{-1}\cdot[\bar{R}^T(\bar{t}_f,\bar{t}_{Nj})\bar{U}+\bar{D}+\bar{Z}],\ N=1,2,\cdots,\bar{N},$$

$$\bar{G}_N \equiv 0,\ N=0, \tag{3.59}$$

and define the $(1 \times n)$ matrix, $\bar{g}_o$, to be

$$\bar{g}_o \equiv [\bar{M}-\bar{M}\bar{R}(\bar{t}_f,\bar{t}_{Nj})\bar{G}_N],\ N=0,1,\cdots,\bar{N}. \tag{3.60}$$

Then, from Eq. 3.55 with N replacing $\bar{N}$, δt_s is written

$$\delta t_s = -\bar{G}_N\Phi(\bar{t}_f,\bar{t}_o)\delta x_o, \tag{3.61}$$

and, from Eq. 3.56 with N replacing $\bar{N}$, δt_f is written

$$\delta t_f = -\bar{g}_o\Phi(\bar{t}_f,\bar{t}_o)\delta x_o. \tag{3.62}$$

Define the neighboring switch-time vector to be

$$t_s \equiv \begin{bmatrix} t_{1j} - t_o \\ t_{2j} - t_o \\ \vdots \\ t_{Nj} - t_o \end{bmatrix}. \tag{3.63}$$

---

* The total number of switch times along the nominal path is $\bar{N}$. If $N \leq \bar{N}$, then N is interpreted to be the number of remaining switch times along the nominal path, when used, instead of $\bar{N}$, in the calculations of the previous sections. Recall that, in these sections, it was assumed that the number of neighboring switch times is identical to the number of nominal switch times.

Then, using Eq. 3.8, Eq. 3.61, and Eq. 3.62, the open-loop estimates for the switch times and the final time, for the neighboring path, are given by

$$t_s = \bar{t}_s - \bar{G}_N \Phi(\bar{t}_f, \bar{t}_o)[x(t_o) - \bar{x}(\bar{t}_o)], \tag{3.64}$$

$$t_f - t_o = \bar{t}_f - \bar{t}_o - \bar{g}_o \Phi(\bar{t}_f, \bar{t}_o)[x(t_o) - \bar{x}(\bar{t}_o)] \ . \tag{3.65}$$

The closed-loop estimates for the switch times and the final time, for a neighboring path with current state $x(t)$, are obtained from Eq. 3.64 and Eq. 3.65 by replacing t_o with t and $\bar{t}_o$ with $\bar{t}$ *:

$$t_s = \bar{t}_s - \bar{G}_N \Phi(\bar{t}_f, \bar{t})[x(t) - \bar{x}(\bar{t})] \ , \quad t_{(N+1)j} < t \leq t_{Nj} \ , \quad \bar{t}_{(N+1)j} < \bar{t} \leq \bar{t}_{Nj} \ , \tag{3.66}$$

$$t_f - t = \bar{t}_f - \bar{t} - \bar{g}_o \Phi(\bar{t}_f, \bar{t})[x(t) - \bar{x}(\bar{t})] \ , \quad t_{(N+1)j} < t \leq t_{Nj} \ , \quad \bar{t}_{(N+1)j} < \bar{t} \leq \bar{t}_{Nj} \ , \tag{3.67}$$

where t replaces t_o, and $\bar{t}$ replaces $\bar{t}_o$, in the definitions of t_s and $\bar{t}_s$, respectively. The need for distinguishing between real time, t, and nominal time, $\bar{t}$, is apparent in Eq. 3.66 and Eq. 3.67. The determination of $\bar{t}$ is discussed in Chapter IV.

The neighboring optimal feedback control law is stated in terms of Eq. 3.66, Eq. 3.67, and the step changes in the nominal control law (Eq. 3.6):

---

* When $N = \bar{N}$, $\bar{t}_{(N+1)j}$ and $t_{(N+1)j}$ are defined to be $\bar{t}_0$ and t_0, respectively.

Neighboring Optimal Feedback Control Law

Let N be the number of switch times along the neighboring path. When $t = t_{ij}$, $i \in [1,\cdots,N]$, as determined from Eq. 3.66, then $u_j(t) = u_j(t_{ij}^-) - \Delta_i \bar{u}_j$, $t \geq t_{ij}$. When $t = t_f$, as determined from Eq. 3.67, then $u(t) = 0$, $t \geq t_f$.

An algorithm, which mechanizes this control law, is presented in the next chapter.

CHAPTER IV

IMPLEMENTATION OF FEEDBACK CONTROL LAW

In this chapter, an algorithm is developed which implements the neighboring optimal control law derived in Chapter III. The main features of this algorithm are the determination of the nominal time and the use of the open-loop control law to choose the correct feedback gains. The "time-to-go" concept of Speyer and Bryson [10] is used to choose $\bar{t}$, and the open-loop control law is used to ascertain the number of switch times and the initial control function for the neighboring path.

The neighboring optimal control law was derived by assuming that the state and switch-time perturbations are infinitesimal. The following inequalities are a consequence of this assumption, and were utilized in Chapter III to derive the neighboring optimal control law:

$$t_0 < t_{Nj} < t_{(N-1)j} < \cdots < t_{2j} < t_{1j} < t_f \ , \quad j \in [1,\cdots,m] \ , \tag{4.1}$$

$$\bar{t}_{ij} + \delta t_{ij} < \bar{t}_{(i-1)j} \ , \ i = 2,\cdots, N \ , \tag{4.2}$$

$$\bar{t}_{ij} + \delta t_{ij} < \bar{t}_f \ . \tag{4.3}$$

Since the neighboring control law will be applied to states which are a finite distance from the nominal path, the switch times and switch-time perturbations for the neighboring path will, in general, not satisfy the above inequalities. This situation is illustrated in Fig. 4.1 by a neighboring control history which violates some of the above inequalities. The mechanization of the neighboring control law must, therefore, be designed to account for possible non-satisfaction of Eq. 4.1 - Eq. 4.3 .

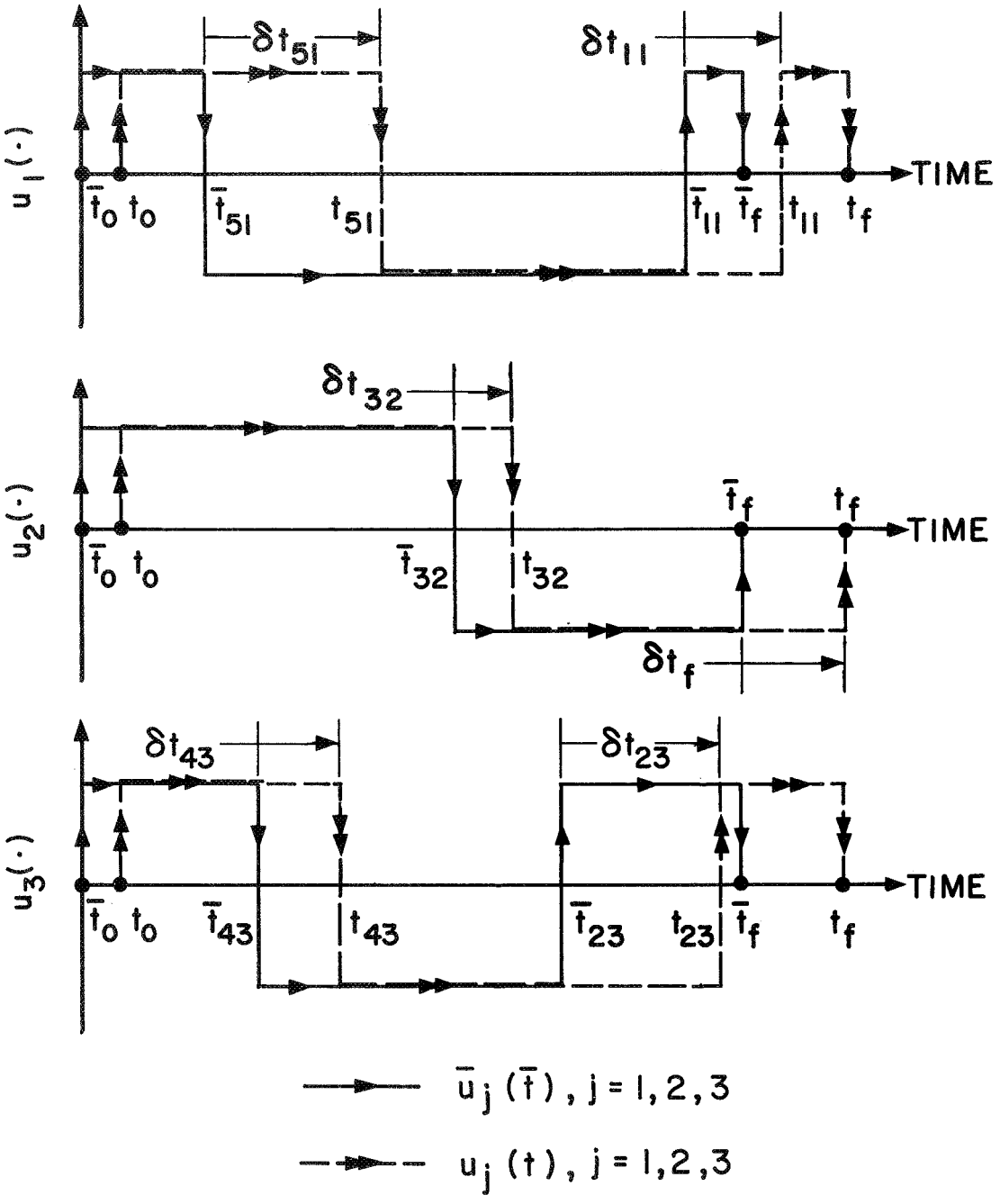

Figure 4.1. An Example Control History for Which Eq. 4.1 - Eq. 4.3 Are Violated: $t_{51} > t_{43}$; $t_{23} > t_{11}$, $t_{51} > t_{43}$; $t_{11} > t_f$.

4.1 Switching Functions Based Upon Nominal Time

The number of remaining switch times along the neighboring (and nominal) trajectories, in the time interval $[t,t_f]$, has been denoted by N . The total number of switch times, in the time interval $[\bar{t}_0,\bar{t}_f]$, along the nominal path, has been denoted by $\bar{N}$. To mechanize the neighboring control law it is necessary to assume that the maximum number of neighboring switch times is less than or equal to $\bar{N}$. That is, $N \in [0,1,\cdots,\bar{N}]$.

For each possible value of N , the matrix of gains, $\bar{G}_N$, can be calculated from Eq. 3.59 . These gains are used to calculate the current estimate of the neighboring switch times (see Eq. 3.66):

$$t_s = \bar{t}_s - \bar{G}_N \Phi(\bar{t}_f,\bar{t})[x(t) - \bar{x}(\bar{t})] \quad , \quad t_{(N+1)j} < t \leq t_{Nj} \quad , \qquad (4.4)$$

$$\bar{t}_{(N+1)j} < \bar{t} \leq \bar{t}_{Nj} \quad .$$

Designate the N^{th} -row of $\bar{G}_N$ by $\bar{g}_N$. Then, from Eq. 4.4, the N^{th}-switch time for the neighboring path is given by

$$t_{Nj} = t + \bar{t}_{Nj} - \bar{t} - \bar{g}_N \Phi(\bar{t}_f,\bar{t})[x(t) - \bar{x}(\bar{t})] \quad , \quad t_{(N+1)j} < t \leq t_{Nj} \quad , \qquad (4.5)$$

$$\bar{t}_{(N+1)j} < \bar{t} \leq \bar{t}_{Nj} \quad .$$

From Eq. 3.60 and Eq. 3.67 , the final time is given by

$$t_f = t + \bar{t}_f - \bar{t} - \bar{M}\Phi(\bar{t}_f,\bar{t})[x(t) - \bar{x}(\bar{t})] \quad , \quad t_{1j} < t \leq t_f \quad , \qquad (4.6)$$

$$\bar{t}_{1j} < \bar{t} \leq \bar{t}_f \quad .$$

Now define $S_{Nj}(t,\bar{t})$ and $S_f(t,\bar{t})$ as follows:

$$S_{Nj}(t,\bar{t}) \equiv \bar{t}_{Nj} - \bar{t} - \bar{g}_N \Phi(\bar{t}_f,\bar{t})[x(t) - \bar{x}(\bar{t})] \ , \ N = 1,\cdots,\bar{N} \ ; \ j \in [1,\cdots,m],$$

$$\bar{t}_{(N+1)j} < \bar{t} \leq \bar{t}_{Nj} \ , \ t_{(N+1)_j} < t \leq t_{Nj} \ , \tag{4.7}$$

$$S_f(t,\bar{t}) \equiv \bar{t}_f - \bar{t} - \bar{M}\Phi(\bar{t}_f,\bar{t})[x(t) - \bar{x}(\bar{t})], \ t_{1j} < t \leq t_f, \ \bar{t}_{1j} < \bar{t} \leq \bar{t}_f \ . \tag{4.8}$$

Substituting Eq. 4.7 and Eq. 4.8 into Eq. 4.5 and Eq. 4.6 , respectively, one sees that $S_{Nj}(t,\bar{t})$ and $S_f(t,\bar{t})$ have the following properties:

$$S_{Nj}(t_{Nj},\bar{t}) = 0 \ , \ S_{Nj}(t,\bar{t}) > 0 \text{ for } t < t_{Nj} \ , \ N = 1,\cdots,\bar{N} \ , \tag{4.9}$$

$$S_f(t_f,\bar{t}) = 0 \ , \ S_f(t,\bar{t}) > 0 \text{ for } t < t_f \ . \tag{4.10}$$

Thus, $S_{Nj}(t,\bar{t})$ is the N^{th}-switching function for the j^{th}-component of the control function, and $S_f(t,\bar{t})$ is the final-time switching function. That is, when $S_{Nj}(t_{Nj},\bar{t}) = 0$, then $u_j(t) = u_j(t_{Nj}^-) - \Delta_N \bar{u}_j, t \geq t_{Nj}$, and when $S_f(t_f,\bar{t}) = 0$, then $u(t) = 0$, $t \geq t_f$. Note that since $S_{Nj}(t,\bar{t})$, $N = 1,\cdots, \bar{N}$, is linear in the state, $x(t)$, the switching surface defined by the neighboring control law is simply a linear approximation of the nominal switching surface at the nominal switch points.

The switching functions, defined by Eq. 4.7 and Eq. 4.8 , are utilized in Section 4.4 to mechanize the neighboring control law. They are, however, a function of the nominal time as well as of the neighboring state, $x(t)$. Thus, a technique for determining an appropriate nominal time must first be specified. This is the subject of the next section.

4.2 Choice of Nominal Time

The choice of $\bar{t}$ is somewhat arbitrary. When calculating the N^{th}-switch time, the only restriction upon this choice is that $\bar{t}$ lie in the interval $(\bar{t}_{(N+1)j}, \bar{t}_{Nj}]$. The best technique for choosing $\bar{t}$ is, in general, dependent upon the particular application of interest. The concept of "time-to-go" is used to determine an appropriate $\bar{t}$ in this study.

This concept may be applied by two different techniques:

1) Choose $\bar{t} \in (\bar{t}_{(N+1)j}, \bar{t}_{Nj}]$ such that the time-to-go until the final time is the same for both neighboring and nominal paths. That is, choose $\bar{t}$ such that

$$\bar{t}_f - \bar{t} = t_f - t \ , \ \bar{t}_{(N+1)j} < \bar{t} \leq \bar{t}_{Nj} \ , \ t_{(N+1)j} < t \leq t_{Nj} \ , \qquad (4.11)$$

where t_f is the predicted final time for the neighboring path.

2) Choose $\bar{t} \in (\bar{t}_{(N+1)j} \ , \ \bar{t}_{Nj}]$ such that the time-to-go until the next switch time is the same for both the neighboring and nominal paths. That is, choose $\bar{t}$ such that

$$\bar{t}_{Nj} - \bar{t} = t_{Nj} - t \ , \ \bar{t}_{(N+1)j} < \bar{t} \leq \bar{t}_{Nj} \ , \ t_{(N+1)j} < t \leq t_{Nj} \ , \qquad (4.12)$$

where t_{Nj} is the predicted value of the next switch time for the neighboring path.

Two classes of problems should be considered: fixed terminal-time and free terminal-time optimization problems. A basic distinction between these two classes of problems is the following: The optimal switching surface, in state-space, for a fixed terminal-time problem is a function of the initial state of the system, whereas the optimal

switching surface for a free terminal-time problem is invariant to the initial state of the system.

It is conjectured that the first of the above techniques for determining $\bar{t}$ is most appropriate for fixed terminal-time problems, whereas the second technique is most appropriate for free terminal-time problems. When the switching surfaces for the neighboring and nominal trajectories are identical, as is the case for free terminal-time problems, it seems reasonable to expect that the neighboring and nominal trajectories will possess similar characteristics with respect to their switching surface. Choosing $\bar{t}$ by the second technique described above insures that this is the case. When the switching surfaces for the neighboring and nominal trajectories are different, as is the case for fixed terminal-time problems, a similarity between the two trajectories, with respect to their respective switching surfaces, should not be expected. For fixed terminal-time problems, therefore, it seems more reasonable to choose $\bar{t}$ by the first technique described above.

It is emphasized that the above discussion is merely conjectural. The ultimate test for determining the most appropriate technique for choosing $\bar{t}$ is a simulation of the particular problem of interest. For the example problems considered in Chapter V, the conjecture proved to be correct. Hence, the procedure for determining $\bar{t}$ described above will be adopted in the remainder of this study.

Finally, it should be noted that choosing $\bar{t}$ by the first technique is particularly appealing when the terminal time is fixed, since estimation of the final time, t_f, is no longer necessary. Also, for free terminal-time problems, the second technique for determining $\bar{t}$

is more appealing since one only needs to estimate the next switch time, t_{N_j} , instead of the final time, t_f .

4.3 Choice of Nominal Path

The proper choice of the nominal path is essential in order to insure the success of the neighboring control scheme. In Chapter III, the terms higher than second-order, in the expansion of the performance index, were dropped. It should be expected, therefore, that the neighboring control law is nearly optimal only when these higher-order terms are small compared to the second-order terms. Hence, when using the neighboring control scheme, the perturbations in the state should be kept as small as possible.

To accomplish this, one should choose a nominal trajectory which lies within the region of expected initial states of the system. This is the primary guideline for choosing a nominal trajectory. If the region of expected initial states is large, it would probably be necessary to generate multiple nominal trajectories, and corresponding control laws, each assigned to control a particular region in state-space. The size of these regions, and the number of nominal trajectories required, would depend upon the particular application , and would have to be determined by a problem simulation.

In addition to these considerations, the nominal trajectory must satisfy two further requirements. The first was mentioned in Section 4.1 . The number of switch times along the nominal path must be at least as large as the maximum number of switch times expected along a neighboring path. In most applications, one would have to perform a simulation in order to determine an appropriate value for $\bar{N}$.

The second requirement is based upon an assumption made in the derivation of the neighboring control law. In Section 3.2, it was

assumed that $u(t_f) = \bar{u}(\bar{t}_f)$. Since the number of remaining neighboring and nominal switch times is identical, satisfaction of this condition insures that the feedback gains, utilized along a given segment of the neighboring trajectory, are associated with the corresponding segment of the nominal trajectory. This requirement can be satisfied by again generating multiple nominal trajectories, each having a final control vector matching that of the expected initial states of the system. The final control vector, $u(t_f)$, for a given initial state, and hence the correct nominal trajectory and control law, can then be determined from a simple algorithm which utilizes the open-loop neighboring control law derived in Chapter III. This algorithm, along with a complete description of the mechanization of the neighboring feedback control law, is presented in the next section.

4.4 Neighboring Feedback Control Algorithm

In this section, an algorithm is presented which mechanizes the neighboring control law derived in Chapter III. Initially, it is assumed that the terminal time is free. The algorithm for free terminal-time problems is modified to handle fixed terminal-time problems at the end of this section. It is assumed that $N \leq \bar{N}$, where an appropriate $\bar{N}$ has been determined by an analysis of the problem and system dynamics. The number of switch times, N , the initial control vector, $u(t_0)$, and the correct nominal path are assumed to be unknown. If any of this information is known, for a particular application, the appropriate steps in the algorithm are deleted.

The first phase of the mechanization involves the determination of the number of switch times, the initial control vector, and the correct

feedback gains. This is essentially an open-loop procedure and requires a finite amount of computation time. In the description below, it is assumed that these computations are performed in negligible time. In practice, one would measure the present initial state, $x(t_0)$, and predict the future state, $x(t_0 + t_c)$, where t_c is the estimated computation time required for this phase of the mechanization. All calculations would then be based upon $x(t_0 + t_c)$ instead of $x(t_0)$. The magnitude of t_c is dependent upon the particular application, and reduces in size when information regarding N, $u(t_0)$, or $u(t_f)$, is available. For the applications considered in Chapter V, t_c is very small compared to the total operating time of the control scheme. Hence, at least for the problems considered in this study, the open-loop phase of the control law mechanization does not seriously impair the overall performance of the neighboring control scheme.

The following data are precalculated and stored in the computer for use in the open-loop phase of the mechanization: the initial neighboring state, $x(t_0)$; the sets of gains, $\bar{G}_i$ and $\bar{g}_0$, $i = 1,\cdots,\bar{N}$, for each nominal trajectory; the switch-time vector, $\bar{t}_s$, the final time, $\bar{t}_f$, the control level changes, $\Delta_i \bar{u}_j$, $i = 1,\cdots,\bar{N}$, and the final control vector, $\bar{u}(\bar{t}_f)$, for each nominal trajectory; the state history, $\bar{x}(\bar{t})$, $\bar{t}_0 \leq \bar{t} \leq \bar{t}_f$, and the state transition matrix history, $\Phi(\bar{t}_f,\bar{t})$, $\bar{t}_0 \leq \bar{t} \leq \bar{t}_f$, for each nominal trajectory.* It is assumed that the number of available nominal trajectories is sufficient to insure that

---

* Instead of storing $\bar{x}(\bar{t})$ and $\Phi(\bar{t}_f,\bar{t})$, $\bar{t}_0 \leq \bar{t} \leq \bar{t}_f$, it is usually more expedient to integrate the defining dynamical equations to determine a desired value of $\bar{x}(\bar{t})$ or $\Phi(\bar{t}_f,\bar{t})$, $\bar{t} \in [\bar{t}_o,\bar{t}_f]$. This was the procedure which was followed in the examples of Chapter V.

at least one nominal trajectory has a final control vector equal to the optimal final control vector for the neighboring initial state.

The open-loop phase of the neighboring control law mechanization, for free terminal-time problems, is now stated as follows:

Open-Loop Phase of Mechanization for Free Terminal-Time Problems

Step 1. Set $t = t_0$, $\bar{t} = \bar{t}_0$, and $N' = \bar{N}$, where N' is an integer constant. Choose, arbitrarily, one of the available nominal trajectories which lies in the region surrounding $x(t_0)$. Using the gains, $\bar{G}_{N'}$ and $\bar{g}_0$, associated with this nominal trajectory , calculate t_s and t_f using Eq. 3.66 and Eq. 3.67, respectively

$$t_s = \bar{t}_s - \bar{G}_{N'}\Phi(\bar{t}_f,\bar{t})[x(t_0) - \bar{x}(\bar{t})] \quad , \tag{4.13}$$

$$t_f = t_0 + \bar{t}_f - \bar{t} - \bar{g}_0\Phi(\bar{t}_f,\bar{t})[x(t_0) - \bar{x}(\bar{t})] \ . \tag{4.14}$$

Step 2. If $t_{N'j}$, as determined by Eq. 4.13 with $N' = \bar{N}$, is negative, set $N' = \bar{N} - 1$ and repeat Step 1 using the same nominal trajectory (i.e. use $\bar{G}_{(\bar{N}-1)}$, and the corresponding $\bar{g}_0$, to calculate t_s and t_f). Continue in this manner until $t_{N'j} > 0$ and $t_{(N'+1)j} < 0$ for some integer $N' \leq \bar{N}$.

Step 3. Choose $\bar{t}$ such that time-to-go until the next switch time is the same for both neighboring and nominal trajectories (see Eq. 4.12):

$$\bar{t} = t_0 + \bar{t}_{N'j} - t_{N'j} \ . \tag{4.15}$$

Then, substituting Eq. 4.15 into Eq. 4.13, recalculate $t_{N'j}$. Continue this procedure, using Eq. 4.15 to determine $\bar{t}$ and then recalculating $t_{N'j}$, until $(t_{N'j})_{New}$ is, to within any desired numerical accuracy, equal to $(t_{N'j})_{Old}$. Then compute $t_{(N'+1)j}$. If $t_{(N'+1)j} > 0$, revaluate N' to be $N' = (N')_{Old} + 1$, and then continue the calculation. If, during this calculation, $t_{N'j}$ becomes negative, revaluate N' to be $N' = (N')_{Old} - 1$, and then continue the calculation.*

Step 4. Calculate t_s and t_f by substituting $\bar{t}$ and N', determined in Step 3, into Eq. 4.13 and Eq. 4.14. Evaluate N to be the number of components of t_s which lie in the interval $[t_0, t_f]$. The neighboring initial control function, $u(t_0)$, is given by $\bar{u}'(\bar{t})$, where $\bar{u}'(\cdot)$ is the control function for the arbitrarily chosen nominal trajectory. The neighboring final control function, $u(t_f)$, is determined from $\bar{u}'(\bar{t}_f)$ and $\Delta_i \bar{u}_j'$, $i = 1, \cdots, N' - N$, by repeated use of Eq. 3.6.**

Step 5. Choose a new nominal trajectory, with final control function $\bar{u}(\bar{t}_f)$, such that $\bar{u}(\bar{t}_f) = u(t_f)$.

Step 6. Set $N' = N$ and repeat Step 3, using the gains associated with the new nominal trajectory. Then check to see if $t_{Nj} > 0$, $t_{(N+1)j} < 0$, and $t_{1j} < t_f$. If, in fact, these inequalities are satisfied, it is concluded that N is the number of neighboring switch times, and that the gains, $\bar{G}_i$ and $\bar{g}_0$, $i = 1, \cdots, N$, associated with the new nominal trajectory, are the

---

* For the examples considered in Chapter V, convergence to $t_{N'j}$ and N' was always accomplished in less than 11 iterations with $|(t_{N'j})_{New} - (t_{N'j})_{Old}| \leq .02$. On the average, only 5 iterations were required.

** If $N' = N$, then $u(t_f) = \bar{u}'(\bar{t}_f)$, and the chosen nominal path is appropriate for the given initial state.

feedback gains appropriate for initial state $x(t_0)$. If, however, these inequalities are not satisfied, one simply revaluates N and/or chooses a new nominal trajectory by repeating Steps 3-5.* Finally, calculate t_s and t_f, using $N' = N$ and the nominal time, $\bar{t}$, determined in Step 3. This completes the open-loop phase of the neighboring control law mechanization.

The number of neighboring switch times, N, the appropriate set of feedback gains, $\bar{G}_i$ and $\bar{g}_0$, $i = 1,\cdots, N$, the initial control vector, $u(t_0)$, and the step changes in the control function, $\Delta_i \bar{u}_j$, $i = 1,\cdots, N$, are now considered to be prescribed, having been determined by the above open-loop algorithm. The switch-time vector, t_s, and the final time, t_f, calculated in Step 6, define the open-loop control law for the initial state $x(t_0)$. This is true since it was assumed that $t = t_0$ in all of the above computations. Knowledge of the open-loop control law is utilized in the feedback mechanization of the neighboring control law, to be described below.

For free final-time problems, $\bar{t} = \bar{t}_{Nj}$ at the N^{th}-neighboring switch time (see Eq. 4.12), and $\bar{t} = \bar{t}_f$ at the neighboring final time. The N switching functions for the N neighboring switch times, and the final-time switching function, may thus be written (Eq. 4.7 and Eq. 4.8):

$$S_{ij}(t,\bar{t}_{ij}) = -\bar{g}_i \Phi(\bar{t}_f,\bar{t}_{ij})[x(t)-\bar{x}(\bar{t}_{ij})],\ i = 1,\cdots,N, \qquad (4.16)\ \text{cont.}$$

---

* This calculation was not performed in the example problems of Chapter V since the inequalities were always satisfied.

$$t_{(i+1)j} < t \leq t_{ij} \ , \tag{4.16}$$

$$S_f(t,\bar{t}_f) = -\bar{M}[x(t) - \bar{x}(\bar{t}_f)] \ , \ t_{1j} < t \leq t_f \ . \tag{4.17}$$

Hence, when $S_{ij}(t,\bar{t}_{ij}) = 0$, the j^{th}-component of the neighboring control function switches discontinuously, and when $S_f(t,\bar{t}_f) = 0$, the neighboring control function switches off.

Since the neighboring control law will be applied to states which are a finite distance from the nominal trajectory, the mechanization of the control law must allow for a possible reordering of the switch times.* That is, for two control components, $u_j(\cdot)$ and $u_{j'}(\cdot)$, $j \neq j'$, with nominal switch times related by $\bar{t}_{ij} < \bar{t}_{i'j'}$, $i > i'$, the mechanization must allow for the possibility that the neighboring switch times are related by $t_{i'j} < t_{ij}$, $i > i'$ (see Fig. 4.1) .

Allowing for this possibility, the feedback phase of the neighboring control law mechanization is described as follows:

Feedback Mechanization for Free Terminal-Time Problems

Monitor the functions $S_{i1}(t,\bar{t}_{i1})$, $S_{i2}(t,\bar{t}_{i2})$,$\cdots$, $S_{im}(t,\bar{t}_{im})$, $i \in [1,\cdots,N]$, where each $S_{ij}(t,\bar{t}_{ij})$ is the switching function for the next switch time for the j^{th}-component of the control function. When any one of these switching functions becomes zero, say $S_{i'j'}(t,\bar{t}_{i'j'})$, then the i'^{th}-neighboring switch time, $t_{i'j'}$, $i' \in [1,\cdots,N]$, is determined, and $u_{j'}(t)$, $t \geq t_{i'j'}$,

---

* An example, in which a reordering of the switch times occurs is presented in Section 5.3 .

becomes (see Eq. 3.6)

$$u_{j'}(t) = u_{j'}(t_{i'j'}) - \Delta_{i'}\bar{u}_{j'} \ , \ t \geq t_{i'j'} \ . \tag{4.18}$$

After time $t_{i'j'}$, replace $S_{i'j'}(t,\bar{t}_{i'j'})$ by $S_{i''j'}(t,\bar{t}_{i''j'})$, $i'' < i'$, in the sequence of switching functions being monitored, where $S_{i''j'}(t,\bar{t}_{i''j'})$ is the switching function for the next switch time, after $t_{i'j'}$, for the j'^{th}-component of the control function. After all N switchings have occurred, monitor $S_f(t,\bar{t}_f)$. When $S_f(t,\bar{t}_f)$ becomes zero, set $u(\cdot) = 0$, thus terminating the control scheme.

This phase of the mechanization of the neighboring control law results in a feedback control scheme since $S_{ij}(t,\bar{t}_{ij})$, $i = 1,\cdots,N$, and $S_f(t,\bar{t}_f)$ are functions, only, of the state, $x(t)$, and prescribed quantities associated with the nominal trajectory. Caution must be used when implementing this control scheme, however, since the switching functions are, in general, not monotonic functions of real time t . That is, as t increases from t_0 , the switching functions may pass thru zero several times before actual switching is supposed to occur. From Eq. 4.16 , $S_{ij}(t,\bar{t}_{ij})$ is a valid switching function only when $t_{(i+1)j} < t \leq t_{ij}$. This restriction on t is a consequence of the assumption that the state perturbations are infinitesimal. Since finite state perturbations will be allowed, t need not satisfy this inequality. If, however, t is far removed from the time interval $[t_{(i+1)j} \ , \ t_{ij}]$, one can no longer expect that $S_{ij}(t,\bar{t}_{ij})$ will possess the properties of a switching function (Eq. 4.9).

This problem is circumvented by utilizing the open-loop switch-time vector, t_s , calculated in the open-loop phase of the mechanization. This vector gives the approximate switch times for the neighboring control law, and will usually indicate the actual ordering of the neighboring switch times. Provided that $S_{ij}(t,\bar{t}_{ij})$, i= 1,$\cdots$, N , are well behaved functions (which was found to be the case for the problems considered in Chapter V), they will satisfy the properties given in Eq. 4.9 when t is "reasonably close" to t_{ij}. Hence, by monitoring $S_{ij}(t,\bar{t}_{ij})$, i = 1,$\cdots$, N, only after t is "reasonably close" to the open-loop switch time, t_{ij}, one insures that $S_{ij}(t,\bar{t}_{ij})$ is, in fact, the switching function for the switch time t_{ij}. Defining "reasonably close" must be done by a problem simulation. At least for the problems discussed in Chapter V, it was found that one could safely monitor $S_{ij}(t,\bar{t}_{ij})$,i = 1,$\cdots$, N, well before the associated open-loop switch times. This completes the description of the feedback mechanization of the neighboring control law for free terminal-time problems. A block diagram of this mechanization is shown in Fig. 4.2.

The control law mechanization for fixed terminal-time problems differs from that for free terminal-time problems in the choice of the nominal time. Since $t_f = \bar{t}_f$, Eq. 4.11 indicates that $\bar{t} = t$ is the appropriate choice for the nominal time. The resulting modifications in the above mechanization, made necessary in order to handle fixed terminal-time problems, are now presented:

Open-Loop Phase of Mechanization for Fixed Terminal-Time Problems

This phase of the mechanization is identical to that for free terminal-time problems when the following modifications are made:

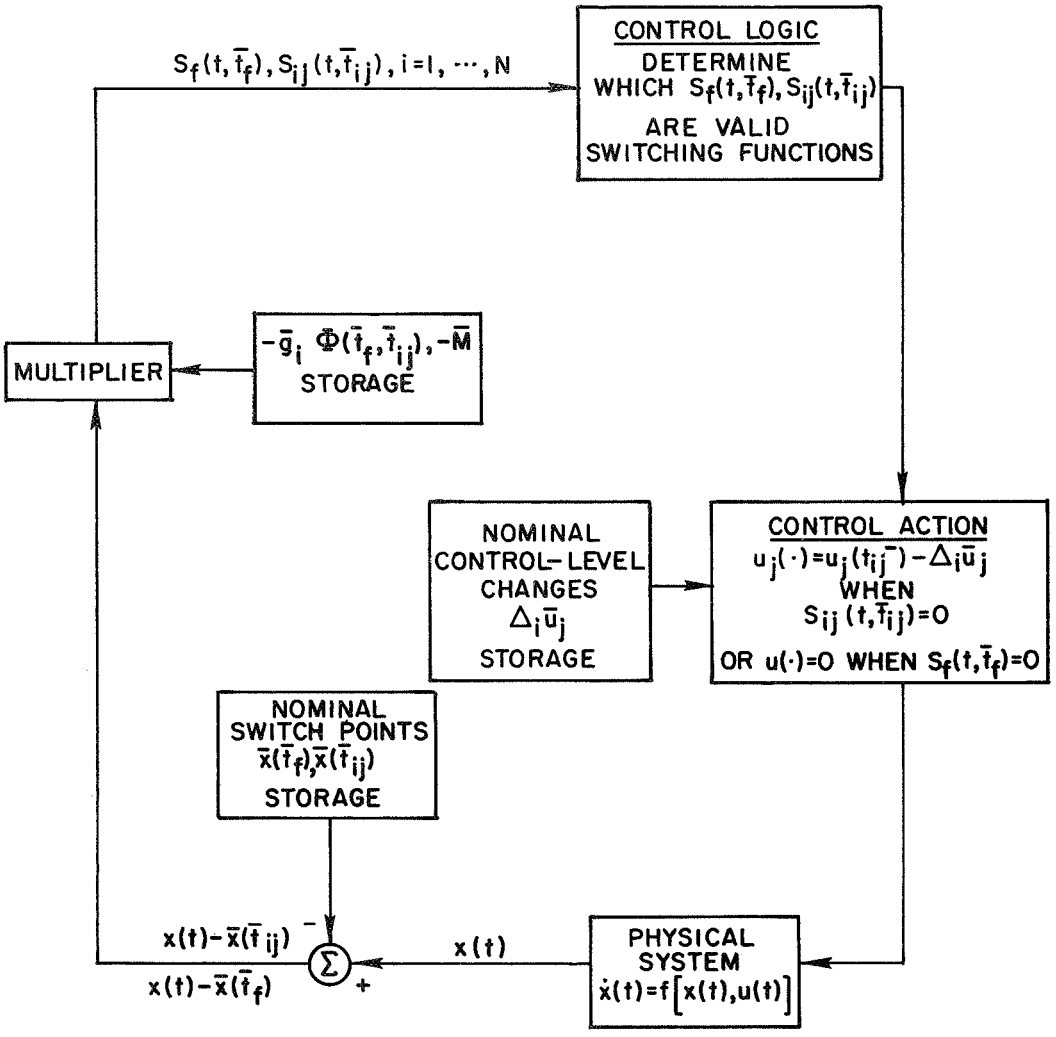

Figure 4.2. Feedback Mechanization of Neighboring Optimal Control Law for Free Terminal-Time Problems.

1. Since $t_f = \bar{t}_f$, and hence $\bar{t} = t$, it follows that $t = t_0 = \bar{t} = \bar{t}_0$ during this phase of the mechanization. Thus, Eq. 4.13 is modified to become

$$t_s = \bar{t}_s - \bar{G}_N \cdot \Phi(\bar{t}_f, t_0)[x(t_0) - \bar{x}(t_0)] , \qquad (4.13')$$

and Eq. 4.14 is omitted.

2. Since $\bar{t} = t$, Step 3 is omitted.

Since no iterative technique is required to calculate $\bar{t}$, it is seen that this phase of the mechanization is simpler than that for free terminal-time problems. Consequently, the open-loop computation time, t_c , is considerably smaller for this class of problems.

The closed-loop phase of the mechanization is described as follows:

Feedback Mechanization for Fixed Terminal-Time Problems

The feedback mechanization for fixed terminal-time problems is identical to that for free terminal-time problems when the following two modifications are made:

1. Since $\bar{t} = t$, the switching functions (Eq. 4.16) are redefined to be (see Eq. 4.7)

$$S_{ij}(t,t) = \bar{t}_{ij} - t - \bar{g}_i \Phi(\bar{t}_f, t)[x(t) - \bar{x}(t)], \quad i = 1, \cdots, N,$$

$$t_{(i+1)j} < t \leq t_{ij} , \quad \bar{t}_{(i+1)j} < t \leq \bar{t}_{ij} , \qquad (4.16')$$

and, since $t_f = \bar{t}_f$, the final-time switching function (Eq. 4.17) is omitted.

2. From Eq. 4.16′, $S_{ij}(t,t)$ is the switching function for the i^{th}-neighboring switch time, t_{ij}, only if $t \leq \bar{t}_{ij}$. If $t_{ij} > \bar{t}_{ij}$, Eq. 4.16′ is modified to become

$$S_{ij}(t,t) = \bar{t}_{ij} - t - \bar{g}_i \Phi(\bar{t}_f,t)[x(t)-\bar{x}(\bar{t}_{ij})], \quad i = 1,\cdots,N, \tag{4.16″}$$

$$t_{(i+1)j} < t \leq t_{ij} \ , \ t > \bar{t}_{ij} \ .$$

Hence, in the time interval $(\bar{t}_{ij},t_{ij}]$, $\bar{x}(t)$ is equated to $\bar{x}(\bar{t}_{ij})$ since only values of $\bar{x}(\bar{t})$, $\bar{t} \leq \bar{t}_{ij}$, are allowed in Eq. 4.7 . This completes the description of the neighboring feedback control scheme for fixed terminal-time problems. A block diagram of this mechanization is shown in Fig. 4.3.

Note that Eq. 4.16′ and Eq. 4.16″ do, in fact, result in a feedback mechanization of the neighboring control law since $S_{ij}(t,t)$, $i = 1,\cdots,N$, are functions of the current state, $x(t)$.* The neighboring feedback control law mechanization described in this chapter is summarized, for convenience, in Section 4.5 .

4.5 Summary of Control Law Mechanization

The mechanization of the neighboring control law, described in this chapter, is summarized in this section. The modifications in the mechanization, made necessary when the terminal time is fixed, are

---

* McNeal's mechanization is open-loop when $t_{ij} > \bar{t}_{ij}$ (see [6], Eq. 5.11). He replaces $x(t)$ with $x(\bar{t}_{ij})$ in the switching function when $t_{ij} > \bar{t}_{ij}$.

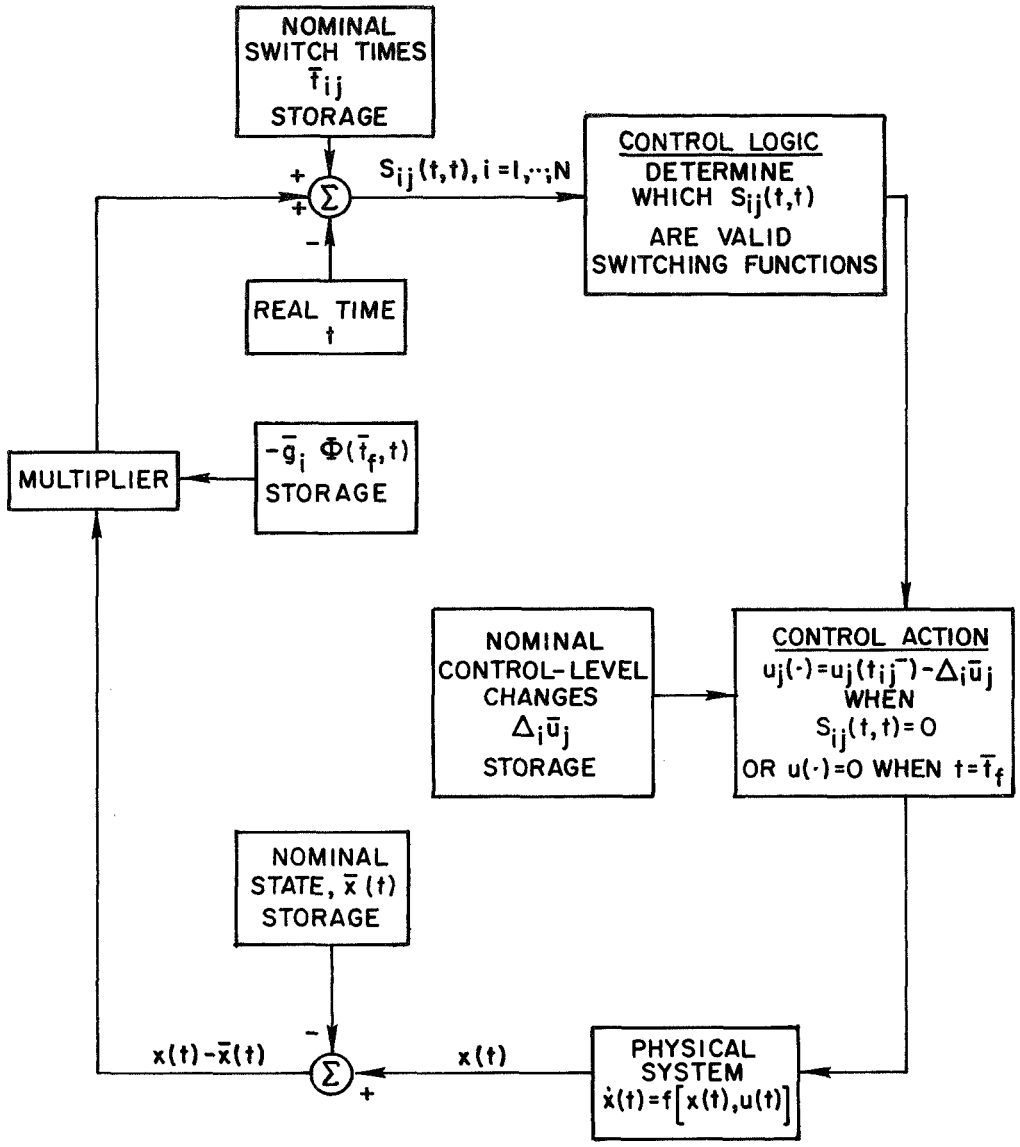

Figure 4.3. Feedback Mechanization of Neighboring Optimal Control Law for Fixed Terminal-Time Problems.

indicated. The neighboring control law mechanization is summarized as follows:

Summary of Preliminary Computations

1. Determine, by problem simulation and/or analysis, the number of nominal switch times, $\bar{N}$, such that for each neighboring initial state, $x(t_0)$, of interest, the number of neighboring switch times, N , satisfies the inequality $N \leq \bar{N}$.

2. Generate a sufficient number of nominal trajectories (see Section 3.1), each having $\bar{N}$ control discontinuities, such that each $x(t_0)$ of interest lies near one of the nominal trajectories, and such that the final control vector, $\bar{u}(\bar{t}_f)$, of that nominal trajectory, is equal to the final control vector, $u(t_f)$, associated with the optimal neighboring trajectory for $x(t_0)$.

3. For each nominal trajectory, calculate and store the following data for use in the control law mechanization:

   a. The gains, $\bar{G}_i$ and $\bar{g}_0$, $i = 0,\cdots, \bar{N}$, (see Eq. 3.59-Eq. 3.60).

   b. The nominal switch-time vector, $\bar{t}_s$ (see Eq. 3.63).

   c. The nominal final time, $\bar{t}_f$.

   d. The control level changes, $\Delta_i \bar{u}_j$, $i = 1,\cdots,\bar{N}$, (see Eq. 3.6).

   e. The nominal final control vector, $\bar{u}(\bar{t}_f)$.

   f. The nominal state history, $\bar{x}(\bar{t})$, $\bar{t}_0 \leq \bar{t} \leq \bar{t}_f$, or an integration routine (Eq. 2.8) which determines $\bar{x}(\bar{t})$, $\bar{t} \in [\bar{t}_0, \bar{t}_f]$.

   g. The state transition matrix history, $\Phi(\bar{t}_f, \bar{t})$, $\bar{t}_0 \leq \bar{t} \leq \bar{t}_f$, or an integration routine (Eq. 3.21) which determines $\Phi(\bar{t}_f, \bar{t})$, $\bar{t} \in [\bar{t}_0, \bar{t}_f]$.

Summary of Open-Loop Phase of Control Law Mechanization

4. Set $t = t_0$ and $\bar{t} = \bar{t}_0$. (Set $t = t_0 = \bar{t} = \bar{t}_0$ when the terminal time is fixed.) Use the gains, $\bar{G}_i$ and $\bar{g}_0$, $i = 1,\cdots, \bar{N}$, associated with an arbitrary nominal trajectory, to determine N' such that $t_{N'j} > 0$ and $t_{(N'+1)j} < 0$ (Step 1 and Step 2 in Section 4.4). (When the terminal time is fixed, replace Eq. 4.13 by Eq. 4.13′ and neglect Eq. 4.14.)

5. Determine $\bar{t}$ such that time-to-go until the next switch time is the same for both neighboring and nominal trajectories, revaluating N' whenever necessary (Step 3 in Section 4.4). (When the terminal time is fixed, omit this step.)

6. Using the current values of $\bar{t}$ and N', evaluate N, $u(t_0)$, and $u(t_f)$, associated with neighboring initial state $x(t_0)$ (Step 4 in Section 4.4).

7. Choose a new nominal trajectory such that $\bar{u}(\bar{t}_f) = u(t_f)$. Then recompute $\bar{t}$ (only if the terminal time is free) and check to see if $t_{Nj} > 0$, $t_{(N+1)j} < 0$, and $t_{1j} < t_f$. If these inequalities are not satisfied, revaluate N and/or choose a new nominal trajectory. Then recompute $\bar{t}$ and again check to see if the above inequalities are satisfied (Step 5 and Step 6 in Section 4.4).

Summary of Neighboring Feedback Control Law Mechanization

8a. For free terminal-time problems, monitor the functions (see Eq. 4.16) $S_{ij}(t,\bar{t}_{ij})$, $j = 1,\cdots, m$; $i \in [1,\cdots,N]$, where each $S_{ij}(t,\bar{t}_{ij})$ is the switching function for the next switch time for the j^{th}-component of the control function. No individual switching function should be monitored until t is "reasonably close" to the corresponding open-loop switch time. When any one of these switching functions becomes

zero, say $S_{i',j'}(t,\bar{t}_{i',j'})$, $u_{j'}(\cdot)$ undergoes a discontinuity and is given by Eq. 4.18 . Then replace $S_{i',j'}(t,\bar{t}_{i',j'})$ by the next switching function for $u_{j'}(\cdot)$ in the sequence of monitored switching functions.

8b. For fixed terminal-time problems, monitor the functions (see Eq. 4.16′) $S_{ij}(t,t)$, $j = 1,\cdots, m$; $i \in [1,\cdots,N]$, where each $S_{ij}(t,t)$ is the switching function for the next switch time for the j^{th}-component of the control function. Then proceed as in 8a. If $t_{ij} > \bar{t}_{ij}$, replace $S_{ij}(t,t)$ in the monitored sequence, defined in Eq. 4.16′ , with $S_{ij}(t,t)$, defined in Eq. 4.16″ .

9. When all N switchings have occurred, monitor $S_f(t,\bar{t}_f)$, defined in Eq. 4.17 , and set $u(\cdot) = 0$ when $S_f(t,\bar{t}_f) = 0$. (For fixed terminal-time problems, set $u(\cdot) = 0$ when $t = \bar{t}_f$.)

The neighboring control scheme summarized above is utilized, in the next chapter, to solve one minimum-fuel and two minimum-time optimization problems.

CHAPTER V

APPLICATION TO CONTROL PROBLEMS

In this chapter, the neighboring optimal feedback control law developed in the previous chapters is utilized to solve three control problems. First, the problem of minimum-fuel control, to the origin, of the $1/s^2$ plant is considered. This problem is solved analytically and demonstrates the control law mechanization for fixed terminal-time problems. The second problem considered is the minimum-time control, to the origin, of the $1/s(s^2+1)$ plant. The optimal switching surface and trajectories for this problem are known [15] , and hence are compared to those generated by the neighboring control scheme. Also, this problem demonstrates the control law mechanization for free terminal-time problems. Both of these problems involve scalar control of low-order systems. To demonstrate the effect of the neighboring control scheme upon high-order, multi-input systems, the minimum-time satellite attitude-acquisition problem is considered. The simulation of the satellite dynamics, and the associated neighboring optimal feedback control law, was performed in single precision on the Stanford University IBM 360/67 digital computer.

The results presented in this chapter, for these three control problems, demonstrate the feasibility of a neighboring optimal control scheme, and lend credence to the feedback mechanization of this control scheme, described in Chapter IV. In addition, these results show the action of the neighboring control scheme when applied to states which are a significant distance from the nominal trajectory.

5.1 Minimum-Fuel Control of $1/s^2$ Plant

The problem considered in this section is the well-known problem of minimum-fuel control, to the origin, of the $1/s^2$ plant. The system dynamics are given by

$$\begin{aligned} \dot{x}_1(t) &= x_2(t) \ , \ x_1(t_0) = x_{10} \ , \\ \dot{x}_2(t) &= u(t) \ , \ x_2(t_0) = x_{20} \ , \end{aligned} \tag{5.1}$$

where the scalar control function is subject to the constraint

$$|u(t)| \leq 1.0 \ , \ t_0 \leq t \leq t_f \ . \tag{5.2}$$

The final time, t_f , is specified. The performance index is given by

$$\bar{J} = \int_{t_0}^{t_f} |u(t)| \ dt \ . \tag{5.3}$$

By augmenting the state (Eq. 2.5) , the performance index may be written

$$\bar{J} = F[x(t_f)] = x_3(t_f) \tag{5.4}$$

where

$$\dot{x}_3(t) = |u(t)| \ , \ x_3(t_0) = 0 \ . \tag{5.5}$$

The terminal constraints are written

$$\Psi[x(t_f)] = \begin{bmatrix} x_1(t_f) \\ x_2(t_f) \end{bmatrix} = \begin{bmatrix} 0 \\ 0 \end{bmatrix} . \tag{5.6}$$

It is known that at most two discontinuities in the optimal control function can occur [16], and hence $\bar{N} = 2$. It is assumed that

the initial state, (x_{10},x_{20}) , is such that the origin is reachable in time (t_f-t_0) . Recall that the neighboring control scheme is only valid when applied to states which are controllable in time (t_f-t_0).

Set $t_0 = \bar{t}_0 = 0.0$ and $t_f = \bar{t}_f = 3.0$. Choose the nominal, initial state to be $(\bar{x}_{10},\bar{x}_{20}) = (1.25, 0.0)$. The nominal, minimum-fuel trajectory for this initial state and terminal time is easily determined (see, for example, [16]) , and is shown in Fig. 5.1 . The nominal switch-time vector is found to be $\bar{t}_s = (2.5, 0.5)$, and the resulting minimum-fuel cost is $\bar{J}_{op} = 1.0$. The initial control function is $\bar{u}(\bar{t}_0) = -1.0$ and the final control function is $\bar{u}(\bar{t}_f) = +1.0$.

To determine the neighboring control law, the weighting matrix, W , is set equal to the second-order identity matrix, and the scalar gain, K , is allowed to become arbitrarily large (see Eq. 2.10). Since the system dynamics are linear, Eq. 3.57, in conjunction with Eq. 3.61, is used to calculate the feedback gains, $\bar{G}_2$ and $\bar{G}_1$, which are given as follows:

$$\bar{G}_2 = \begin{bmatrix} 0.5 & -1.25 & 0.0 \\ -0.5 & 0.25 & 0.0 \end{bmatrix} , \tag{5.7}$$

$$\bar{G}_1 = \begin{bmatrix} -0.4 & -0.8 & 0.0 \end{bmatrix} . \tag{5.8}$$

Using these gains, the neighboring optimal feedback control scheme for fixed terminal-time problems was applied to the following initial states:

$$\text{Example I:} \quad x_0 = \begin{bmatrix} 1.375 \\ -.125 \end{bmatrix}$$

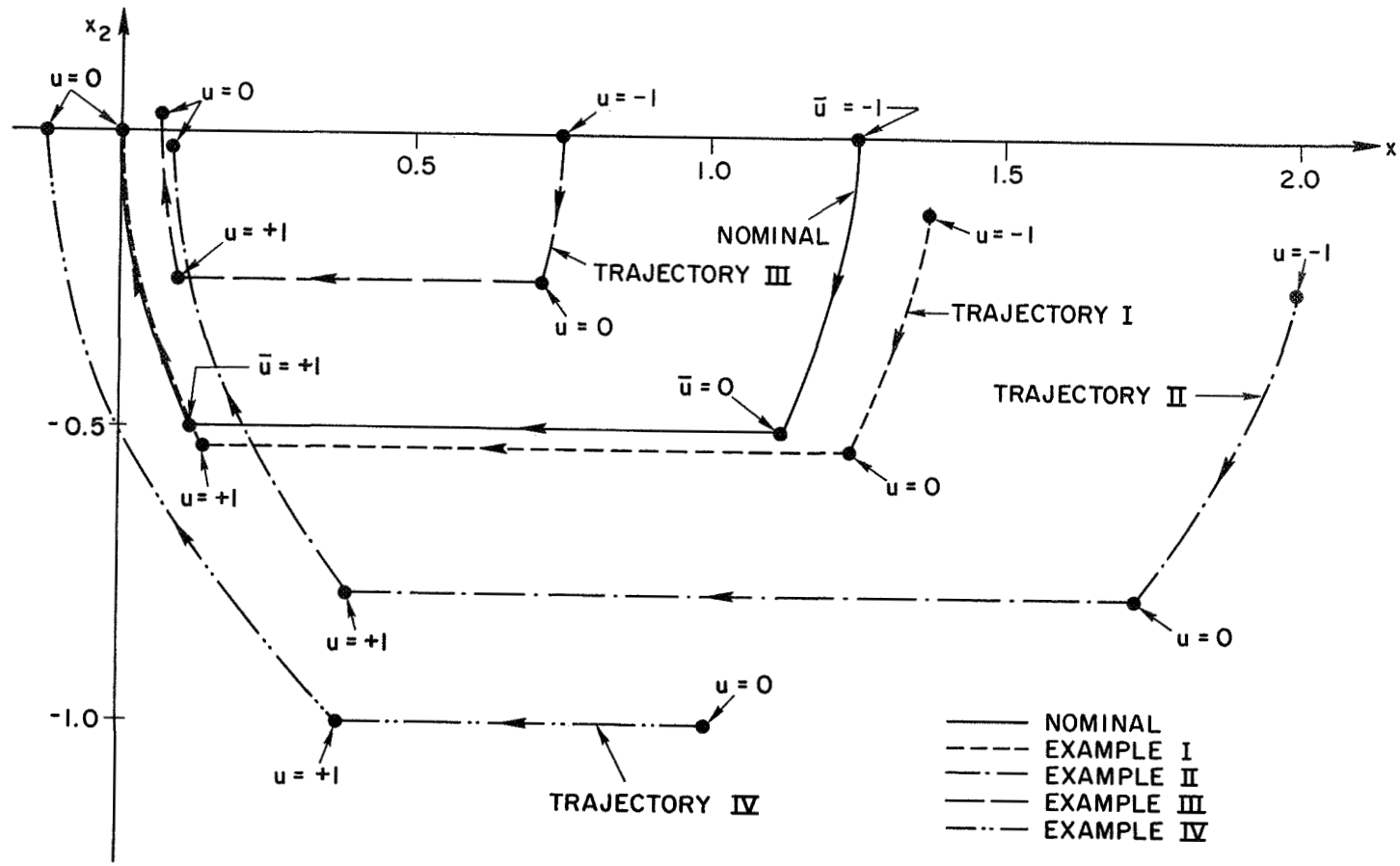

Figure 5.1. Neighboring Trajectories for Problem of Minimum-Fuel Control of $1/s^2$ Plant.

Example II: $x_0 = \begin{bmatrix} 2.00 \\ -.25 \end{bmatrix}$

Example III: $x_0 = \begin{bmatrix} 0.75 \\ 0.0 \end{bmatrix}$

Example IV: $x_0 = \begin{bmatrix} 1.0 \\ -1.0 \end{bmatrix}$

In each case, the open-loop phase of the neighboring control law mechanization (see Section 4.4) verified that the chosen nominal trajectory is, indeed, appropriate for these chosen initial states. The neighboring optimal trajectories, for each of these initial states, are shown in Fig. 5.1 , and are specified by the number of neighboring switch times, the neighboring switch-time vector, the initial and final control functions, and the final state, in Table 5.1 .

Also included in Table 5.1 are the optimal switch-time vectors, $(t_s)_{op}$, the neighboring and optimal costs, $\bar{J}$ and $\bar{J}_{op}$*, and a measure of the effectiveness of the neighboring control scheme, $||x(t_f)|| / ||x_0||$, for each neighboring trajectory. The optimal switch times and optimal costs were obtained by solving Optimization Problem I, for each neighboring initial state, by the technique developed in [16]. Note that $\bar{J} \leq \bar{J}_{op}$ for each of the example trajectories. This is expected since the terminal constraints, Eq. 5.6 , are not satisfied exactly by any

* The neighboring cost, $\bar{J}$, listed in Table 5.1 , is the nominal performance index (Eq. 5.4) evaluated along the neighboring trajectory. Thus, non-satisfaction of the terminal constraints is not reflected by the magnitude of $\bar{J}$.

Trajectory	Nominal	Example I	Example II	Example III	Example IV
Initial State, x_0	$\begin{bmatrix} 1.25 \\ 0.0 \end{bmatrix}$	$\begin{bmatrix} 1.375 \\ -.125 \end{bmatrix}$	$\begin{bmatrix} 2.00 \\ -.25 \end{bmatrix}$	$\begin{bmatrix} 0.75 \\ 0.0 \end{bmatrix}$	$\begin{bmatrix} 1.0 \\ -1.0 \end{bmatrix}$
Initial Control Function, $u(t_0)$	-1.0	-1.0	-1.0	-1.0	0.0
Final Control Function, $u(t_f)$	+1.0	+1.0	+1.0	+1.0	+1.0
Number of Switch Times, N	2	2	2	2	1
Switch-Time Vector, t_s	$\begin{bmatrix} 2.5 \\ 0.5 \end{bmatrix}$	$\begin{bmatrix} 2.471 \\ 0.406 \end{bmatrix}$	$\begin{bmatrix} 2.250 \\ 0.528 \end{bmatrix}$	$\begin{bmatrix} 2.719 \\ 0.250 \end{bmatrix}$	.625
Optimal Switch-Time Vector, $(t_s)_{op}$	$\begin{bmatrix} 2.5 \\ 0.5 \end{bmatrix}$	$\begin{bmatrix} 2.466 \\ 0.409 \end{bmatrix}$	$\begin{bmatrix} 2.155 \\ 0.595 \end{bmatrix}$	$\begin{bmatrix} 2.725 \\ 0.275 \end{bmatrix}$	.5
Final State, $x(t_f)$	$\begin{bmatrix} 0.0 \\ 0.0 \end{bmatrix}$	$\begin{bmatrix} 0.0039 \\ -.0018 \end{bmatrix}$	$\begin{bmatrix} 0.0868 \\ -.0278 \end{bmatrix}$	$\begin{bmatrix} 0.0708 \\ 0.0312 \end{bmatrix}$	$\begin{bmatrix} -.125 \\ 0.0 \end{bmatrix}$
$\|\|x(t_f)\|\| / \|\|x_0\|\|$	0.0	0.0031	0.0452	0.1031	0.0884
Neighboring Cost, J	1.0	0.935	1.278	0.531	1.0
Optimal Cost, J_{op}	1.0	0.943	1.44	0.55	1.0

Table 5.1. Data and Results for Problem of Minimum-Fuel Control of $1/s^2$ Plant.

of the neighboring trajectories, and hence the neighboring fuel requirement should be less than that required to satisfy the terminal constraints exactly. The distance from x(t) to the origin is defined by

$$||x(t)|| \equiv \sqrt{\sum_{i=1}^{n} x_i^2(t)} \quad . \tag{5.9}$$

Hence, $||x(t_f)|| \; / \; ||x_0||$ is the ratio of the distances, from the origin, of the neighboring final and initial states. This ratio reduces in magnitude when the neighboring initial states approach the nominal trajectory, as indicated by the results in Table 5.1 .

In Fig. 5.1 , Trajectory I lies closest to the nominal path and is very nearly optimal. The remaining neighboring trajectories are a significant distance from the nominal path and are, therefore, sub-optimal, as indicated by their non-satisfaction of the terminal constraints. Since K was allowed to become arbitrarily large, the sub-optimality of these trajectories is due entirely to the large deviations in the neighboring states away from the nominal path, and not due to the relaxation of the terminal constraints, required in order to obtain the neighboring feedback control law (see Section 2.3).

When solving Example IV, the open-loop phase of the neighboring control law mechanization dictated that N = 1 and $u(t_0) = 0$. This means that the minimum-fuel trajectory, to the origin, requires time $t_f \leq \bar{t}_f = 3.0$. Hence, the calculation of this trajectory becomes a free terminal-time problem, subject to the constraint $t_f \leq \bar{t}_f$. The feedback gains, $\bar{M}$ and $\bar{G}_1$, associated with free terminal-time trajectories, are given by (Eq. 3.32 and Eq. 3.59)

$$\bar{M} = \begin{bmatrix} 0.0 & 1.0 & 0.0 \end{bmatrix} , \tag{5.10}$$

$$\bar{G}_1 = \begin{bmatrix} -2.0 & 0.0 & 0.0 \end{bmatrix} . \tag{5.11}$$

These gains were used, in conjunction with the free terminal-time neighboring control law mechanization, to generate Trajectory IV in Fig. 5.1 . The neighboring final time was calculated to be $t_f = 1.625 < \bar{t}_f$. The optimal final time for this example is $(t_f)_{op} = 1.50$.

Finally, note that $t_{21} > \bar{t}_{21}$ for Trajectory II and $t_{11} > \bar{t}_{11}$ for Trajectory III. Hence, the switching function defined by Eq. 4.16″ was utilized to calculate these particular switch times.

5.2 Minimum-Time Control of $1/s(s^2+1)$ Plant

A problem considered by Flügge-Lotz and Mih Yin [15] is discussed in this section, namely, the minimum-settling-time problem for the $1/s(s^2+1)$ plant. The system dynamics are given by*

$$\begin{aligned} \dot{x}_1(t) &= x_2(t) \quad , \quad x_1(t_0) = x_{10} \quad , \\ \dot{x}_2(t) &= -x_1(t) + u(t) \quad , \quad x_2(t_0) = x_{20} \quad , \\ \dot{x}_3(t) &= u(t) \quad , \quad x_3(t_0) = x_{30} \quad , \end{aligned} \tag{5.12}$$

where the scalar control function is subject to the constraint

$$|u(t)| \leq 1.0 \quad , \quad t_0 \leq t \leq t_f \, . \tag{5.13}$$

---

* Eq. 5.12 is the normal form of the state equations for the $1/s(s^2+1)$ plant (see[15], pg. 35).

The performance index is

$$\bar{J} = t_f - t_0 \ . \tag{5.14}$$

By augmenting the state (Eq. 2.5) , the performance index may be written

$$\bar{J} = F[x(t_f)] = x_4(t_f) \tag{5.15}$$

where

$$\dot{x}_4(t) = 1 \quad , \quad x_4(t_0) = 0 \ . \tag{5.16}$$

The terminal constraints for this problem are written

$$\Psi[x(t_f)] = \begin{bmatrix} x_1(t_f) \\ x_2(t_f) \\ x_3(t_f) \end{bmatrix} = \begin{bmatrix} 0 \\ 0 \\ 0 \end{bmatrix} \ . \tag{5.17}$$

The number of nominal switch times is chosen to be $\bar{N} = 4$. Neighboring initial states which are controllable, and which require no more than four switch times, are considered. Set $t_0 = \bar{t}_0 = 0.0$ and choose the nominal initial state to be $(\bar{x}_{10}, \bar{x}_{20}, \bar{x}_{30}) = (-3.600, 2.000, -3.665)$. The minimum-time trajectory, to the origin, from this initial state is known (see [15], Fig. 3.6), and is shown in both Fig. 5.2A and Fig. 5.2B . The nominal switch-time vector is $\bar{t}_s = (8.360, 6.789, 2.077, 0.506)$, and the nominal final time is $\bar{t}_f = 9.930$. The nominal initial control function is $\bar{u}(\bar{t}_0) = +1.0$, and the nominal final control function is $\bar{u}(\bar{t}_f) = +1.0$.

Again, as in the second-order example (Section 5.1) , set the weighting matrix, W, equal to the third-order identity matrix, and let the scalar gain, K, become arbitrarily large (see Eq. 2.10). The

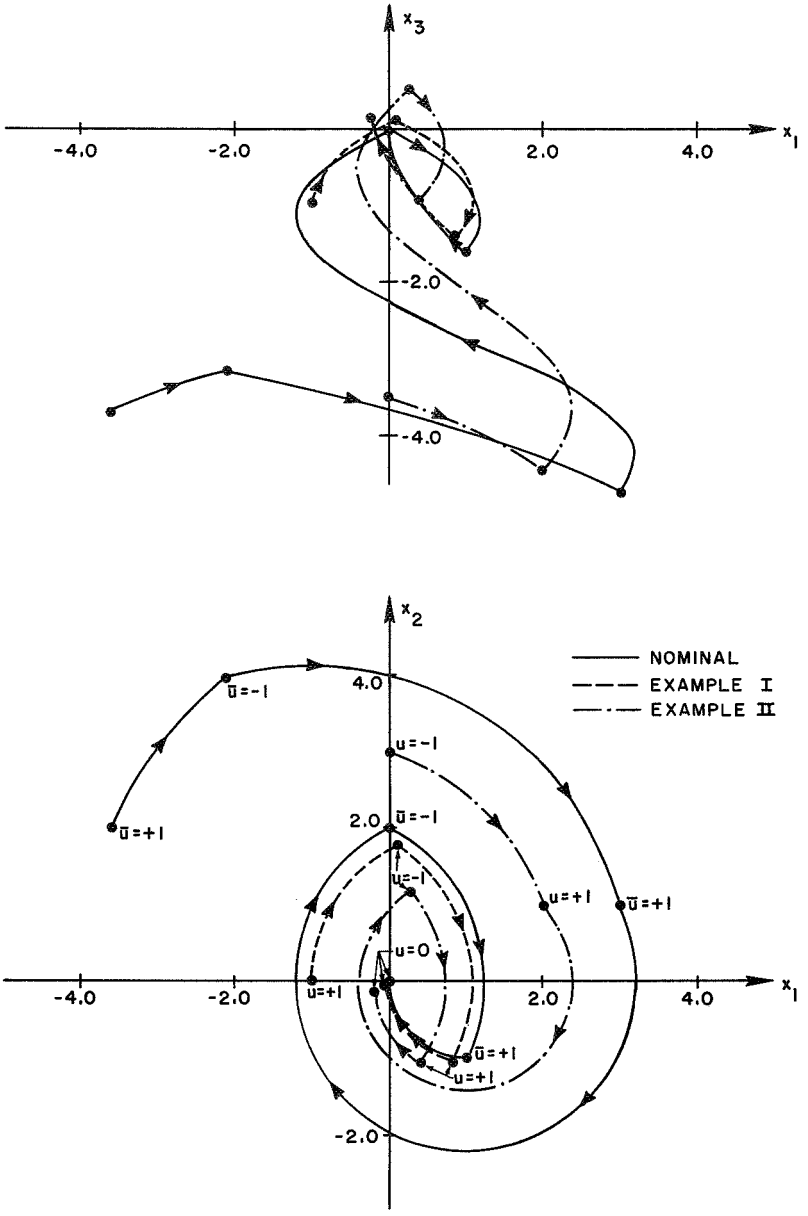

Figure 5.2A. Neighboring Trajectories for Problem of Minimum-Time Control of $1/s(s^2 + 1)$ Plant: Example I and Example II.

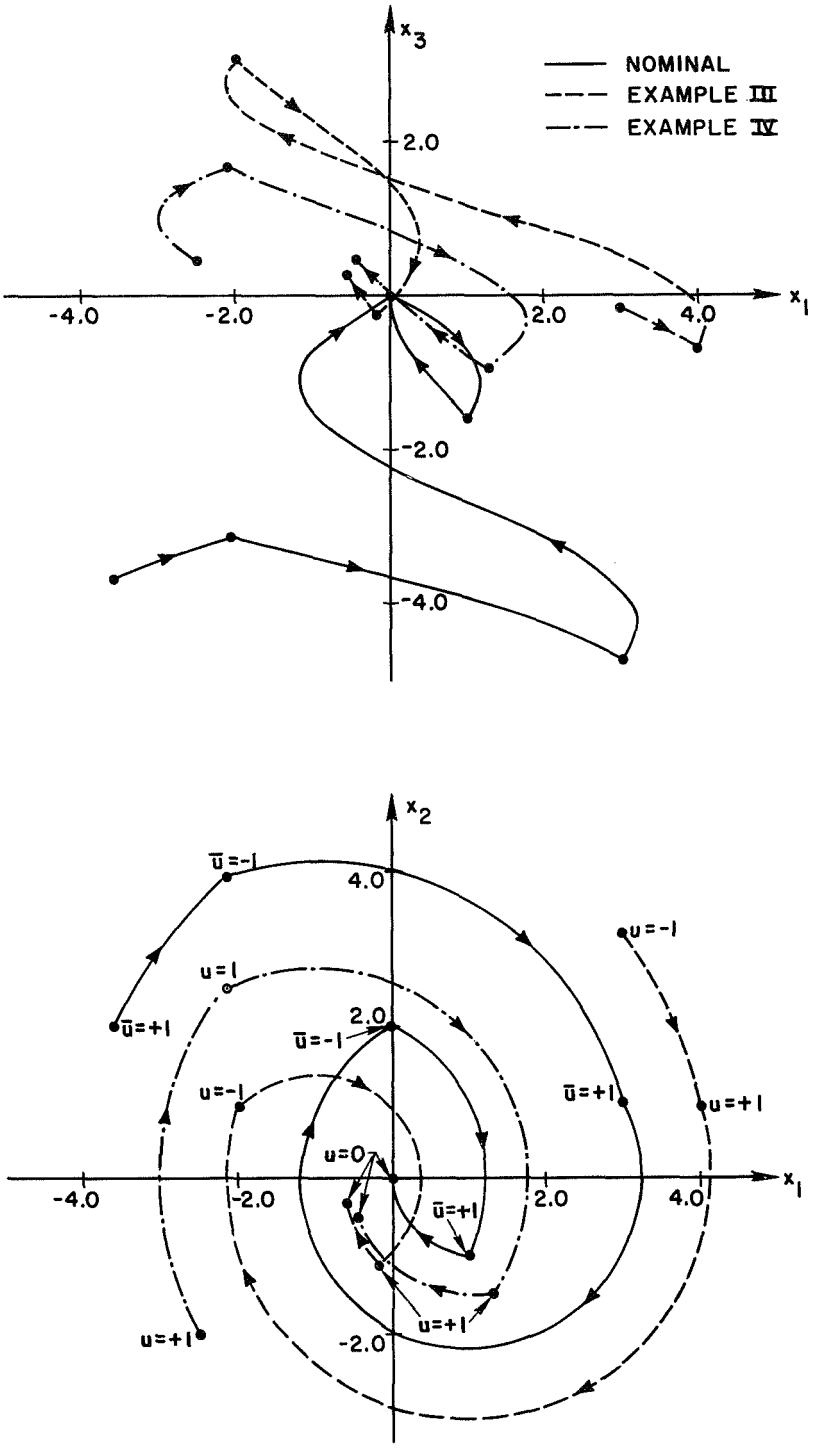

Figure 5.2B. Neighboring Trajectories for Problem of Minimum-Time Control of $1/s(s^2 + 1)$ Plant: Example III and Example IV.

system dynamics (Eq. 5.12) are linear, and hence Eq. 3.57, in conjunction with Eq. 3.61, is again used to calculate the feedback gains, $\bar{G}_N$ and $\bar{g}_0$, N = 1,$\cdots$, 4 . These gains, along with the final-time feedback gain, $\bar{M}$ (Eq. 3.32 or Eq. 3.60 with N = 0) , are given in Table 5.2 .

Using the feedback gains in Table 5.2 , the neighboring optimal feedback control scheme for free terminal-time problems was applied to the following initial states:

$$\text{Example I:} \quad x_0 = \begin{bmatrix} -1.000 \\ 0.0 \\ -0.965 \end{bmatrix}$$

$$\text{Example II:} \quad x_0 = \begin{bmatrix} 0.0 \\ 3.0 \\ -3.5 \end{bmatrix}$$

$$\text{Example III:} \quad x_0 = \begin{bmatrix} 2.970 \\ 3.190 \\ -0.175 \end{bmatrix}$$

$$\text{Example IV :} \quad x_0 = \begin{bmatrix} -2.500 \\ -2.000 \\ 0.488 \end{bmatrix}$$

For each of these initial states, the open-loop phase of the neighboring control scheme (see Section 4.4) deduced that $u(t_f) = +1.0$, verifying that the chosen nominal trajectory, with $\bar{u}(\bar{t}_f) = +1.0$, is appropriate for these initial states. The neighboring trajectories for these states are shown in Fig. 5.2 A and Fig. 5.2 B, and are specified in

Number of Switch Times	Feedback Gain $\bar{G}_N$	$\bar{g}_0$
N = 4	$\begin{bmatrix} -0.250 & 0.0 & 0.0 & 0.0 \\ -0.125 & -0.125 & 0.125 & 0.0 \\ -0.250 & 0.0 & 0.0 & 0.0 \\ -0.125 & -0.125 & 0.125 & 0.0 \end{bmatrix}$	$\begin{bmatrix} -0.5 & 0.5 & 0.5 & 0.0 \end{bmatrix}$
N = 3	$\begin{bmatrix} -0.25 & 0.0 & 0.0 & 0.0 \\ -0.25 & -0.25 & 0.25 & 0.0 \\ -0.25 & 0.0 & 0.0 & 0.0 \end{bmatrix}$	$\begin{bmatrix} -0.5 & 0.5 & 0.5 & 0.0 \end{bmatrix}$
N = 2	$\begin{bmatrix} -0.50 & 0.0 & 0.0 & 0.0 \\ -0.25 & -0.25 & 0.25 & 0.0 \end{bmatrix}$	$\begin{bmatrix} -0.5 & 0.5 & 0.5 & 0.0 \end{bmatrix}$
N = 1	$\begin{bmatrix} -0.333 & 0.166 & -0.166 & 0.0 \end{bmatrix}$	$\begin{bmatrix} -0.333 & 0.667 & 0.333 & 0.0 \end{bmatrix}$
N = 0	$\begin{bmatrix} 0.0 & 0.0 & 0.0 & 0.0 \end{bmatrix}$	$\begin{bmatrix} 0.0 & 0.5 & 0.5 & 0.0 \end{bmatrix}$

Table 5.2. Neighboring Feedback Gains for Problem of Minimum-Time Control of $1/s(s^2+1)$ Plant.

Table 5.3 by the initial and final control function, the number of switch times, the switch-time vector, the final time, and the final state.

In Fig. 5.2A, Trajectory I, with two switch times, lies quite close to the nominal trajectory and is very nearly optimal, as indicated by $x(t_f)$ for Example I in Table 5.3. Trajectory II, with three switch times, lies farther from the nominal path, but is still reasonably close to being optimal. Again, since K was allowed to become

Trajectory	Nominal	Example I	Example II	Example III	Example IV
Initial State, x_0	$\begin{bmatrix} -3.600 \\ 2.000 \\ -3.665 \end{bmatrix}$	$\begin{bmatrix} -1.000 \\ 0.0 \\ -0.965 \end{bmatrix}$	$\begin{bmatrix} 0.0 \\ 3.0 \\ -3.5 \end{bmatrix}$	$\begin{bmatrix} 2.970 \\ 3.190 \\ -0.175 \end{bmatrix}$	$\begin{bmatrix} -2.500 \\ -2.000 \\ 0.488 \end{bmatrix}$
Initial Control Function, $u(t_0)$	+1.0	+1.0	-1.0	-1.0	+1.0
Final Control Function, $u(t_f)$	+1.0	+1.0	+1.0	+1.0	+1.0
Number of Switch Times, N	4	2	3	3	2
Switch-Time Vector, t_s	$\begin{bmatrix} 8.360 \\ 6.789 \\ 2.077 \\ 0.506 \end{bmatrix}$	$\begin{bmatrix} 2.63 \\ 1.10 \end{bmatrix}$	$\begin{bmatrix} 7.28 \\ 5.88 \\ 0.93 \end{bmatrix}$	$\begin{bmatrix} 7.55 \\ 4.24 \\ 0.49 \end{bmatrix}$	$\begin{bmatrix} 3.77 \\ 1.19 \end{bmatrix}$
Final Time, t_f	9.930	4.030	8.260	8.110	5.200
Final State, $x(t_f)$	$\begin{bmatrix} 0.0 \\ 0.0 \\ 0.0 \end{bmatrix}$	$\begin{bmatrix} -0.0353 \\ 0.0005 \\ 0.0054 \end{bmatrix}$	$\begin{bmatrix} -0.2048 \\ -0.0927 \\ 0.1037 \end{bmatrix}$	$\begin{bmatrix} -0.5751 \\ -0.3084 \\ 0.3333 \end{bmatrix}$	$\begin{bmatrix} -0.4484 \\ -0.5180 \\ 0.5270 \end{bmatrix}$
$\|\|x(t_f)\|\| \; / \; \|\|x_0\|\|$	0.0	0.0257	0.0536	0.1678	0.2669

Table 5.3. Data and Results for Problem of Minimum-Time Control of $1/s(s^2 + 1)$ Plant.

arbitrarily large when calculating the feedback gains in Table 5.2, the sub-optimality of these trajectories, as well as of those in Fig. 5.2B , is due entirely to the finite deviations in the neighboring states away from the nominal path.

Trajectory III and Trajectory IV, in Fig. 5.2B, show the action of the neighboring control scheme when applied to states which are far from the nominal path. As indicated by $||x(t_f)|| \; / \; ||x_0||$, given for each neighboring trajectory in Table 5.3, the degree of optimality of these trajectories is seriously reduced. Nonetheless, considering the magnitudes of the deviations in the neighboring states away from the nominal path, the neighboring control scheme performs reasonably well, even though the terminal constraints are not satisfied.

In Fig. 5.3, the neighboring and true optimal trajectories for Example III and Example IV are compared. The optimal trajectories for these initial states were determined by the techniques described in [15]. The optimal and neighboring switch times and final times, for these example trajectories, are compared in Table 5.4 .

	Example III	Example IV
Neighboring Switch-Time Vector, t_s	$\begin{bmatrix} 7.55 \\ 4.24 \\ 0.49 \end{bmatrix}$	$\begin{bmatrix} 3.77 \\ 1.19 \end{bmatrix}$
Optimal Switch-Time Vector, $(t_s)_{op}$	$\begin{bmatrix} 6.975 \\ 4.014 \\ 0.698 \end{bmatrix}$	$\begin{bmatrix} 3.840 \\ 0.890 \end{bmatrix}$
Neighboring Final Time, t_f	8.110	5.200
Optimal Final Time, $(t_f)_{Min}$	7.500	5.410

Table 5.4. Comparison of Neighboring and Optimal Switch Times and Final Times for Example III and Example IV.

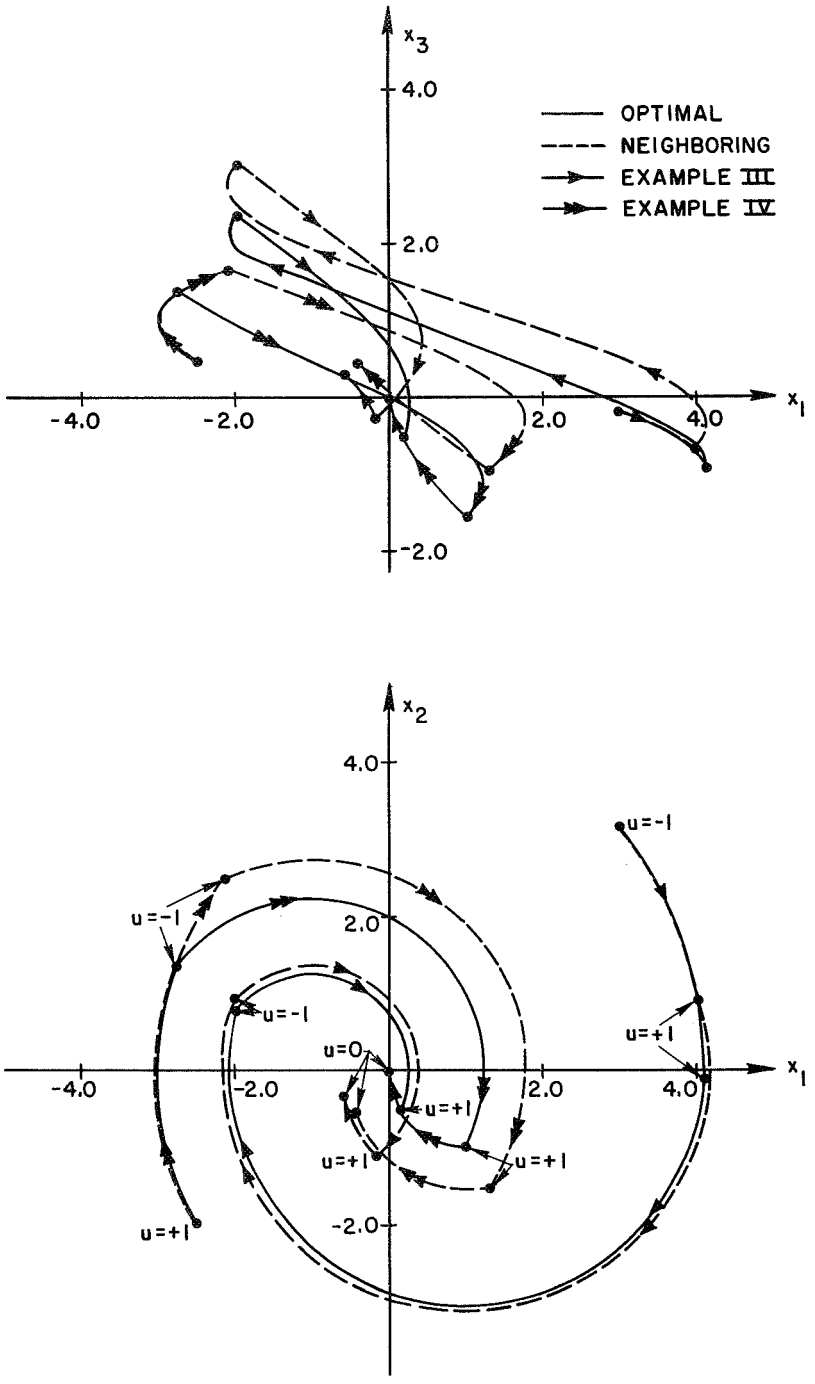

Figure 5.3. Neighboring and Optimal Trajectories for Problem of Minimum-Time Control of $1/s(s^2 + 1)$ Plant: Example III and Example IV.

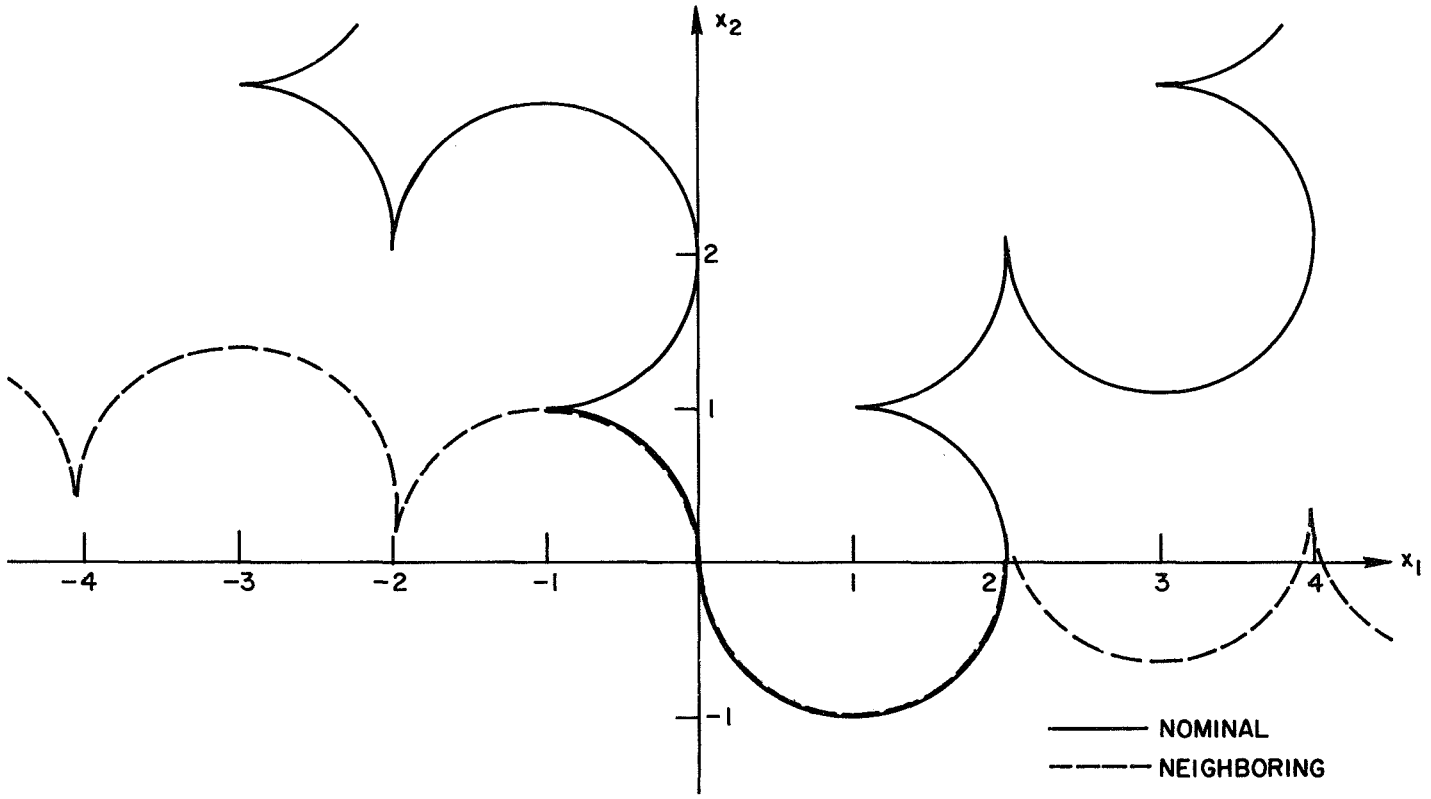

Figure 5.4. The Projections of the Optimal Nominal and Neighboring Switching Curves Onto the x_1x_2-Plane: Example III and Example IV.

Finally, recall that the switching surface generated by the neighboring control scheme is, in a sense, a linear approximation of the nominal switching surface at the nominal switch points (see Section 4.1). The projection of the optimal, nominal switching curve, onto the x_1x_2 -plane, is shown in Fig. 5.4 (see [15], Fig. 3.6). The projection of the optimal switching curve for the neighboring initial states of Example III and Example IV is also shown in Fig. 5.4 (see [15], Fig. 3.3). The irregularity of the optimal switching surface, and the geometric dissimilarity of the switching surface at the nominal and neighboring optimal switch points, are indicated in Fig. 5.4 by these projections. Hence, for these example trajectories, one cannot expect that a linearization of the switching surface at the nominal switch points is a good approximation to the optimal switching surface at the neighboring switch points.* It is therefore concluded that this example problem is a severe test for the neighboring optimal control scheme developed in this paper. One should expect improvement in the performance of the neighboring control scheme when applied to problems with better behaved optimal switching surfaces.

5.3 Minimum-Time Satellite Attitude-Acquisition Problem

The problem considered in this section is the problem of minimum-time attitude control of an earth-orbiting satellite. It is assumed that the attitude of the satellite is controlled by three high-torque

---

* It would be interesting to compare the numerical results obtained here with those of Frederick [17] for the $1/s(s^2+1)$ plant. He designed linear and piecewise-linear switching functions for the quasi-minimum-time control of this plant.

cold gas jets fixed to the satellite and alligned with the three principal axes of the satellite. The torque level generated by the cold gas jets is assumed to be large compared to the gravity-gradient and disturbance torques acting on the vehicle. The satellite is assumed to be a rigid body and the earth is taken to be an inertially fixed point mass.

The problem considered here is the minimum-time attitude-acquisition problem. That is, given an initial state, x_0 , use the neighboring optimal feedback control scheme to acquire a desired state, x_f , in minimum time. The three-axis Euler angles, θ_i , i = 1,2,3, defined in Appendix C(yaw, roll, and pitch angles, respectively), and the associated inertial angular velocity components, ω_i , i= 1,2,3, are chosen to be the state variables for this system.* Hence, the (6 x 1) state vector is defined to be

$$x(t) \equiv \begin{bmatrix} \theta_1(t) \\ \theta_2(t) \\ \theta_3(t) \\ \omega_1(t) \\ \omega_2(t) \\ \omega_3(t) \end{bmatrix}, \quad t_0 \leq t \leq t_f , \tag{5.18}$$

where $\theta_i(t)$, i = 1,2,3, are measured in radians, and $\omega_i(t)$, i = 1,2,3, are measured in radians per second. Since a feedback control law is utilized in the solution of this problem, the state must be measurable.

---

* The angular velocity components, ω_i, i = 1,2,3, are inertial under the assumption that the earth is inertially fixed. This is made evident in Appendix C.

A brief discussion on possible techniques for measuring $\theta_i(t)$ and $\omega_i(t)$, i = 1,2,3, is presented in Appendix D.

The dynamical and kinematical equations for the satellite are discussed in detail in Appendix C. For simplicity, the discussion here is limited to satellites in circular orbit with angular velocity r(i.e. $\dot{\theta}$ = r in Eq. C.6 of Appendix C). Then, using Eq. 5.18 in Eq. C.4 and Eq. C.6 of Appendix C, the state dynamical equations are written as follows:

$$
\begin{aligned}
\dot{x}_1(t) &= \frac{1}{c_2}[x_4(t)c_3 - x_5(t)s_3 + rc_1s_2] \ , \ x_1(t_0) = \theta_{10} \ , \\
\dot{x}_2(t) &= x_4(t)s_3 + x_5(t)c_3 - rs_1, \ x_2(t_0) = \theta_{20} \ , \\
\dot{x}_3(t) &= \frac{1}{c_2}[-x_4(t)s_2c_3 + x_5(t)s_2s_3 + x_6(t)c_2 - rc_1], x_3(t_0) = \theta_{30}, \\
\dot{x}_4(t) &= u_1(t) - k_1x_5(t)x_6(t) \ , \ x_4(t_0) = \omega_{10} \ , \\
\dot{x}_5(t) &= u_2(t) - k_2x_6(t)x_4(t) \ , \ x_5(t_0) = \omega_{20}, \\
\dot{x}_6(t) &= u_3(t) - k_3x_4(t)x_5(t) \ , \ x_6(t_0) = \omega_{30} \ ,
\end{aligned}
\tag{5.19}
$$

where $s_i = \sin(x_i(t))$, i = 1,2,3, and $c_i = \cos(x_i(t))$, i = 1,2,3. In Eq. 5.19, the control vector components, $u_i(t)$, i = 1,2,3, have the dimensions of radians per second per second (see Eq. C.3 in Appendix C).

The particular satellite, considered in this study, is the same as the satellite considered by Wolske [2] . The principal moments of inertia (see Appendix C)are given by

$$
I_1 = 800 \text{ slug-ft}^2 \ , \tag{5.20 cont.}
$$

$$I_2 = 581 \text{ slug-ft}^2 \ ,$$

$$I_3 = 300 \text{ slug-ft}^2 \ , \tag{5.20}$$

and the resulting inertia parameters (Eq. C.2 in Appendix C) are

$$k_1 = -0.351 \ ,$$

$$k_2 = \ 0.860 \ , \tag{5.21}$$

$$k_3 = -0.730 \ .$$

Also, from Wolske, $\beta_1 \equiv \beta_2 \equiv \beta_3 \equiv \beta = 0.206\ \pi/180.0$ rad/sec^2 (see Eq. 2.2). That is, the control vector components must satisfy the constraints

$$|u_i(t)| \leq \beta = \frac{0.206}{180.0}\,\pi\ \frac{\text{rad}}{\text{sec}^2} \ , \ i = 1,2,3; \ t_0 \leq t \leq t_f \ . \tag{5.22}$$

The orbital angular velocity, r , is chosen to be

$$r = 1.0583 \times 10^{-3}\ \frac{\text{rad}}{\text{sec}} \ , \tag{5.23}$$

which corresponds to a circular orbit with an approximate period of 99 minutes.

The chosen control objective is to give the satellite zero angular velocity and zero angular displacement relative to the orbital reference axes (see Fig. C.1 and Fig. C.2 in Appendix C). That is, the control objective is to make the satellite earth-pointing, with one principal axis of the satellite directed toward the earth and another principal axis directed normal to the orbit plane. To achieve this objective, the terminal constraints are written as follows:

$$\Psi[x(t_f)] = \begin{bmatrix} x_1(t_f) \\ x_2(t_f) \\ x_3(t_f) \\ x_4(t_f) \\ x_5(t_f) \\ x_6(t_f) - r \end{bmatrix} = \begin{bmatrix} 0 \\ 0 \\ 0 \\ 0 \\ 0 \\ 0 \end{bmatrix} . \qquad (5.24)$$

Again, by augmenting the state (Eq. 2.5) , the performance index is written

$$\bar{J} = F[x(t_f)] = x_7(t_f) , \qquad (5.25)$$

where

$$\dot{x}_7(t) = 1 , \; x_7(t_0) = 0 . \qquad (5.26)$$

A number of optimal, nominal trajectories were generated by integrating backwards, simultaneously, the adjoint and state equations for different values of the final adjoint vector. It was found that, for the initial states of interest, only three nominal switch times were required, one for each component of the control vector. Thus, the number of nominal switch times was chosen to be $\bar{N} = 3$. The nominal final control vector was chosen to be $\bar{u}(\bar{t}_f) = (+\beta , +\beta , +\beta)$. Therefore, only neighboring initial states for which $u(t_f) = (+\beta, +\beta, +\beta)$ are considered in the examples of this section. The chosen nominal, minimum-time trajectory and control history are shown in both Fig. 5.5A,B,C and Fig. 5.6 A,B,C . The nominal initial state, initial control vector, switch-time vector, time-sequence of the nominal control-component switchings, and final time, are given in Table 5.5 .

To calculate the feedback gains, the nominal and neighboring initial times were set equal to zero, and the weighting matrix, W (see Eq. 2.10) , was chosen to be the sixth-order identity matrix.

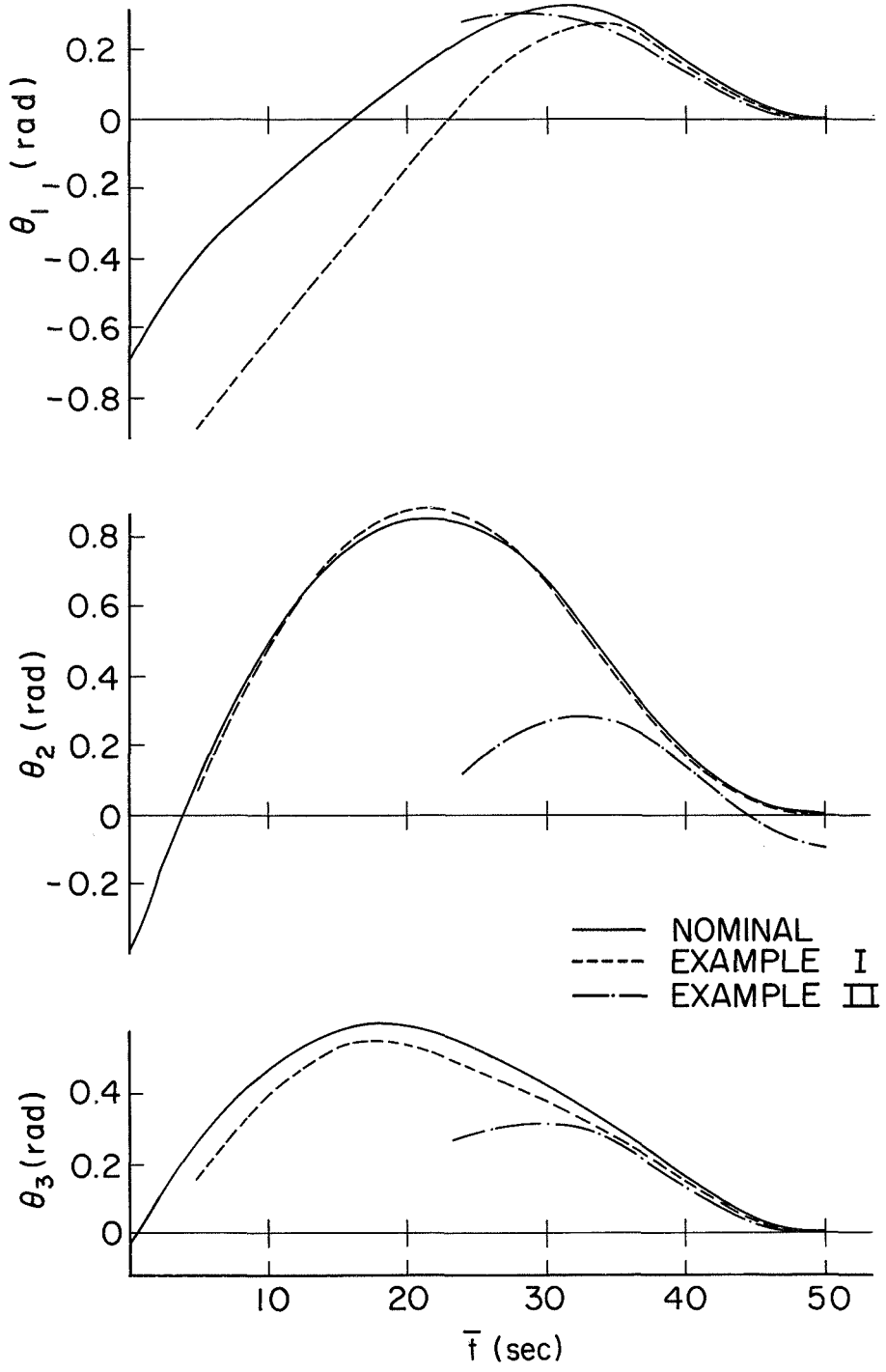

Figure 5.5A. Neighboring Euler Angle Time History: Example I and Example II of Satellite Attitude-Acquisition Problem.

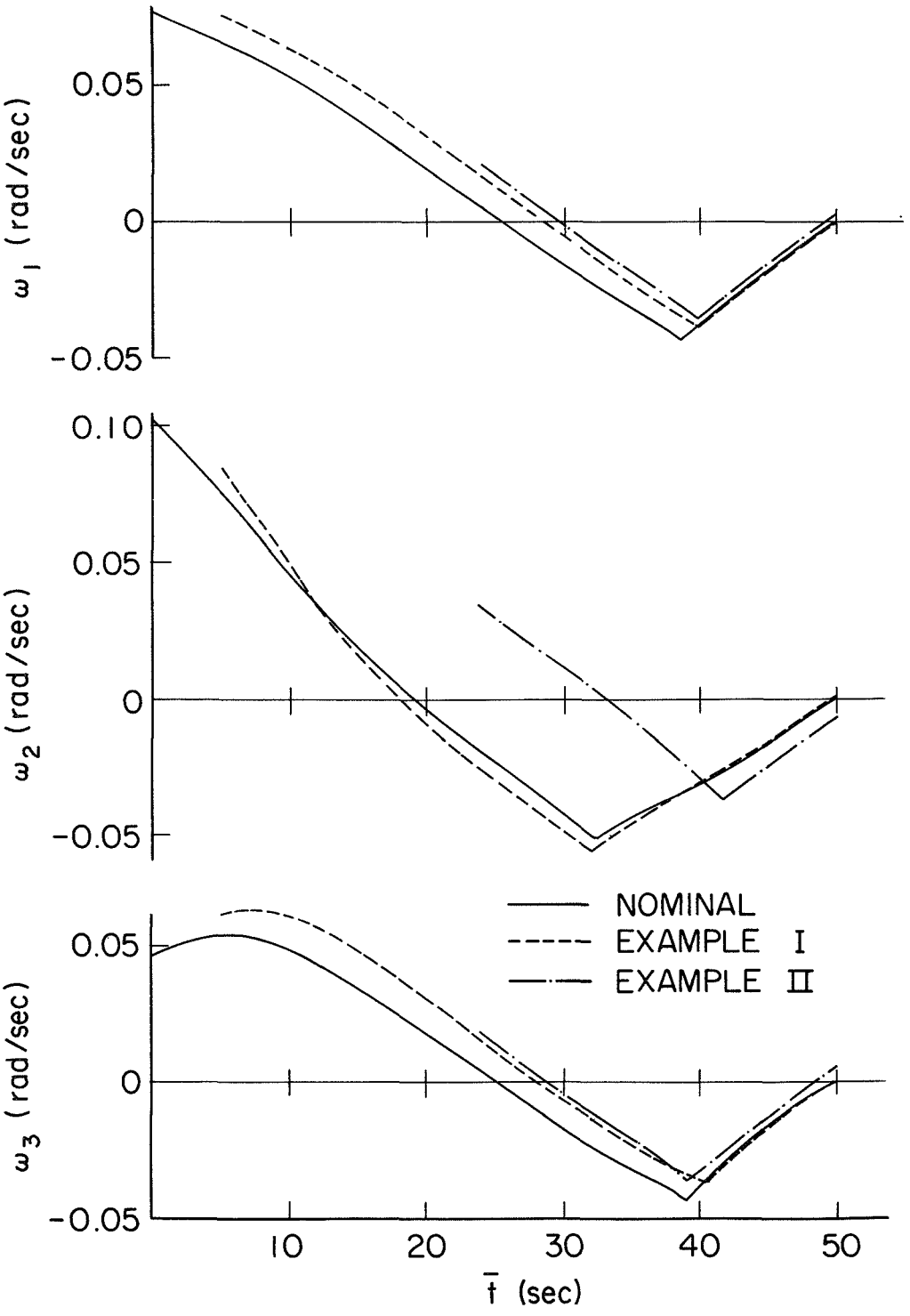

Figure 5.5B. Neighboring Angular Velocity Time History: Example I and Example II of Satellite Attitude-Acquisition Problem.

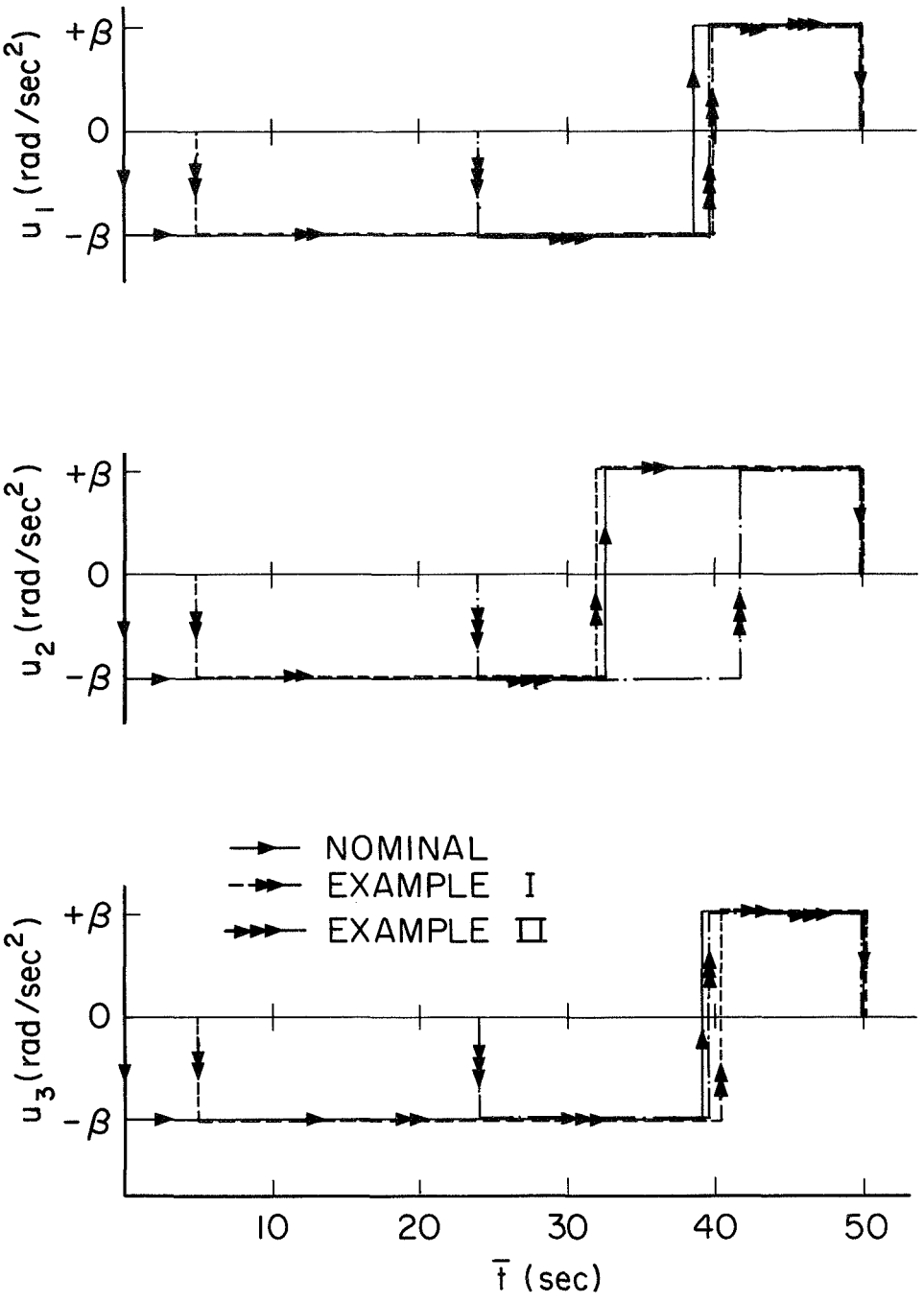

Figure 5.5C. Neighboring Control Function Time History: Example I and Example II of Satellite Attitude-Acquisition Problem.

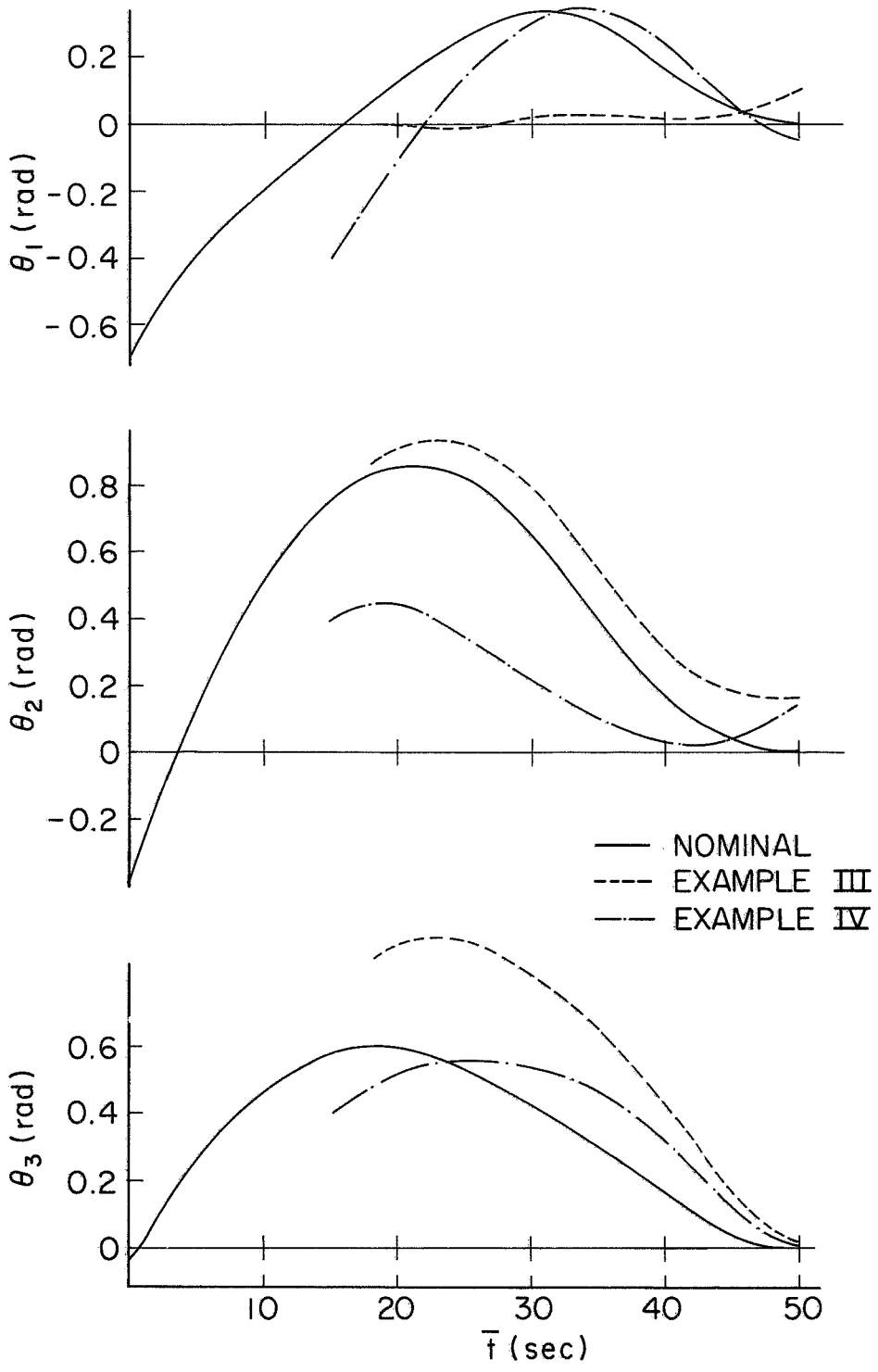

Figure 5.6A. Neighboring Euler Angle Time History: Example III and Example IV of Satellite Attitude-Acquisition Problem.

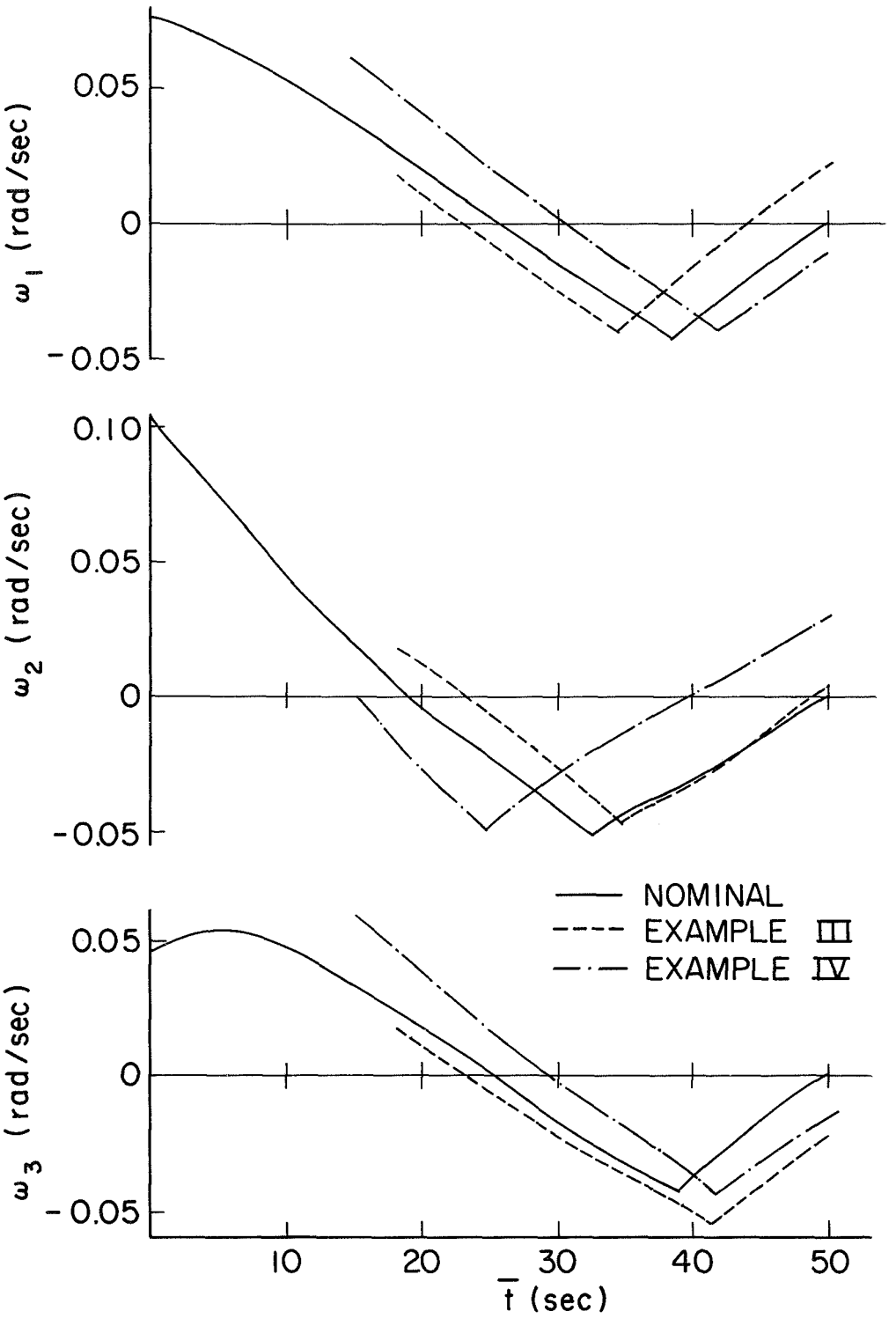

Figure 5.6B. Neighboring Angular Velocity Time History: Example III and Example IV of Satellite Attitude-Acquisition Problem.

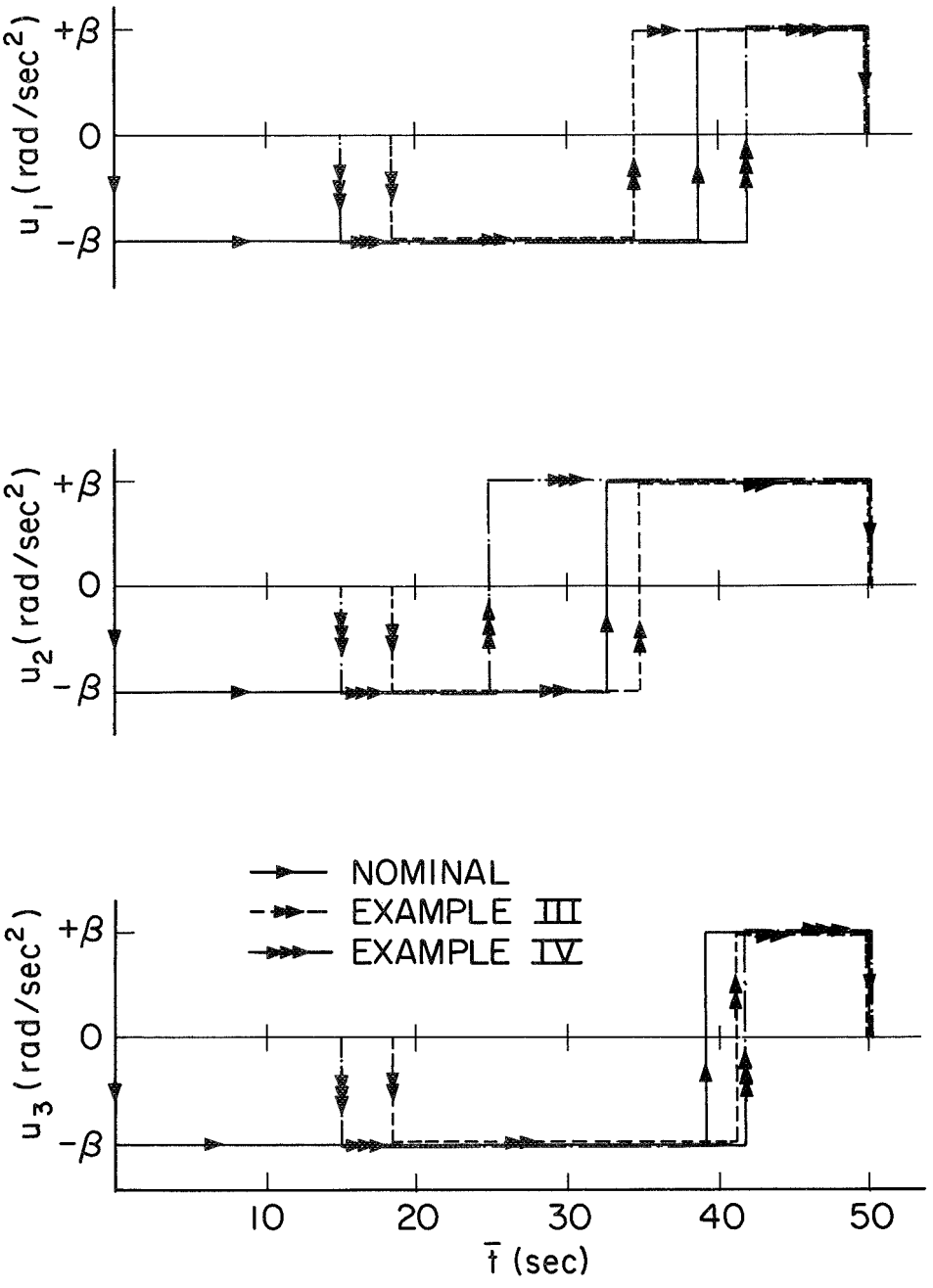

Figure 5.6C. Neighboring Control Function Time History: Example III and Example IV of Satellite Attitude-Acquisition Problem.

Trajectory	Nominal	Example I	Example II	Example III	Example IV
Initial State, x_0	$\begin{bmatrix} -.69464 \\ -.38946 \\ -.02859 \\ .07633 \\ .10914 \\ .04704 \end{bmatrix}$	$\begin{bmatrix} -.89055 \\ .06821 \\ .15746 \\ .07526 \\ .08445 \\ .06174 \end{bmatrix}$	$\begin{bmatrix} .28001 \\ .12066 \\ .27800 \\ .02096 \\ .03375 \\ .01774 \end{bmatrix}$	$\begin{bmatrix} 0.0 \\ 0.87266 \\ 0.87266 \\ 0.01693 \\ 0.01807 \\ 0.01813 \end{bmatrix}$	$\begin{bmatrix} -.40000 \\ 0.40000 \\ 0.40000 \\ 0.06000 \\ 0.0 \\ 0.06000 \end{bmatrix}$
Initial Control Vector, $u(t_0)$ - rad/sec^2	$\begin{bmatrix} -\beta \\ -\beta \\ -\beta \end{bmatrix}$	$\begin{bmatrix} -\beta \\ -\beta \\ -\beta \end{bmatrix}$	$\begin{bmatrix} -\beta \\ -\beta \\ -\beta \end{bmatrix}$	$\begin{bmatrix} -\beta \\ -\beta \\ -\beta \end{bmatrix}$	$\begin{bmatrix} -\beta \\ -\beta \\ -\beta \end{bmatrix}$
Final Control Vector, $u(t_f)$ - rad/sec^2	$\begin{bmatrix} +\beta \\ +\beta \\ +\beta \end{bmatrix}$	$\begin{bmatrix} +\beta \\ +\beta \\ +\beta \end{bmatrix}$	$\begin{bmatrix} +\beta \\ +\beta \\ +\beta \end{bmatrix}$	$\begin{bmatrix} +\beta \\ +\beta \\ +\beta \end{bmatrix}$	$\begin{bmatrix} +\beta \\ +\beta \\ +\beta \end{bmatrix}$
Number of Switch Times, N	3	3	3	3	3
Switch-Time Vector, t_s-sec	$\begin{bmatrix} 39.1652 \\ 38.7611 \\ 32.5010 \end{bmatrix}$	$\begin{bmatrix} 35.395 \\ 34.995 \\ 27.147 \end{bmatrix}$	$\begin{bmatrix} 15.550 \\ 15.900 \\ 17.649 \end{bmatrix}$	$\begin{bmatrix} 23.048 \\ 16.200 \\ 16.450 \end{bmatrix}$	$\begin{bmatrix} 26.547 \\ 26.797 \\ 9.550 \end{bmatrix}$
Time-sequence of Control-Component Switchings	$\bar{u}_2, \bar{u}_1, \bar{u}_3$	u_2, u_1, u_3	u_3, u_1, u_2	u_1, u_2, u_3	u_2, u_3, u_1
Final Time, t_f- sec	50.0	45.043	25.997	31.696	34.795
Final State, $x(t_f)$	$\begin{bmatrix} 0.0 \\ 0.0 \\ 0.0 \\ 0.0 \\ 0.0 \\ r \end{bmatrix}$	$\begin{bmatrix} -.00543 \\ .00192 \\ -.00124 \\ -.00021 \\ .00028 \\ .00106 \end{bmatrix}$	$\begin{bmatrix} -00364 \\ -.09557 \\ .00545 \\ .00289 \\ -.00707 \\ .00573 \end{bmatrix}$	$\begin{bmatrix} .09686 \\ .16594 \\ .02072 \\ .02148 \\ .00312 \\ -.02324 \end{bmatrix}$	$\begin{bmatrix} -.04598 \\ .13538 \\ .01807 \\ -.01209 \\ .02958 \\ -.01631 \end{bmatrix}$

Table 5.5. Data and Results for Minimum-Time Satellite Attitude-Acquisition Problem.

The scalar gain, K (see Eq. 2.10), was set equal to 10^5 . The system dynamics for this problem (Eq. 5.19) are nonlinear in the state, and hence no simplifications in the feedback gains, $\bar{G}_N$ and $\bar{g}_0$, $N = 1,2,3,$ as defined in Eq. 3.59 and Eq. 3.60, are possible.* These gains, along with the final-time feedback gain, $\bar{M}$ (Eq. 3.32 or Eq. 3.60 with $N = 0$), are given in Table 5.6 .

The neighboring optimal feedback control scheme for free terminal-time problems was applied to four initial states, listed in Table 5.5.** For each of these examples, the open-loop phase of the neighboring control scheme (see Section 4.4) verified that the chosen nominal trajectory is appropriate for the chosen initial state (i.e. $u(t_f) = \bar{u}(\bar{t}_f)$ for each example trajectory). The neighboring state and control time histories for these initial states are shown in Fig. 5.5A,B,C and Fig. 5.6A, B, C . Since the neighboring control law algorithm is based upon time-to-go until the next switch time, and until the final time, these trajectories are plotted to terminate at the nominal final time. This allows one to make a better comparison between the neighboring and nominal, state and control, time histories. Each neighboring trajectory is also specified in Table 5.5 by the initial and final control vector, the number of switch times, the switch-time vector, the time-sequence of control-component switchings, the final time, and the final state.

---

* The calculation of the feedback gains in Section 5.1 and Section 5.2 was simplified since the system dynamics for the problems considered there are linear in the state.

* Example III corresponds, numerically, to the minimum-time problem considered by Wolske ([2], pp. 63-72). He obtains a sub-optimal, bang-zero-bang control function with a 37 sec. operating time. It is interesting to compare his results with those obtained in this section.

Number of Switch Times	Feedback Gains: $\bar{G}_N, \bar{g}_0$	
N = 3	$\bar{G}_3$	$\begin{bmatrix} -2.2494 & -.3564 & -12.8022 & .4155 & .3014 & -.6849 & 0.0 \\ -11.8812 & -3.0110 & .2969 & -.6230 & .1879 & .4606 & 0.0 \\ 1.7870 & -8.1730 & .3778 & .1209 & -.3840 & .2668 & 0.0 \end{bmatrix}$
	$\bar{g}_0$	$\begin{bmatrix} -9.0834 & -4.9777 & -9.0529 & 92.9890 & 92.2471 & 92.9412 & 0.0 \end{bmatrix}$
N = 2	$\bar{G}_2$	$\begin{bmatrix} -2.0921 & -1.0755 & -12.7690 & .4262 & .2676 & -.6614 & 0.0 \\ -11.9693 & -2.6079 & .2783 & -.6290 & .2069 & .4474 & 0.0 \end{bmatrix}$
	$\bar{g}_0$	$\begin{bmatrix} -9.6150 & -2.5462 & -9.1653 & 92.9530 & 92.3613 & 92.8618 & 0.0 \end{bmatrix}$
N = 1	$\bar{G}_1$	$\begin{bmatrix} -.2054 & -.6644 & -12.8128 & .5253 & .2350 & -.7320 & 0.0 \end{bmatrix}$
	$\bar{g}_0$	$\begin{bmatrix} -.1518 & -.4843 & -9.3853 & 93.4503 & 92.1978 & 92.5080 & 0.0 \end{bmatrix}$
N = 0	$\bar{G}_0$	$\begin{bmatrix} 0.0 & 0.0 & 0.0 & 0.0 & 0.0 & 0.0 & 0.0 \end{bmatrix}$
	$\bar{M}$	$\begin{bmatrix} -.0013 & .0024 & 0.0 & 93.0655 & 92.0256 & 93.0442 & 0.0 \end{bmatrix}$

Table 5.6. Neighboring Feedback Gains for Minimum-Time Satellite Attitude-Acquisition Problem.

Trajectory I in Fig. 5.5 A,B,C is very nearly optimal, as indicated by $x(t_f)$ for Example I in Table 5.5. Only the initial yaw angle $(\theta_1(t_0))$ deviates significantly from the nominal. This is reflected by the fact that $\theta_1(t_f)$ is several times larger than $\theta_2(t_f)$ and $\theta_3(t_f)$. Also note that the order in which the control components switch along this example trajectory is the same as that for the nominal trajectory.

The deviations in the neighboring states away from the nominal path, for each of the three remaining examples, are much larger than those in Example I. The performance level of the neighboring control scheme is, therefore, reduced. Also, the order in which the control components switch, for each of these three examples, differs from that for the nominal path (see Table 5.5, Fig. 5.5C, and Fig. 5.6C). For the range of initial states considered here, the final yaw angle $(\theta_1(t_f))$ does not exceed 5.6^o, the final roll angle $(\theta_2(t_f))$ does not exceed 9.5^o, and the final pitch angle $(\theta_3(t_f))$ does not exceed 1.2^o. The final yaw, roll, and pitch rates ($\omega_1(t_f)$, $\omega_2(t_f)$, $\omega_3(t_f)$, respectively), for these examples, never exceed 1.7^o/sec.

These deviations away from the desired terminal constraints (Eq. 5.24) can be reduced by generating nominal trajectories which are closer to the neighboring initial states. However, it should be kept in mind that, in general, the terminal constraints will never be satisfied exactly. This is due to the fact that, as one approaches the terminal state, the number of remaining switch times is not sufficient in number to satisfy the terminal constraints. Therefore, the neighboring control scheme should be used as a neighborhood-acquisition control law. When the degree of non-satisfaction of the terminal constraints is

beyond allowed tolerances, a high-accuracy, station-keeping control scheme should be used to reduce the deviations in the final state away from its desired value.

	Example I	Example II
Neighboring Switch-Time Vector, t_s - sec	$\begin{bmatrix} 35.395 \\ 34.995 \\ 27.147 \end{bmatrix}$	$\begin{bmatrix} 15.550 \\ 15.900 \\ 17.649 \end{bmatrix}$
Optimal Switch-Time Vector, $(t_s)_{op}$ - sec	$\begin{bmatrix} 35.314 \\ 34.950 \\ 27.232 \end{bmatrix}$	$\begin{bmatrix} 15.511 \\ 15.736 \\ 16.283 \end{bmatrix}$
Neighboring Final Time, t_f - sec	45.043	25.997
Optimal Final Time, $(t_f)_{Min}$ - sec	45.000	25.000

Table 5.7. Comparison of Neighboring and Optimal Switch Times and Final Times for Example I and Example II.

Finally, in order to make a direct comparison between the optimal and neighboring control laws, the optimal and neighboring switch-time vectors and final times, for Example I and Example II, are shown in Table 5.7 . The deviations, from their optimal values, in the neighboring switch times and final times, are easily deduced from Table 5.7 for these examples. These deviations are felt to be representative of those encountered when applying the neighboring control scheme to initial states which are similarly displaced away from any generated nominal path.

CHAPTER VI

SUMMARY AND CONCLUSIONS

The concept of neighboring optimal feedback control of high-order, nonlinear systems, with multi-dimensional, discontinuous control functions, has been investigated in this paper. The neighboring optimal feedback control law for this class of systems was derived, and the implementation of this control law was discussed. The derivation of the control law was based upon the assumption that all state and switch-time perturbations are infinitesimal. The implementation of this control law was constructed to allow for finite, and possibly large, deviations in the neighboring state away from the nominal trajectory.

By allowing for finite state and switch-time perturbations, the region, in state-space, for which the neighboring feedback control scheme gives meaningful results, is greatly enlarged. When these perturbations are finite, use of the neighboring control scheme will, in general, not result in exact satisfaction of the terminal constraints, even when the scalar gain, K (see Eq. 2.10) , approaches infinity. This is due to the fact that the terms higher than second-order in the expansion of the performance index, which were neglected in the calculation of the neighboring control law, are no longer negligible. However, by properly choosing the nominal time, and by allowing for a possible reordering of the control-component switching sequence, use of the neighboring control scheme can result in approximate satisfaction of the terminal constraints. By generating a sufficient number of nominal trajectories, one should be able to construct a neighboring control scheme which insures satisfaction of the terminal constraints to within any desired degree of accuracy.

The technique described to choose the nominal time, and the open-loop algorithm which determines the number of switch times, the initial and final control functions, and the appropriate nominal trajectory, are presented without any rigorous mathematical justifications. No such justification is possible since the state and switch-time perturbations are assumed to be finite, and hence, strictly speaking, the concept of neighboring optimal control is no longer applicable. These ideas are supported, however, by a heuristic argument, and by the results presented in Chapter V. At least for the example problems considered in this study, the open-loop algorithm performed without fail, and the technique for choosing the nominal time, described in Section 4.2 , performed better than all other techniques investigated. Of course, if the neighboring initial state is too far removed from the nominal trajectory, use of the neighboring optimal control scheme can no longer be expected to give meaningful results.

It can be stated, however, that when the region of interest, in state-space, is known and is small, the neighboring feedback control scheme, developed in this paper, is very nearly optimal. When this region is unknown, or is large, the neighboring feedback control scheme can be used as a neighborhood-acquisition control law. That is, when one is not willing to generate a large number of nominal trajectories, the neighboring control scheme can be used to acquire a terminal state which lies in a finite neighborhood of the desired terminal state. In any event, to determine the performance level of the neighboring control scheme for a particular application, one must perform a systems analysis and simulation similar to those performed in Chapter V.

For future investigations, effort might be directed toward reducing the errors in the terminal state vector. Since the terminal state is, in general, quite sensitive to switch-time perturbations, one approach to accomplish this might be to perform all computations in double precision. One might investigate the effect of re-initiating the control scheme after acquiring a certain neighborhood of the desired terminal state. One might also devise and test different techniques for choosing $\bar{t}$. Finally, the action of the neighboring control scheme should be examined when noise is present in the system, when some components of the control vector are continuous, when the control history is composed of both continuous and discontinuous segments, and when the optimization problem of interest is singular.

APPENDIX A

CALCULATION OF FIRST- AND SECOND-ORDER PERTURBATIONS IN THE STATE

The first-order perturbation, $\delta x_I(\bar{t})$, is the first-order solution of the first-order, perturbed dynamical equations:

$$\dot{\delta x}(\bar{t}) = \bar{f}_x(\bar{t})\delta x(\bar{t}) + \bar{f}_u(\bar{t})\delta u(\bar{t}) \ , \ \delta x(\bar{t}_0) = \delta x_0 \tag{A.1}$$

where, based on the assumed functional dependence of $f[\cdot,\cdot]$ upon $u(\cdot)$, $\bar{f}_u(\bar{t})\delta u(\bar{t})$ is evaluated to be

$$\begin{aligned} &\bar{f}_u(\bar{t})\delta u(\bar{t}) = \Delta_i \bar{f} \ , \ \bar{t}_{ij} < \bar{t} < \bar{t}_{ij} + \delta t_{ij} \ , \ i = 1,\cdots, \bar{N}; \\ &j \in [1,\cdots,m] \ , \ \bar{f}_u(\bar{t})\delta u(\bar{t}) = 0 \ , \text{ otherwise .} \end{aligned} \tag{A.2}$$

Eq. A.2 is valid only when a first-order solution of Eq. A.1 is desired. Let the state transition matrix for Eq. A.1 be $\Phi(\cdot,\cdot)$. Then the solution of Eq. A.1 is

$$\delta x(\bar{t}) = \Phi(\bar{t},\bar{t}_0)\delta x_0 + \int_{\bar{t}_0}^{\bar{t}} \Phi(\bar{t},\tau)\bar{f}_u(\tau)\delta u(\tau)d\tau \ . \tag{A.3}$$

It has been assumed that $\delta t_f > 0$ and $\delta t_{ij} > 0$, $i = 1,\cdots, \bar{N}$. Since the switch times are distinct, and δt_{ij} , $i = 1,\cdots,\bar{N}$, are infinitesimal, $\bar{t}_{ij} + \delta t_{ij} < \bar{t}_{(i-1)j}$, $i = 2,\cdots, \bar{N}$, and $\delta t_{1j} + \bar{t}_{1j} < \bar{t}_f$. Then, using Eq. A.2 in Eq. A.3 , $\delta x(\bar{t})$, to first-order, and evaluated at $\bar{t} = \bar{t}_{kj}$, is

$$\delta x_I(\bar{t}_{kj}) = \Phi(\bar{t}_{kj},\bar{t}_0)\delta x_0 + \sum_{i=k+1}^{\bar{N}} \Phi(\bar{t}_{kj},\bar{t}_{ij})\Delta_i \bar{f}\delta t_{ij} \ , \ k = 1,\cdots,\bar{N} \ , \tag{A.4}$$

and $\delta x(\bar{t})$, to first-order, and evaluated at $\bar{t} = \bar{t}_f$, is

$$\delta x_I(\bar{t}_f) = \Phi(\bar{t}_f,\bar{t}_0)\delta x_0 + \sum_{i=1}^{\bar{N}} \Phi(\bar{t}_f,\bar{t}_{ij})\Delta_i \bar{f}\delta t_{ij} \ . \tag{A.5}$$

The second-order perturbation, $\delta x_{II}(\bar{t})$, is the second-order solution of the second-order, perturbed dynamical equations. The i^{th}-component of $\delta x(\bar{t})$, between nominal switch times, must satisfy

$$\begin{aligned} \delta\dot{x}^i(\bar{t}) &= \bar{f}_x{}^i(\bar{t})\delta x(\bar{t}) + \bar{f}_u{}^i(\bar{t})\delta u(\bar{t}) + \delta x_I^T(\bar{t})\bar{f}_{xu}^i(\bar{t})\delta u(\bar{t}) \\ &+ \frac{1}{2}\,\delta x_I{}^T(\bar{t})\bar{f}_{xx}^i(\bar{t})\delta x_I(\bar{t}) \ , \ \delta x(\bar{t}_0) = \delta x_0 \end{aligned} \tag{A.6}$$

where the fact that $\bar{f}_{uu}(\bar{t}) \equiv 0$ has been utilized.* The following notation has been used in writing Eq. A.6 :

$$\bar{f}_x{}^i(\bar{t}) \equiv \left[\frac{\partial \bar{f}_i(\bar{t})}{\partial x_1} \ \cdots \ \frac{\partial \bar{f}_i(\bar{t})}{\partial x_n} \right] , \tag{A.7}$$

$$\bar{f}_u{}^i(\bar{t}) \equiv \left[\frac{\partial \bar{f}_i(\bar{t})}{\partial u_1} \ \cdots \ \frac{\partial \bar{f}_i(\bar{t})}{\partial u_m} \right] , \tag{A.8}$$

$$\bar{f}_{xu}^i(\bar{t}) \equiv \begin{bmatrix} \dfrac{\partial^2 \bar{f}_i(\bar{t})}{\partial x_1 \partial u_1} & \cdots & \dfrac{\partial^2 \bar{f}_i(\bar{t})}{\partial x_1 \partial u_m} \\ \vdots & & \vdots \\ \dfrac{\partial^2 \dot{\bar{f}}_i(\bar{t})}{\partial x_n \partial u_1} & \cdots & \dfrac{\partial^2 \dot{\bar{f}}_i(\bar{t})}{\partial x_n \partial u_m} \end{bmatrix} , \tag{A.9}$$

---

* It has been assumed that $f[\cdot,\cdot]$ is linear in $u(\cdot)$.

$$\bar{f}_{xx}^{\,i}(\bar{t}) \equiv \begin{bmatrix} \dfrac{\partial^2 \bar{f}_i(\bar{t})}{\partial x_1^2} & \cdots & \dfrac{\partial^2 \bar{f}_i(\bar{t})}{\partial x_1 \partial x_n} \\ \vdots & & \vdots \\ \dfrac{\partial^2 \bar{f}_i(\bar{t})}{\partial x_n \partial x_1} & \cdots & \dfrac{\partial^2 \bar{f}_i(\bar{t})}{\partial x_n^2} \end{bmatrix} , \tag{A.10}$$

$$\dot{\delta x}^{i}(\bar{t}) \equiv (\dot{\delta x}(\bar{t}))_i . \tag{A.11}$$

The state transition matrix for Eq. A.6 is again $\Phi(\cdot,\cdot)$. The first-order perturbation, $\delta x_I(\bar{t})$, appearing in Eq. A.6, is the first-order solution of Eq. A.1, and is thus considered as a prescribed function of $\bar{t}$. The solution of Eq. A.6 for $\delta x^i(\bar{t}_f)$ is thus

$$\delta x^i(\bar{t}_f) = [\Phi(\bar{t}_f,\bar{t}_0)\delta x_0]_i + \frac{1}{2}\int_{\bar{t}_0}^{\bar{t}_f} \sum_{j=1}^{n} \Phi_{ij}(\bar{t}_f,\tau)\delta x_I^T(\tau)\bar{f}_{xx}^{\,j}(\tau)\delta x_I(\tau)\delta\tau$$

$$+ \left[\int_{\bar{t}_0}^{\bar{t}_f} \Phi(\bar{t}_f,\tau)\bar{f}_u(\tau)\delta u(\tau)d\tau\right]_i + \int_{\bar{t}_0}^{\bar{t}_f} \sum_{j=1}^{n} \Phi_{ij}(\bar{t}_f,\tau)\delta x_I^T(\tau)\bar{f}_{xu}^{\,j}(\tau)\delta u(\tau)d\tau . \tag{A.12}$$

Again, based on the assumed functional dependence of $f[\cdot,\cdot]$ upon $u(\cdot)$, $\bar{f}_u(\bar{t})\delta u(\bar{t})$ and $\bar{f}_{xu}^{\,j}(\bar{t})\delta u(\bar{t})$ are evaluated to be

$$\begin{aligned} &\bar{f}_u(\bar{t})\delta u(\bar{t}) = \Delta\bar{f}(\bar{t}) \\ &\bar{f}_{xu}^{\,j}(\bar{t})\delta u(\bar{t}) = [\Delta\bar{f}_x^{\,j}(\bar{t})]^T \end{aligned} \quad , \bar{t}_{ij} < \bar{t} < \bar{t}_{ij} + \delta t_{ij} \ , i = 1,\cdots,\bar{N},$$

$$\begin{aligned} &\bar{f}_u(\bar{t})\delta u(\bar{t}) = 0 \\ &\bar{f}_{xu}^{\,j}(\bar{t})\delta u(\bar{t}) = 0 \end{aligned} \quad , \text{otherwise} , \tag{A.13}$$

where $\Delta\bar{f}(\bar{t})$ and $\Delta\bar{f}_x^{\,j}(\bar{t})$ are defined to be

$$\Delta\bar{f}(\bar{t}) \equiv f[\bar{x}(\bar{t}),\bar{u}(\bar{t}_{ij}^{-})] - f[\bar{x}(\bar{t}),\bar{u}(\bar{t}_{ij}^{+})] \qquad (A.14)$$

$$\Delta\bar{f}_x^{\,j}(\bar{t}) \equiv f_x^{\,j}[\bar{x}(\bar{t}),\bar{u}(\bar{t}_{ij}^{-})] - f_x^{\,j}[\bar{x}(\bar{t}),\bar{u}(\bar{t}_{ij}^{+})]$$

$$, \bar{t}_{ij} < \bar{t} < \bar{t}_{ij} + \delta t_{ij} \,, \quad i = 1,\cdots,\bar{N} \,.$$

The last two terms in Eq. A.12 are now combined by using Eq. A.13 and rearranging terms:

$$\left[\int_{\bar{t}_0}^{\bar{t}_f} \Phi(\bar{t}_f,\tau)\bar{f}_u(\tau)\delta u(\tau)d\tau\right]_i + \int_{\bar{t}_0}^{\bar{t}_f} \sum_{j=1}^{n} \Phi_{ij}(\bar{t}_f,\tau)\delta x_I^{\,T}(\tau)\bar{f}_{xu}^{\,j}(\tau)\delta u(\tau)d\tau$$

$$= \left[\sum_{k=1}^{\bar{N}} \int_{\bar{t}_{kj}}^{\bar{t}_{kj}+\delta t_{kj}} \Phi(\bar{t}_f,\tau)[\Delta\bar{f}(\tau) + \Delta\bar{f}_x(\tau)\delta x_I(\tau)]d\tau\right]_i \qquad (A.15)$$

The integral term in Eq. A.15 is now expanded in a Taylor's series, retaining terms only through second-order:

$$\int_{\bar{t}_{kj}}^{\bar{t}_{kj}+\delta t_{kj}} \Phi(\bar{t}_f,\tau)[\Delta\bar{f}(\tau) + \Delta\bar{f}_x(\tau)\delta x_I(\tau)]d\tau$$

$$= \Phi(\bar{t}_f,\bar{t}_{kj})\Big[[\Delta\bar{f}(\bar{t}_{kj}) + \Delta\bar{f}_x(\bar{t}_{kj})\delta x_I(\bar{t}_{kj})]\delta t_{kj} + \frac{1}{2}[\dot{\bar{f}}_x(\bar{t}_{kj}^{+})\Delta\bar{f}(\bar{t}_{kj}) + \dot{\Delta\bar{f}}(\bar{t}_{kj})]\,\delta t_{kj}^2\Big] \,. \qquad (A.16)$$

Finally, recalling that $\dot{\Delta\bar{f}}(\bar{t}_{kj}) = \Delta_k\dot{\bar{f}}_x\bar{f}(\bar{t}_{kj}^{-})$, Eq. A.16 and Eq. A.15 are substituted into Eq. A.12 to give*

---

* This result agrees with that of McNeal ([6], Eq. A.18 and Eq. A.19), obtained for a scalar control variable by a slightly different derivation.

$$\delta x^i(\bar{t}_f) = [\Phi(\bar{t}_f,\bar{t}_0)\delta x_0]_i + \frac{1}{2}\int_{\bar{t}_0}^{\bar{t}_f}\sum_{j=1}^{n}\Phi_{ij}(\bar{t}_f,\tau)\delta x_I^T(\tau)\bar{f}_{xx}^{\ j}(\tau)\delta x_I(\tau)d\tau$$

$$+\left[\sum_{k=1}^{\bar{N}}\left\{\Phi(\bar{t}_f,\bar{t}_{kj})\left[\left(\Delta_k\bar{f} + \Delta_k\bar{f}_x\delta x_I(\bar{t}_{kj})\right)\delta t_{kj} + \frac{1}{2}\left(-\bar{f}_x(\bar{t}_{kj}^{+})\Delta_k\bar{f}\right.\right.\right. \qquad \text{(A.17)}$$

$$\left.\left.\left. + \Delta_k\bar{f}_x\bar{f}(\bar{t}_{kj}^{-})\right)\delta t_{kj}^2\right]\right\}\right]_i$$

Finally, $\delta x_{II}^{\ i}(\bar{t}_f)$ is composed of the second-order terms in Eq. A.17:

$$\delta x_{II}^{\ i}(\bar{t}_f) = \frac{1}{2}\int_{\bar{t}_0}^{\bar{t}_f}\sum_{j=1}^{n}\Phi_{ij}(\bar{t}_f,\tau)\delta x_I^T(\tau)\bar{f}_{xx}^{\ j}(\tau)\delta x_I(\tau)d\tau$$

(A.18)

$$+\left[\sum_{k=1}^{\bar{N}}\left\{\Phi(\bar{t}_f,\bar{t}_{kj})\left[\Delta_k\bar{f}_x\delta x_I(\bar{t}_{kj})\delta t_{kj} + \frac{1}{2}\left(-\bar{f}_x(\bar{t}_{kj}^{+})\Delta_k\bar{f} + \Delta_k\bar{f}_x\bar{f}(\bar{t}_{kj}^{-})\right)\delta t_{kj}^2\right]\right\}\right]_i .$$

APPENDIX B

SOME NECESSARY COMPUTATIONS

The following computation is required in order to obtain the expansion of the performance index as it appears in Eq. 3.30:

$$\frac{\bar{\lambda}^T(\bar{t}_f)}{2}\begin{bmatrix} \int_{\bar{t}_0}^{\bar{t}_f} \sum_{j=1}^{n} \Phi_{1j}(\bar{t}_f,\tau)[\delta x_1{}^T(\tau)\bar{f}_{xx}^{\,j}(\tau)\delta x_I(\tau)]d\tau \\ \vdots \\ \int_{\bar{t}_0}^{\bar{t}_f} \sum_{j=1}^{n} \Phi_{nj}(\bar{t}_f,\tau)[\delta x_I{}^T(\tau)\bar{f}_{xx}^{\,j}(\tau)\delta x_I(\tau)]d\tau \end{bmatrix}$$

$$= \frac{1}{2}\int_{\bar{t}_0}^{\bar{t}_f} \sum_{i=1}^{n}\sum_{j=1}^{n} \delta x_I{}^T(\tau)\bar{\lambda}_i(\bar{t}_f)\Phi_{ij}(\bar{t}_f,\tau)\bar{f}_{xx}^{\,j}(\tau)\delta x_I(\tau)d\tau$$

$$= \frac{1}{2}\int_{\bar{t}_0}^{\bar{t}_f} \delta x_I{}^T(\tau)\Big[\sum_{i=1}^{n}\sum_{j=1}^{n} \bar{\lambda}_i(\bar{t}_f)\Phi_{ij}(\bar{t}_f,\tau)\bar{f}_{xx}^{\,j}(\tau)\Big]\delta x_I(\tau)d\tau$$

$$\overset{(3.23)}{=} \frac{1}{2}\int_{\bar{t}_0}^{\bar{t}_f} \delta x_I{}^T(\tau)\Big[\sum_{j=1}^{n} \bar{\lambda}_j(\tau)\bar{f}_{xx}^{\,j}(\tau)\Big]\,\delta x_I(\tau)d\tau$$

$$\overset{(3.1)}{=} \frac{1}{2}\int_{\bar{t}_0}^{\bar{t}_f} \delta x_I{}^T(\tau)\bar{H}_{xx}(\tau)\delta x_I(\tau)d\tau\ . \qquad (B.1)$$

The numbers in parentheses above the equality signs refer to equations in the text which justify the ensuing step in the computation.

When determining the optimal switch-time perturbation, δt_{kj}, in Section 3.4, it is necessary to differentiate Eq. B.1 with respect to

δt_{kj} . This differentiation is performed as follows:

$$\frac{\partial}{\partial \delta t_{kj}} \left[\frac{1}{2} \int_{\bar{t}_0}^{\bar{t}_f} \delta x_I^T(\tau) \bar{H}_{xx}(\tau) \delta x_I(\tau) d\tau \right]$$

$$= \int_{\bar{t}_0}^{\bar{t}_f} \left[\frac{\partial \delta x_I(\tau)}{\partial \delta t_{kj}} \right]^T \bar{H}_{xx}(\tau) \delta x_I(\tau) d\tau \ , \qquad \text{(B.2)}$$

where $\frac{\partial}{\partial \delta t_{kj}} \bar{H}_{xx}(\bar{t}) \equiv 0$, $\bar{t} \in [\bar{t}_0, \bar{t}_f]$, since $\bar{H}_{xx}(\cdot)$ is a function of the nominal control vector only. For $\bar{t}_0 \leq \bar{t} \leq \bar{t}_{kj}$, $\frac{\partial \delta x_I(\bar{t})}{\partial \delta t_{kj}} \equiv 0$.

Thus

$$\int_{\bar{t}_0}^{\bar{t}_f} \left[\frac{\partial \delta x_I(\tau)}{\partial \delta t_{kj}} \right]^T \bar{H}_{xx}(\tau) \delta x_I(\tau) d\tau = \int_{\bar{t}_{kj}}^{\bar{t}_f} \left[\frac{\partial \delta x_I(\tau)}{\partial \delta t_{kj}} \right]^T \bar{H}_{xx}(\tau) \delta x_I(\tau) d\tau . \qquad \text{(B.3)}$$

From Eq. 3.29, $\delta x_I(\bar{t})$, $\bar{t} \in [\bar{t}_{kj}, \bar{t}_f]$, is given by

$$\delta x_I(\bar{t}) = \Phi(\bar{t}, \bar{t}_0) \delta x_0 + \sum_{i=k}^{\bar{N}} \Phi(\bar{t}, \bar{t}_{ij}) \Delta_i \bar{f} \delta t_{ij} \ , \quad \bar{t}_{kj} < \bar{t} \leq \bar{t}_{(k-1)j} \ ,$$

$$k = 2, \cdots, \bar{N} \ , \quad \bar{t}_{kj} < \bar{t} \leq \bar{t}_f \ , \quad k = 1 \ . \qquad \text{(B.4)}$$

Thus, differentiating Eq. B.4 with respect to δt_{kj} gives

$$\frac{\partial \delta x_I(\bar{t})}{\partial \delta t_{kj}} = \Phi(\bar{t}, \bar{t}_{kj}) \Delta_k \bar{f} \ , \quad \bar{t}_{kj} < \bar{t} \leq \bar{t}_f \ . \qquad \text{(B.5)}$$

Substituting Eq. B.5 and Eq. B.4 into Eq. B.3 then gives the desired result:

$$\frac{\partial}{\partial \delta t_{kj}} \left[\frac{1}{2} \int_{\bar{t}_0}^{\bar{t}_f} \delta x_I^T(\tau) \bar{H}_{xx}(\tau) \delta x_I(\tau) d\tau \right] =$$

(B.6)

$$\sum_{\ell=2}^{k} \left\{ \int_{\bar{t}_{\ell j}}^{\bar{t}_{(\ell-1)j}} [\Phi(\tau, \bar{t}_{kj}) \Delta_k \bar{f}]^T \bar{H}_{xx}(\tau) [\Phi(\tau, \bar{t}_0) \delta x_0 + \sum_{i=\ell}^{\bar{N}} \Phi(\tau, \bar{t}_{ij}) \Delta_i \bar{f} \delta t_{ij}] d\tau \right\}$$

$$+ \int_{\bar{t}_{1j}}^{\bar{t}_f} [\Phi(\tau, \bar{t}_{kj}) \Delta_k \bar{f}]^T \bar{H}_{xx}(\tau) [\Phi(\tau, \bar{t}_0) \delta x_0 + \sum_{i=1}^{\bar{N}} \Phi(\tau, \bar{t}_{ij}) \Delta_i \bar{f} \delta t_{ij}] d\tau \ .$$

APPENDIX C

SATELLITE ATTITUDE EQUATIONS OF MOTION

In this appendix, the attitude equations of motion for the earth-orbiting satellite, considered in Section 5.3, are presented. These equations are not derived in detail here since they are well known (see, for example, [1], [2] , [18]). The assumptions made in the derivation of these equations, and the coordinate systems used to describe the attitude and dynamics of the satellite, are, however, described in detail in order to make explicit the problem discussed in Section 5.3.

The following assumptions are made in order to simplify the dynamical description of the satellite:

Assumption 1. The satellite attitude is controlled by three cold gas jets, fixed to the satellite, and alligned with the three principal axes of the satellite.

Assumption 2. The gravity-gradient and disturbance torques acting on the satellite are negligible compared to the control torques generated by the cold gas jets.

Assumption 3. The satellite, hereafter designated body B, is a rigid body.

Assumption 4. The earth, hereafter designated attracting body E, is an inertially fixed point mass.

Now let $\bar{b}_i$, i = 1,2,3, be a set of right-handed, mutually orthogonal unit vectors, fixed in B, and parallel to the principal axes of B. Let the mass center, B* , of body B, be the origin of the body-fixed reference axes, denoted by (x_B , y_B , z_B) and specified by $\bar{b}_i$, i = 1,2,3.

Let ω_i, i = 1,2,3, be the $\bar{b}_i^{th}$-component of the angular velocity vector of B relative to E (and hence relative to inertial space by Assumption 4 above). The principal moments of inertia of B, with respect to $\bar{b}_i$, i = 1,2,3, for B*, are denoted by I_i, i = 1,2,3. Finally, let T_i, i = 1,2,3, be the control torques generated by the cold gas jets about $\bar{b}_i$, i = 1,2,3.

Utilizing the above notation and Assumptions 1-4, Euler's dynamical equations of motion for the satellite may be written (see [19], pg. 283):

$$\begin{aligned} T_1 &= \dot{\omega}_1 I_1 - \omega_2\omega_3(I_2 - I_3) \\ T_2 &= \dot{\omega}_2 I_2 - \omega_3\omega_1(I_3 - I_1) \\ T_3 &= \dot{\omega}_3 I_3 - \omega_1\omega_2(I_1 - I_2) \end{aligned} \tag{C.1}$$

Now define the normalized inertia parameters, k_1, k_2, k_3, to be

$$\begin{aligned} k_1 &\equiv \frac{I_3 - I_2}{I_1}, \\ k_2 &\equiv \frac{I_1 - I_3}{I_2}, \\ k_3 &\equiv \frac{I_2 - I_1}{I_3}, \end{aligned} \tag{C.2}$$

and define the control angular accelerations, u_1, u_2, u_3, to be

$$u_i \equiv \frac{T_i}{I_i}, \quad i = 1, 2, 3. \tag{C.3}$$

Substituting Eq. C.2 and Eq. C.3 into Eq. C.1, and rearranging terms, then gives

$$\dot{\omega}_1 = u_1 - \omega_2\omega_3 k_1 \quad ,$$

$$\dot{\omega}_2 = u_2 - \omega_3\omega_1 k_2 \quad , \tag{C.4}$$

$$\dot{\omega}_3 = u_3 - \omega_1\omega_2 k_3 \quad .$$

The earth-fixed (or inertial) reference axes, denoted by (x_E , y_E , z_E), and the orbital reference axes, denoted by (x_R, y_R, z_R) , are shown in Fig. C.1 for a satellite, B , in an elliptic orbit about the earth, E . Both z_E and z_R are normal to the orbit plane. It is convenient to direct x_R along the radius vector, $\bar{\rho}$, and to direct x_E toward the orbit perigee. In Fig. C.1, "a" is the magnitude of the semi-major axis, e is the eccentricity of the orbit, and θ is the true anomaly.

The attitude of B , in inertial space, is specified by the three-axis Euler angles, θ_i , i = 1,2,3 . These angles are defined to be the magnitudes of successive rotations, relative to the (x_R, y_R, z_R) reference frame, about the (x_B, y_B, z_B) reference axes, respectively. A pictorial description of θ_i , i = 1,2,3, is given in Fig. C.2, where (x_R', y_R', z_R') and (x_R'', y_R'', z_R'') represent the intermediate positions, between successive rotations, of the (x_B, y_B, z_B) reference axes. The angles $\theta_1, \theta_2, \theta_3$ are commonly referred to as the yaw, roll, and pitch angles, respectively.

The kinematical equations, relating the three-axis Euler angles to the components of the inertial angular velocity of B , are written as

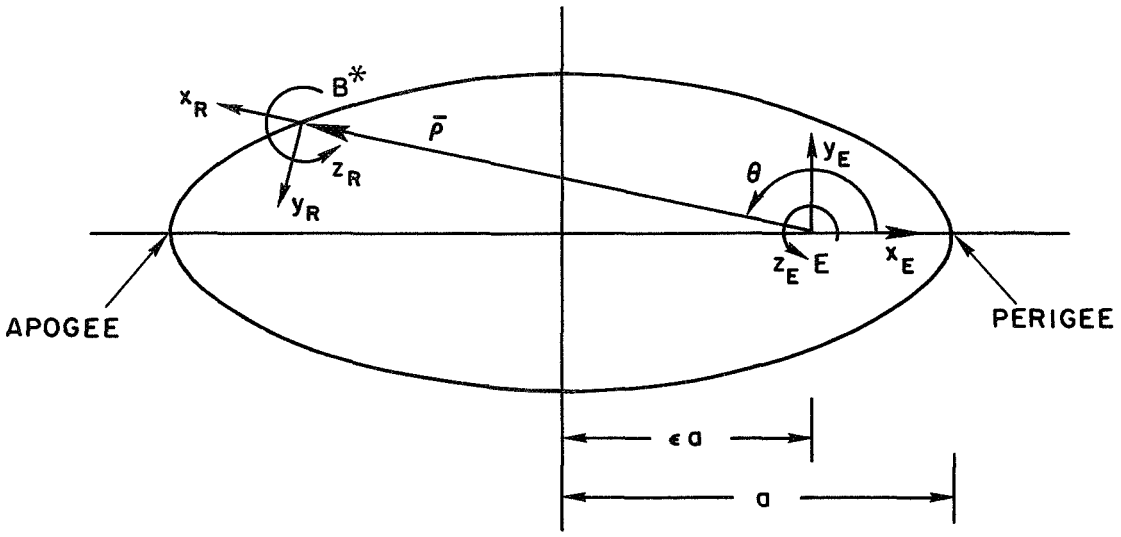

Figure C.1. Reference Frames Associated With Satellite in Elliptical Orbit.

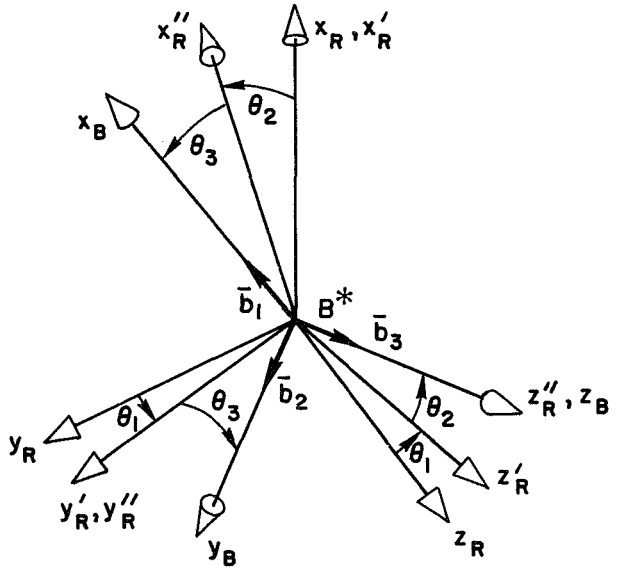

Figure C.2. Pictorial Description of Three-Axis Euler Angles.

follows (see [18] , pg. 9):

$$\omega_1 = \dot{\theta}(s_1 s_3 - c_1 s_2 c_3) + \dot{\theta}_1 c_2 c_3 + \dot{\theta}_2 s_3$$

$$\omega_2 = \dot{\theta}(s_1 c_3 + c_1 s_2 s_3) - \dot{\theta}_1 c_2 s_3 + \dot{\theta}_2 c_3 \qquad \text{(C.5)}$$

$$\omega_3 = \dot{\theta} c_1 c_2 + \dot{\theta}_1 s_2 + \dot{\theta}_3$$

where $s_i = \sin(\theta_i)$, $i = 1,2,3$, and $c_i = \cos(\theta_i)$, $i = 1,2,3$. Solving Eq. C.5 for $\dot{\theta}_1$, $\dot{\theta}_2$, and $\dot{\theta}_3$ gives

$$\dot{\theta}_1 = \frac{1}{c_2} [\omega_1 c_3 - \omega_2 s_3 + \dot{\theta} c_1 s_2] ,$$

$$\dot{\theta}_2 = \omega_1 s_3 + \omega_2 c_3 - \dot{\theta} s_1 , \qquad \text{(C.6)}$$

$$\dot{\theta}_3 = \frac{1}{c_2} [-s_2 c_3 \omega_1 + s_2 s_3 \omega_2 + c_2 \omega_3 - c_1 \dot{\theta}] .$$

Note that a singularity appears in Eq. C.6 when $\theta_2 = 90^\circ$. This difficulty is avoided in Section 5.3 by simply choosing initial states such that $|\theta_2(t)| < 90^\circ$, $t_0 \leq t \leq t_f$. Furthermore, regions of indifference (see [2], pg. 13) exist when specifying the satellite orientation by the three-axis Euler angles, θ_i , $i = 1,2,3$. This is due to the fact that a given geometrical orientation, specified by θ_i , $i = 1,2,3$, may also be specified by $\theta_i \pm 2\pi m$, $i = 1,2,3$, where m is any positive integer. The control problems created by this multi-valued nature of the Euler angles are again avoided in Section 5.3 by choosing initial states such that $|\theta_i(t)| < 180^\circ$, $t_0 \leq t \leq t_f$, $i = 1$, 3.

Eq. C.4 and Eq. C.6 are the equations of motion utilized in Sec-

tion 5.3 to solve the satellite attitude-acquisition problem. In Eq. C.6 , $\dot{\theta}(t)$, $t_0 \leq t \leq t_f$, is determined by the particular orbit of interest, and is therefore considered to be a prescribed function.

APPENDIX D

STATE DETERMINATION FOR MINIMUM-TIME SATELLITE ATTITUDE-ACQUISITION PROBLEM

The neighboring feedback control scheme developed in this dissertation is based upon the assumption that the system state, $x(t)$, is known exactly. McNeal [6] proved a separation theorem which allows one to replace $x(t)$ with an estimate of the state, $\hat{x}(t)$, in the neighboring feedback control law. This theorem is based upon the assumption that the system dynamics and the state measurements are contaminated with additive noise which possesses the properties of white Gaussian random processes. It is assumed that control and estimation are separable in the minimum-time satellite attitude-acquisition problem discussed in Section 5.3. The purpose of this appendix is to briefly discuss, without going into the details of estimation theory, the general approach used to estimate the state of the satellite for this attitude-acquisition problem.

The state variables for this system were chosen to be the three-axis Euler angles, $\theta_i(t), i = 1,2,3$, relative to the orbital reference axes, and the inertial angular velocity components along the principal axes of the satellite, $\omega_i(t)$, $i = 1,2,3$ (see Appendix C). Information about $\omega_i(t)$, $i = 1,2,3$, may be obtained from a three-axis, strapped down, single degree-of-freedom gyro package. This package consists of three single-axis rate or rate-integrating gyros which are fixed to the satellite and whose input axes are parallel to each principal axis of the satellite.*

---

* If the body angular rates are measured about a non-principal axis coordinate system, they can easily be transformed into a principal axis system by a constant 3 x 3 matrix transformation and all computations can then take place in that coordinate frame.

The outputs from these gyros are the angular rates, $\omega_i(t)$, i = 1,2,3, and additive noise due to gyro unbalance, stray magnetic field and temperature effects, gyro-misalignment errors, gyro bearing friction, and other causes. The gyro error is usually modeled by a bias error plus a zero-mean white Gaussian random process. For precise angular rate determination, these errors must be accurately estimated and then subtracted from the gyro-output signal.

Assuming that $\omega_i(t)$, i = 1,2,3, can accurately be determined in this manner, the Euler angles can be calculated by integrating the satellite's kinematical equations, repeated here for convenience (see Eq. C.6):

$$\begin{aligned}
\dot{\theta}_1 &= \frac{1}{c_2}\,[\omega_1 c_3 - \omega_2 s_3 + \dot{\theta} c_1 s_2] \,, \\
\dot{\theta}_2 &= \omega_1 s_3 + \omega_2 c_3 - \dot{\theta} s_1 \,, \\
\dot{\theta}_3 &= \frac{1}{c_2}\,[-s_2 c_3 \omega_1 + s_2 s_3 \omega_2 + c_2 \omega_3 - c_1 \dot{\theta}] \,,
\end{aligned} \tag{D.1}$$

where $\dot{\theta}$ is taken to be a prescribed function. Two fundamental problems arise when using this approach. First, initial values for the Euler angles are usually inaccurate, if available, since they cannot be measured directly. Second, since the gyros possess bias errors, the long-term errors in $\theta_i(t)$, i = 1,2,3, will be unbounded.

Jackson [20] discusses and demonstrates the fact that compensation for the angular rate measurement bias errors and noise is possible when some satellite orientation information is available. In addition, this information may be used to obtain estimates, with bounded long-

term errors, of the three-axis Euler angles. The required orientation information may be obtained by utilizing one or more onboard sensors which may or may not be mounted on gimbals. Horizon sensors, sun sensors, star sensors, and landmark sensors, to name a few, utilize telescopic or photographic devices to detect the horizon, the sun, a specified star, and a specified landmark, respectively. If the sensor is mounted on gimbals, a servomechanism can be utilized, after acquisition, to "hold" the target for as long as the target is in the satellite's field of view. If the sensor is rigidly fixed to the satellite, the sensor outputs are time pulses which occur whenever the target passes the sensor's field of view.

The main feature of the sensors mentioned above is that each determines the representation of a unit vector, $\overline{V}$, in the body fixed reference frame. Denote this representation by $\overline{V}_B$, and let $\overline{V}_R$ denote $\overline{V}$ in the orbital reference frame. After target acquisition, $\overline{V}$ is the unit vector parallel to the sensor's line of sight and directed toward the target. Since the satellite's orbital motion is assumed known, $\overline{V}_R$ is a prescribed function of orbital position.

There exists a real orthogonal transformation matrix, T_{BR} , which maps $\overline{V}_R$ into $\overline{V}_B$. Thus,

$$\overline{V}_B = T_{BR}\overline{V}_R \ . \tag{D.2}$$

For the three-axis Euler angle representation of attitude, the elements of T_{BR} are trigonometric functions of $\theta_i(t)$, $i = 1,2,3$. Thus, the sensor outputs are nonlinear functions of the Euler angles which may or may not supply sufficient information to determine the satellite orientation. In addition, any sensor used to obtain these functions

will be contaminated with noise. This noise must be modeled and compensated for in order to accurately extract the satellite attitude from the given measurements.

Fortunately, existing gyros and sensors often possess error characteristics that can be modeled quite accurately as normally distributed white random processes. This allows one to turn to the extensive literature on linear and nonlinear stochastic estimation theory to implement a system for estimating $\omega_i(t)$, $i = 1,2,3$, as well as $\theta_i(t)$, $i = 1,2,3$ (see, for example, [13] and [20]). Either observers, designed to regulate the transient behavior of the state error $\tilde{x}(t) = x(t) - \hat{x}(t)$, or filters, designed to determine $\hat{x}(t)$ in some optimal sense, can be developed to determine an estimate of the satellite state. The gyro package and at least one attitude sensor are required in order to develop an accurate state estimator.

The existing theory for linear estimators is quite extensive. To be applicable to the system of interest here, the state dynamical equations (Eq. C.4 and Eq. C.6) and the state observations must be linearized about a nominal path. The estimator would then be accurate only when state deviations from the nominal are small. For the neighboring control scheme, this technique would probably work quite well when the nominal path is the optimal path generated by the nominal control law. When the state deviations are large, however, it would probably be necessary to use nonlinear estimation techniques since the dynamical equations for $\theta_i(t)$, $i = 1,2,3$, and the state observations are highly nonlinear. Since nonlinear estimation theory is not as highly developed as linear estimation theory, the performance of a given nonlinear estimator must be determined by a simulation of the particular system of interest. It is noted that all significant sensor errors must

be incorporated in the design of the linear or nonlinear state estimator. In particular, bias errors, when present, must appear explicitly in the estimator dynamics.

It is finally noted that other attitude representations may also be used to specify the system state, such as the Euler parameter and direction cosine representations. A discussion of these representations and their advantages over the Euler angle representation, with regard to nonlinear state estimation, is presented in [20].

REFERENCES

1. K. A. Hales and I. Flügge-Lotz, "Minimum Fuel Attitude Control of a Rigid Body in Orbit by an Extended Method of Steepest Descent," Sudaar No. 257, Department of Aeronautics and Astronautics, Stanford University, Stanford, California, January, 1966. See also International Journal of Non-Linear Mechanics, Volume 3, Pergamon Press, 1968.

2. G. D. Wolske and I. Flügge-Lotz, "Minimum Fuel Attitude Control of a Nonlinear Satellite System with Bounded Control by a Method Based on Linear Programming," Sudaar No. 374 , Department of Aeronautics and Astronautics, Stanford University, Stanford, California, May, 1969. Also, to be published in International Journal of Non-Linear Mechanics, Volume 5, Pergamon Press, 1970.

3. P. Dyer and S. R. McReynolds, "On a New Necessary Condition for Optimal Control Problems with Discontinuities," Space Programs Summary No. 37-48, Volume 3, December 31, 1967, pp. 9-12.

4. P. Dyer and S. R. McReynolds, "On Optimal Control Problems with Discontinuities," J. Math. Anal. Appl., Volume 23, 1968, pp. 585-603.

5. D. H. Jacobson, "Differential Dynamic Programming Methods for Solving Bang-Bang Control Problems," IEEE Trans. Auto. Control, December, 1968, pp. 661-675.

6. Don McNeal, "Neighboring Optimal Control of Nonlinear Systems Using Bounded Control,"Sudaar No. 311, Department of Aeronautics and Astronautics, Stanford University, Stanford, California, May, 1967.

7. J. V. Breakwell, J. L. Speyer, and A. E. Bryson, Jr.,"Optimization and Control of Nonlinear Systems Using the Second Variation," SIAM J. Control, Ser. A, 1, 2, 1963, pp. 193-223.

8. H. J. Kelley, "Guidance Theory and Extremal Fields," IRE Trans. on Automatic Control, AC-7, October, 1962, pp. 75-82.

9. J. E. McIntyre, "Neighboring Optimal Terminal Control with Discontinuous Forcing Functions," AIAA J., 4, 1, January, 1966, pp.141-148.

10. J. L.Speyer and A. E. Bryson, Jr., "A Neighboring Optimum Feedback Control Scheme Based on Estimated Time-to-Go with Application to Re-Entry Flight Paths,"AIAA J., 6 , 5, May, 1968, pp. 769-776.

11. W. F. Powers, "Techniques for Improved Convergence in Neighboring Optimum Guidance," AIAA Paper No. 69-888, AIAA Guidance, Control, and Flight Mechanics Conference, Princeton, New Jersey, August, 1969.

12. E. J. Davison and D. M. Monro, "A Computational Technique for Finding Time Optimal Controls of Nonlinear Time-Varying Systems," Preprints of Technical Papers from the Tenth Joint Automatic Control Conference of the American Automatic Control Council, August, 1969.

13. A. E. Bryson, Jr., and Yu-Chi Ho, Applied Optimal Control: Optimization, Estimation, and Control, Blaisdell Publishing Company, 1969.

14. L. S. Pontryagin, V. G. Boltyanskii, R. V. Gamkrelidze, and E. F. Mishchenko, The Mathematical Theory of Optimal Processes, Interscience Publishers, Inc., New York, 1962.

15. I. Flügge-Lotz and Mih Yin, "On the Optimum Response of Third Order Contactor Control Systems," Stanford University Technical Report No. 125, Division of Engineering Mechanics, Stanford University, Stanford, California , April 25, 1960. See also ASME Journal of Basic Engineering, Volume 83, Series D, 1961, pp. 59-64.

16. I. Flügge-Lotz and H. Marbach, "The Optimal Control of Some Attitude Control Systems for Different Performance Criteria," Sudaar No. 131, Department of Aeronautics and Astronautics, Stanford University, Stanford, California, June, 1962. See also ASME Journal of Basic Engineering, Volume 85, Series D, June, 1963, pp. 165-176.

17. D. K. Frederick, "Piecewise-Linear Switching Functions for Quasi-Minimum-Time Contactor Control Systems," Sudaar No. 178, Department of Aeronautics and Astronautics, Stanford University, Stanford, California, December, 1963. See also IEEE Trans. on Automatic Control , August, 1967.

18. R. Busch and I. Flügge-Lotz, "The Attitude Control of a Satellite In an Elliptic Orbit," Sudaar No. 261, Department of Aeronautics and Astronautics, Stanford University, Stanford, California, April, 1966. See also Journal of Spacecraft and Rockets, Volume 4, No.4, American Institute of Aeronautics and Astronautics, 1967.

19. T. R. Kane, Dynamics , Holt, Rinehart and Winston, Inc., 1968.

20. D. B. Jackson, "Applications of Nonlinear Estimation Theory to Spacecraft Attitude Determination Systems," presented at the Spacecraft Attitude Determination Symposium, El Segundo, California, October, 1969.